The Effects of Different Particle Size of Nano-ZnO and Alumina-based Catalysts on Removal of Atrazine from Water with Ozone

A Thesis Submitted to the College of

Graduate Studies and Research

In Partial Fulfillment of the Requirements

For the Degree of Master of Science

In the Department of Chemical and Biological Engineering

University of Saskatchewan

Saskatoon

By

Azam Sadeghi

© Copyright Azam Sadeghi, December, 2015. All rights reserved.

PERMISSION TO USE

In presenting this thesis in partial fulfillment of the requirements for a Master of Science degree from the University of Saskatchewan, I agree that the libraries of this University may make it freely available for inspection. I further agree that permission for copying of this thesis in any manner, in whole or in part, for scholarly purposes may be granted by the professors who supervised my thesis work, in their absence, by the Graduate Chair of the program or Dean of the College in which my thesis work was done. It is understood that any copying, publication, or use of this thesis or parts thereof for financial gain shall not be allowed without my written permission. It is also understood that due recognition shall be given to me and to the University of Saskatchewan in any scholarly use which may be made of any material in my thesis.

Requests for permission to copy or to make other use of material in this thesis in whole or in part should be addressed to:

Head of the Department of Chemical and Biological Engineering

College of Engineering, 57 Campus Drive

University of Saskatchewan

Canada S7N 5A9

Abstract

Due to the widespread application of pesticides and herbicides in agricultural industries, these substances have been highlighted as emerging contamination of natural ground and surface water resources. Conventional water treatment processes are only effective in removing emerging contaminants in water.

The mechanism of degradation of organic impurities present in water using ozone is known to either directly involve the ozone molecule or to occur by the indirect effect of free hydroxyl radicals (•OH). The latter are produced in the radical chain reaction of ozone decomposition.

A series of experiments were carried out to investigate the effects of particle sizes of nano-ZnO catalysts on removal of atrazine (ATZ). Nano-ZnO catalysts increase the rate of ozone decomposition and atrazine removal by production of hydroxyl radicals as oxidative intermediates. However, different particle sizes have a minimal effect on the rate of ozone decomposition and atrazine removal. It is believed that molecular ozone is adsorbed on the surface of nano-ZnO followed by the oxidation of the ozone molecule. This leads to the production of OH radicals. Therefore, it is reasonable to assume that reaction is carried out in the bulk of the solution and the rate is independent of catalyst's surface area. This is probably the reason for similar reaction rates of different particle sizes of nano-Zno catalysts.

Additionally three different metal oxides (ZnO, Mn_2O_3 and Fe_2O_3) loaded on γ-alumina and γ-alumina (metal oxide-free) were used in catalytic ozonation of aquatic atrazine samples. The findings substantiate the strong influence of molecular ozone on degradation of ATZ and the partial involvement of hydroxyl radicals in the mechanism. Based on adsorption studies, atrazine

has a low affinity towards adsorption on the surface of the catalysts. It is logical to assume that ozone reacts with the hydroxyl groups of the catalyst to form a highly reactive metal-ozone complex. This layer could react with a molecule of atrazine through an electron-transfer mechanism.

The residual concentration of ATZ and total organic carbon (TOC) were determined by High Performance Liquid Chromatography (HPLC) and Total Organic Carbon (TOC) analyses.

ACKNOWLEDGEMENTS

Firstly, I would like to express my deepest gratitude to my supervisor, Dr. Jafar Soltan, whose patience, involvement, and guidance provided an outstanding research environment and led to a fascinating graduate experience. I have been fortunate to have him by my side as a mentor throughout my study.

Secondly, I would like to thank members of my graduate committee, Dr. Venkatesh Meda and Dr. Lifeng Zhang for insightful comments and constructive criticism they provided during my graduate study.

I would like to acknowledge the financial support from the Natural Science and Engineering Research Council of Canada (NSERC) and the Department of Chemical and Biological Engineering of the University of Saskatchewan.

A very special thanks to the previous and present members of my research group who have been outstanding colleagues and provided useful discussions and a fantastic work environment. I would also like to thank Mr. Richard Blondin and Mr. Rlee Prokopishyn for their kind and invaluable assistance throughout the projects.

Dedication

I dedicate this thesis to my Husband Pouyan.

Thank you very much for your love and encouragement throughout

my academic and personal life

Table of Contents

List of Figures

List of Tables

NOMENCLATURE

Ag(I)	Silver(I)
Al_2O_3	Aluminum oxide (Alumina)
AOP	Advanced oxidation process
ATZ	Atrazine ($C_8H_{14}ClN_5$)
BET	Brunauer, Emmett and Teller
Cd(II)	Cadmium (II)
Co(II)	Cobalt(II)
Cr(III)	Chromium(III)
Cu(II)	Copper(II)
DCAA	Dichloroacetic acid ($C_2H_2Cl_2O_2$)
Fe(II)	Iron(II)
Fe(III)	Iron(III)
Fe^{2+}	Iron (II) ion
Fe_2O_3	Iron(III) oxide
Fe_2O_3/γ-Alumina	Iron(III) oxide loaded on γ-alumina

f_{OH}	Fraction of micropollutant degraded by hydroxyl radicals
H_2O_2	Hydrogen peroxide
$H_3PO_4/H_2PO^{4-}/HPO4^{-2}$	Phosphate buffers
HO_2^-	Hydroperoxyl ion
HO_2•	Hydroperoxyl radical
HPLC	High Performance Liquid Chromatography
k_a	Apparent first-order adsorption rate constant (L g^{-1} s^{-1})
k_D	Pseudo first-order ozone decomposition rate constant (s^{-1})
k_{O_3}	Reaction rate constant of micropollutant with molecular ozone (M^{-1} s^{-1})
k_{obs}	Observed reaction rate constant (M^{-1} s^{-1})
k_{OH}	Reaction rate constant of micropollutant with hydroxyl radicals (M^{-1} s^{-1})
K_{ow}	Octanol-Water Partition Coefficient
M	Atrazine concentration (mol L^{-1})
Mn(II)	Manganese (II)
Mn_2O_3 / γ-alumina /O_3	Ozonation process catalyzed by manganese(III) oxide loaded on y-alumina
Mn_2O_3/y-alumina	Manganese(III) oxide loaded on y-alumina

MnO_2	Manganese dioxide
nano-ZnO (35-45 nm)/O_3	Ozonation process catalyzed by nano-ZnO (35-45 nm)
nano-ZnO (35-45 nm)/O_3/TBA	Ozonation process catalyzed by nano-ZnO (35-45 nm) in presence of *tert*-butyl alcohol
Ni(II)	Nickel (II)
$O_2^{\bullet-}$	Superoxide ion radical
O_3	Ozone or non-catalytic ozonation process
O_3^-	Ozonide ion
$O_3^{\bullet}$	Ozonide radical
$O_3^{\bullet-}$	Ozonide ion radical
OH^-	Hydroxide ion
OH•	Hydroxyl radicals
*p*CBA	para-chlorobenzoic acid ($C_7H_5ClO_2$)
pH_{PZC}	pH of point of zero charge
pK_a	Acid dissociation constant
R_{ct}	Ratio of hydroxyl radical concentration to ozone concentration
rpm	Revolutions per minute
S_{BET}	Catalyst specific surface area (m2 g-1)

SHB	Staehelin, Hoigné, and Buhler
TBA	*tert*-butanol ($C_4H_{10}O$)
TCP	2,4,6-trichlorophenol ($C_6H_2Cl_3OH$)
TiO_2	Titanium dioxide
TOC	Total organic carbon
UV	Ultraviolet light
W	Catalyst dose (g L^{-1})
Zn(II)	Zinc(II)
ZnO	Zinc oxide
ZnO/γ-Al_2O_3	Zinc oxide loaded on γ-alumina
ZnO/γ-alumina/O_3	Ozonation process catalyzed by zinc oxide loaded on γ-alumina
ZnO/γ-alumina/O_3/TBA	Ozonation process catalyzed by zinc oxide loaded on γ-alumina in presence of *tert*-butyl alcohol

Chapter1

1. Introduction

Ozonation processes are among the most promising methods of degradation of organic pollutants in water treatment processes. Despite the successful use of ozonation in removal of most common contaminants, the aqueous degradation of some, including atrazine, are slow and hence inefective.[1] Catalytic ozonation is used to increase the efficiency of the ozonation process. Catalytic ozonation has been a major focus in water treatment research for many years, but despite the success of these methods, it has yet to be used as a common treatment process in the water purification industry. Only a few countries such as France and China have incorporated this method of water purification in their water treatment industry. This under-utilization is somewhat related to the knowledge gap in the mechanism and process of such methods.[2] This research aims to investigate methods to increase the effectiveness of catalytic ozonation systems as well as new catalysts for removal of an emerging pollutant.

1.1 Research Motivation

Atrazine is one of the most widely used herbicides in Canada since the 60's. This contaminant is among the most prevalent pollutants detected in sources of potable water in the Great Lakes Region and Lower Fraser Valley Region of British Columbia.[3,4] The chemical structure of atrazine is illustrated in Figure 1. Atrazine is a hydrophobic compound (solubility in water = 30 $mg.L^{-1}$ at pH=7.5, K_{ow}=2.68) which has a high adsorption potential on organic matter. Atrazine is poorly biodegradable; the average half-life of atrazine in the natural aqueous media is reported as 60 days.[5]

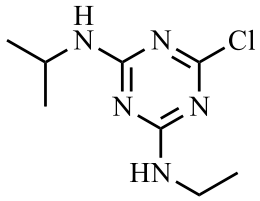

Figure 1. 1. Chemical structure of atrazine

Atrazine (ATZ), the parent compound of the triazine family, is a well-known herbicide which has been monitored in drinking water for three decades. The legal atrazine concentration in drinking water is 3 parts per billion. However EPA's monitoring program has demonstrated that the concentration of atrazine exceeds this limit in some specific seasons.[6]

Atrazine has the potential to cause acute and chronic health issues.[7–10] Studies have shown that even low levels of exposure to atrazine can cause abnormalities in newborns.[11] Additionally, this compound is a hormone-mimicking toxin which can interfere with regular hormone activities in the human body.[12]

The removal of pesticides (including ATZ) from water are achieved mainly through either or a combination of chemical degradation, incineration, adsorption, phytoremediation, and/or biodegradation. Hydrolysis, dehalogenation, photolysis, and oxygenation (oxidation) processes are among the most important means of removal of ATZ from water and wastewater samples.[13,14]

Various compounds have been used in the degradation of this emerging pollutant (EP) from water through a process called catalytic ozonation. Nano material-based catalysts are known to possess outstanding efficiency in catalytic processes. Intrigued by the outstanding properties of nano-catalysts, exploiting the effects of catalyst's particle size for removal of Atrazine is particularly alluring. Additionally the effects of metal oxides (ZnO, Mn_2O_3 and Fe_2O_3) loaded on γ-alumina and γ-alumina (metal oxide-free) in catalytic ozonation of aqueous samples of atrazine is another focus of this thesis.

1.2 Research Objectives

Generally, the surface area of a heterogeneous catalyst is proportional to its particle size and hence the observed reactivity in catalytic ozonation processes. Previous reports have demonstrated that micro, sub-micro, and nano-sized ZnO catalysts are associated with different efficiencies in removal of organic pollutants from water samples. However, to the best of our knowledge, the effects of various sizes of nano-ZnO in catalytic ozonation of Atrazine are not reported. As an initial goal of this project, the effects of three different particle sizes of nano-ZnO in catalytic ozonation of Atrazine are explored.

To explore more effective catalysts for removal of Atrazine through catalytic ozonation processes, the effects of different metals loaded on alumina are investigated.

The aforementioned goals are pursued by the following specific objectives:

- Study of catalyst characterization by measuring the point of zero charge.
- Study of adsorption of Atrazine on catalyst surface.
- Determine and compare effect of different pH on ozone self-decomposition.
- Study of the effect of catalyst dose on ozone decomposition rate.
- Study of the effects of particle sizes of nano-ZnO on ATZ degradation by monitoring the total removal of ATZ during catalytic ozonation.
- Study of the effect of different metals loaded on γ-Alumina on ATZ degradation by monitoring the total removal of ATZ during catalytic ozonation and concentration of ozone.
- Quantify and compare the ability of different catalysts to enhance ozone decomposition into hydroxyl radicals.

- Estimate the contributions of molecular ozone and free radical reactions for atrazine degradation and assess the inhibitory effects of a radical scavenger

Chapter 2

2. Literature Review

The study of the mechanisms involved in the catalytic ozonation of aqueous samples is non-trivial, mostly due to the presence of excess amounts of water. In simple terms, the catalytic ozonation generates hydroxyl radicals which are hyper reactive species. However, the catalytic reactivity of such systems does not necessarily correlate to the generation of hydroxyl radicals. Many instances of catalytic reactivity without the incorporation of hydroxyl radicals exist in the literature. Regardless of the nature of the reactive intermediate, catalytic ozonation processes are relevant in reactions in which, at the same pH, the efficiency of ozonation in the presence of catalyst is higher than without it.[2]

In heterogeneous catalytic ozonation, the catalyst is in a different physical state than the reaction media. Inevitably, the reaction proceeds on the surface of the catalyst (adsorption). Three conditions could be considered for the mechanism (Fig. 2.1):[2]

1. Adsorption of ozone on the surface of the heterogeneous catalyst.
2. Adsorption of organic molecule on the surface of the heterogeneous catalyst.
3. Simultaneous adsorption of ozone and organic molecule on the heterogeneous catalyst's surface.

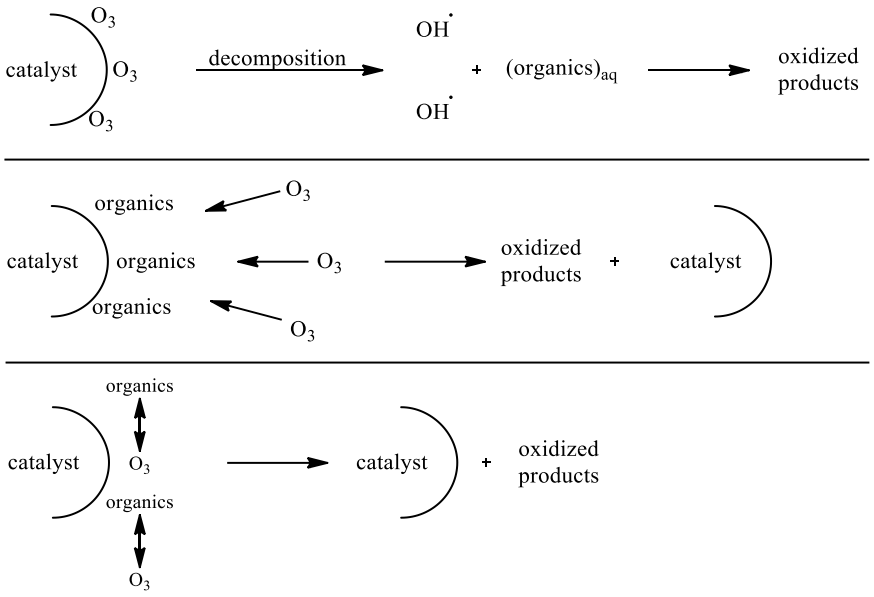

Figure 2. 1. Three possible mechanisms for heterogeneous catalysis[2]

2.1 Rate of Ozone Decomposition

Based on the structure of ozone, it could be seen as a dipole (i.e. an electrophile or nucleophile). It has a relatively short half-life which depends on pH, temperature, and impurities present in water.[1]

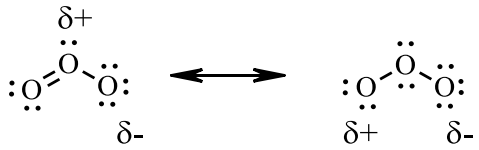

Figure 2. 2. Resonance structures of ozone

Sotelo *et* al.[15] proposed first order kinetics for ozone decomposition rate at a constant pH and temperature. Ozone decomposition rate in water follows the pseudo first-order kinetics (See Appendix A) depicted in equation 1:[15]

$$-rO_3 = -\frac{d[O_3]}{dt} = k_D[O_3] \quad (2.1)$$

In this equation, k_D is the ozone decomposition rate constant in s^{-1}. By rearranging and integrating equation 2.2 is obtained:

$$Ln\frac{[O_3]}{[O_3]_o} = -k_D t \qquad (2.2)$$

Rate constant is determined by plotting ln ($[O_3]/ [O_3]_0$) against the reaction time.

The pH of the media greatly influences the ozone decomposition. In pH<3 the decomposition of ozone is independent of the pH while in mildly basic and basic pHs (i.e. 7< pH< 10) the rate of ozone decomposition is greatly increased (half-life 15-25 min). This is believed to be due to hydroxyl anions (OH^-) serving as initiators for the ozone decomposition (*vide infra*).[1]

The most accepted model for decomposition of ozone was proposed by Staehelin, Hoigné, and Buhler (SHB) in 1984. According to this model ozone is converted to hydroxyl radicals through the following transformations:[16,17]

Initiation reaction

$O_3 + OH^- \longrightarrow HO_2^\bullet + O_2^{\bullet-}$ $\quad k=70\ M^{-1}s^{-1}$ (2.3)

Propagation reactions

$HO_2^\bullet \longrightarrow O_2^{\bullet-} + H^+$ $\quad k= 7.9 \times 10^5\ M^{-1}s^{-1}$ (2.4)

$O_2^{\bullet-} + H^+ \longrightarrow HO_2^\bullet$ $\quad k= 5 \times 10^{10}\ M^{-1}s^{-1}$ (2.5)

$O_2^{\bullet-} + O_3 \longrightarrow O_2 + O_3^{\bullet-}$ $\quad k= 1.6 \times 10^9\ M^{-1}s^{-1}$ (2.6)

$O_3^{\bullet-} + H^+ \longrightarrow HO_3^\bullet$ $\quad k= 5.2 \times 10^{10}\ M^{-1}s^{-1}$ (2.7)

$HO_3^\bullet \longrightarrow O_3^{\bullet-} + H^+$ $\quad k= 3.3 \times 10^2\ M^{-1}s^{-1}$ (2.8)

$HO_3^\bullet \longrightarrow {}^\bullet OH + O_2$ $\quad k= 1.1 \times 10^5\ M^{-1}s^{-1}$ (2.9)

${}^\bullet OH + O_3 \longrightarrow HO_4^\bullet$ $\quad k= 2 \times 10^9\ M^{-1}s^{-1}$ (2.10)

$HO_4^\bullet \longrightarrow HO_2^\bullet + O_2$ $\quad k= 2.8 \times 10^4\ M^{-1}s^{-1}$ (2.11)

Termination reactions

$HO_4^{\bullet} + HO_4^{\bullet} \longrightarrow H_2O_2^{\bullet} + 2O_3$ $k= 5 \times 10^9\, M^{-1}s^{-1}$ (2.12)

$HO_4^{\bullet} + HO_3^{\bullet} \longrightarrow H_2O_2^{\bullet} + O_2 + O_3$ $k= 5 \times 10^9\, M^{-1}s^{-1}$ (2.13)

Later, Tomiyashu *et* al.[17] suggested that hydrogen peroxide and hydroxyl radicals react together to form $HO_2^{\bullet}$ radicals which could also serve as initiators for ozone decomposition.

$\bullet OH + H_2O_2 \longrightarrow HO_2^{\bullet} + H_2O$ $k= 2.7 \times 10^7\, M^{-1}s^{-1}$ (2.14)

$\bullet OH + HO_2^{-} \longrightarrow HO_2^{\bullet} + OH^{-}$ $k= 7.5 \times 10^9\, M^{-1}s^{-1}$ (2.15)

2.2 The effect of Radical Scavengers

Radical scavengers are compounds that terminate the radical chain reaction of ozone decomposition by reacting with free hydroxyl radicals. *Tert*-butanol, carbonate ions, bicarbonate ions, dihydrogen phosphate ion, hydrogen phosphate ion and humic substances are commonly used as radical scavengers.

OH^-, UV, H_2O_2/HO_2^-, Fe^{2+}, and humic substances are initiators for a series of chain radical decomposition reactions of ozone to hydroxyl radicals. In the presence of such compounds, molecular ozone is transformed to superoxide ion $O_2^{-\bullet}$. However, in the presence of radical scavengers $OH^{\bullet}$ is trapped and removed from the chain reaction (equation 2.16 to equation 2.21)

During the termination step and in the presence of hydroxyl radical scavengers, OH radicals react with the scavenger and form semi-sable species. In the absence of such scavengers, hydroxyl radicals undergo the desired reaction with the emerging pollutant or intermediate (equation 2.15).

Generally, the reaction between hydroxyl radicals and organic molecules is slower in the presence of radical scavengers. As mentioned earlier, OH radicals are extremely reactive species

(rate constants beteen 10^5 and10^9 $M^{-1}s^{-1}$) and hence are considered as non-selective oxidants in radical chain reactions. The produced hydroxyl radicals react rapidly and non-selectively with a wide range of species in the reaction (including radical scavengers). Statistically, in the presence of radical scavengers, the interaction probability of the organic molecules and hydroxyl radicals is reduced and the rate is decreased.[17] This is the reason for the observed rate of decomposition difference in the presence of radical scavengers.

$$\bullet OH + O_3 \longrightarrow O_2 + HO_2^{\bullet} \qquad k = 3.0 \times 10^9\ M^{-1}s^{-1} \qquad (2.16)$$

$$\bullet OH + HCO_3^- \longrightarrow OH^- + HCO_3^{\bullet} \qquad k = 1.5 \times 10^7\ M^{-1}s^{-1} \qquad (2.17)$$

$$\bullet OH + CO_3^{2-} \longrightarrow OH^- + CO_3^{-\bullet} \qquad k = 4.2 \times 10^8\ M^{-1}s^{-1} \qquad (2.18)$$

$$\bullet OH + H_2PO_4^- \longrightarrow OH^- + H_2PO_4^{\bullet} \qquad k < 10^5\ M^{-1}s^{-1} \qquad (2.19)$$

$$\bullet OH + HPO_4^{2-} \longrightarrow OH^- + H_2PO_4^- \qquad k < 10^7\ M^{-1}s^{-1} \qquad (2.20)$$

$$\begin{cases} \bullet OH + (CH_3)_3C\text{-}OH \longrightarrow H_2O + (CH_3)_2\text{-}COH\text{-}CH_2\bullet & k = 5.0 \times 10^8\ M^{-1}s^{-1} \\ (CH_3)_2\text{-}COH\text{-}CH_2\bullet \xrightarrow{dimerization} (CH_3)_2\text{-}COH\text{-}CH_2\text{-}CH_2\text{-}COH(CH_3)_2 \end{cases} \qquad (2.21)$$

2.3 Catalytic Ozonation

Catalytic ozonation is used both in air and water purification processes. Catalytic ozonation is theoretically well-defined and has been exploited in industrial air purification.[18] However, catalytic ozonation is poorly understood and underutilized in water and wastewater treatment. Only a few countries have used aquatic catalytic ozonation for water treatment, namely, France and China.[19] Thus far the application of catalytic ozonation in water purification is only limited to laboratory scale systems. The reason for the limited application in industry could be related to lack of knowledge regarding the mechanism. This could be due to the presence of large quantities of water which complicates radical reactions.[2]

Catalytic ozonation processes have been shown to successfully eliminate many emerging pollutants from water and wastewater. These purification processes are generally more effective than non-catalytic ozonation reactions. This boost in the reactivity is believed to be due to facile formation of hydroxyl radicals which oxidize the emerging pollutants. For this reason catalytic ozonation is also termed "Advanced Oxidation Process" (AOP). Although the enhanced reactivity is believed to be directly linked to the presence of hydroxyl radicals, some reports have shown that catalytic ozonation processes could proceed without the incorporation of hydroxyl radicals.[2]

A better efficiency in catalytic ozonation processes means that in such reactions, the amounts of degraded emerging pollutants at the same pH and temperatures are higher than catalyst-free ozonation processes.[2]

Aquatic catalytic ozonation processes could also be classified in two types: homogeneous and heterogeneous catalytic ozonation processes.

2.3.1 Homogeneous Catalytic Ozonation

In homogeneous catalytic ozonation, the dissolved ions are responsible for the catalytic reactivity. Different transition metals such as Fe(II), Mn(II), Zn(II), Ni(II), Cd(II), Cu(II), Ag(I), Co(II), and Cr(III) are commonly used for homogeneous catalytic ozonation.[1]

Two types of mechanisms are possible for homogeneous catalytic ozonation: One, formation of hydroxyl radicals as a result of the reaction of molecular ozone and the catalyst (which serves as the initiator for the reaction). Two, formation of a complex between catalyst and the emerging pollutant followed by the oxidation of the emerging pollutant by molecular ozone.[1]

A number of studies have focused on the efficiency of catalytic ozonation processes and metal-free ozonation reactions for wastewater treatments. Based on TOC removal of the organics,

it was demonstrated that the amount of degradation of organics in the presence of metals such as Fe(II), Mn(II), Ni(II) and Co(II) sulphate are more than metal-free ozonation reactions.[20] Gracia *et* al.[21] studied the catalytic ozonation of humic substances in the presence of Mn(II), Fe(II), Fe(III), Cr(III), Ag(I), Cu(II), Zn(II), Co(II) and Cd(II) sulphate in water. Based on their findings, reactions of ozone with humic substances are very fast. However, high concentrations of ozone are required to obtain complete degradation of the emerging pollutant (conversion to CO_2). In such systems, low ozone concentrations lead to partial oxidation of organics into lighter by-products. Their findings suggest that the TOC removal of humics in the presence of Mn(II) or Ag(I) is about 60% and other transition metals have negligible effect on the degradation of organics. Additionally, it was shown that in all of the catalytic ozonation reactions carried out in the presence of transition metals, the amount of ozone required for a complete degradation of organics is less than metal-free ozonation reactions.[1] The effects of such transition metals in catalytic ozonation were explained by their ability to initiate the ozone decomposition chain reactions. Superoxide ions $O_2^{\bullet-}$ are formed as a result of the initiation reaction. This is followed by the electron transfer from $O_2^{\bullet-}$ to O_3 to form $O_3^{\bullet-}$ and finally generation of OH radicals[21] which subsequently leads to the oxidation of the emerging pollutants.

Piera *et* al.[22] have proposed a similar mechanism for the reaction of ozone and Fe(II). The proposal involves a transfer of oxygen from ozone to ferrous iron (equation 2.22 and equation 2.23)

$$Fe^{2+} + O_3 \rightarrow FeO^{2+} + O_2 \qquad (2.22)$$

$$FeO^{2+} + H_2O \rightarrow Fe^{3+} + HO^{\bullet} + OH^{-} \qquad (2.23)$$

In the mechanism suggested by Hart[23] for reaction of ozone with Fe(II), an electron transfer from Fe(II) to ozone generates Fe(III) and $O3^{-\bullet}$ which leads to formation of OH radicals.

$$Fe^{2+} + O_3 \rightarrow Fe^{3+} + O_3^{-\bullet} \quad (2.24)$$

$$O_3^{-\bullet} + H^+ \rightleftharpoons HO_3 \rightarrow OH^\bullet + O_2 \quad (2.25)$$

$$Fe^{2+} + OH^\bullet \rightarrow Fe^{3+} + OH^- \quad (2.26)$$

Pines and Reckhow[24] proposed a different mechanism for a homogeneous catalytic ozonation. Initially the metal and the oxalate anions form a complex on the surface of the catalyst. This reactive complex is then oxidized by molecular ozone (rather than hydroxyl radicals) (Figure 2.3)

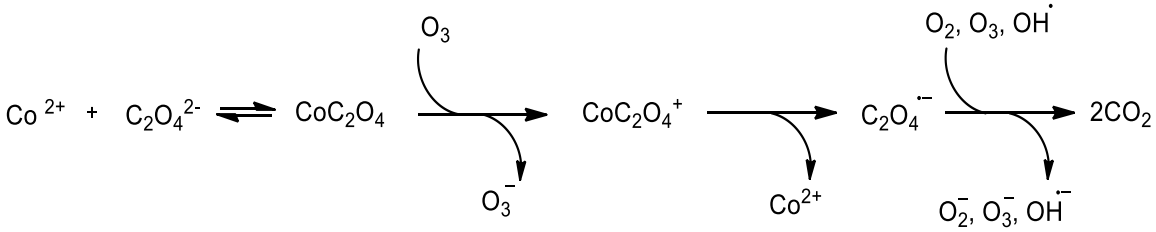

Figure 2. 3. Proposed mechanism for Co(III)-mediated ozonation of oxalic acid.[1]

Co(II)–oxalate complex is more reactive than free Co(II), this is related to partial donation of electron density from oxalate to Co(II). Molecular ozone could react with such reactive species to form Co(III)–complexes which would finally result in formation of Co(II) and oxalate radicals. These radicals could undergo another oxidation with species such as ozone, hydroxyl radicals and oxygen to complete the degradation process.[24]

2.3.2 Heterogeneous Catalytic Ozonation

Different types of heterogeneous catalysts in solid state such as metals, metal oxides and metals or metal oxides on metal oxide supports are used in heterogeneous catalytic ozonation.

Heterogeneous catalytic ozonation reactions could be carried out in bulk or on the surface of the catalysts. The efficiency of the catalytic ozonation process is greatly influenced by the surface properties of catalyst and the pH of the solution. It has been shown that pH levels influence the rate of ozone decomposition and catalysis on the surface's active sites.[1]

2.3.3 Surface Properties of Metal Oxides

In order to understand the mechanisms of heterogeneous catalytic ozonation, catalyst surface properties should be taken into consideration. For the purpose of catalyst selection one must consider catalyst's physical properties (such as surface area, density, pore volume, porosity, pore size distribution, mechanical strength, and purity), commercial availability and chemical properties such as chemical stability and especially the presence of active surface sites such as Lewis acid groups.

Acidity and basicity of catalysts are directly proportional to the number of hydroxyl groups on the surface of metal oxides.[1] Furthermore, it is genreally accepted that the number of hydroxyl radicals on the surface is directly proportional to the rate of ozone decomposition.[25] Surface properties of metals in hetereohenous catalysis are often characterized by the Point of Zero Charge (pH_{PZC}) of that catalyst. At pH_{PZC} the catalyst's electrical charge denstity is zero and hence the surface charge is neural. At $pH < pH_{PZC}$ is catalyst's surface is protonated and at $pH > pH_{PZC}$ the surficial OH groups are deprotonated:

$$pH < pH_{PZC} : MeOH + H+ \Leftrightarrow MeOH_2^+ \quad (2.27)$$

$pH > pH_{PZC}$: $MeOH + OH^- \Leftrightarrow MeO^- + H_2O$ (2.28)

Based on these equations, catalysts have higher activities and more free hydroxyl groups on the surface at their pH_{PZC}.[25]

2.4 General Mechanism of Ozone Decomposition on the Surface of Catalysts in Water

A number of mechanisms have been proposed in order to elucidate the ozone decomposition reactions in water, one of which consists of the initial chemisorption of the molecular ozone on the catalyst's surface followed by the generation of adsorbed oxygen-containing species such as ozonide, superoxide, and atomic oxygen. These species will then react with another molecule of ozone to continue the propagation of the ozone decomposition.[1,17] A study by Bulanin *et* al. has provided evidence of such mechanism by detecting the reactive oxygen-containing molecules using Fourier Transform Infra-Red (FT-IR) analysis (two peaks at 1034 and 1108 cm^{-1}).[26]

Lin *et* al.[27] has shown that the adsorption of ozone and decomposition ability of the catalyst are factors which influence the aquatic decomposition of molecular ozone. Furthermore, the authors suggest that the activity and desorption abilities of oxygen (which is the product of ozone decomposition) from the surface of the catalyst are other crucial factors involved in the decomposition of ozone.

Beltrán *et* al.[28] carried out a series of catalytic ozonation reactions in the presence of activated carbon as the catalyst. Although the reactions of activated carbon are not within the scope of this thesis, the proposed mechanism of such systems may be applicable to other catalytic ozonation systems. In the proposed mechanism, it is hypothesized that homogenous reactions take

place concurrently with heterogeneous reactions in aqueous media and reactions of this sort were taken into consideration in the mechanism of aquatic catalytic ozonation.

In addition, it is well-known that pH of the solution greatly influences the nature of ozone decomposition. As a result, different reaction paths are proposed at different pH of solution. This property of the reaction media also affects the formation of hydroxyl radicals that directly influence the decomposition of ozone. Beltrán *et al.*[28] has proposed the most accepted mechanism in heterogeneous ozone decomposition in water in two different pH ranges:

At pH 2–6:

$$O_3 + S \rightleftarrows O_3{-}S \quad (2.29)$$

$$O_3{-}S \rightleftarrows O{-}S + O_2 \quad (2.30)$$

$$O{-}S + O_3 \rightleftarrows 2O_2 + S \quad (2.31)$$

At pH > 6:

$$OH^- + S \rightleftarrows OH{-}S \quad (2.32)$$

$$O_3 + OH{-}S \rightleftarrows \bullet O_3{-}S + HO\bullet \quad (2.33)$$

$$\bullet O_3{-}S \rightleftarrows \bullet O - S + O_2 \quad (2.34)$$

$$O_3 + \bullet O - S \rightleftarrows O2^{-\bullet} + S + O_2 \quad (2.35)$$

In these reactions S is the catalyst surface (the initiator of ozone decomposition).

According to equation 2.5 under acidic and neutral conditions, the ozone decomposition does not produce hydroxyl radicals (possibly due to the facile reaction of hydroxyl radicals with proton ions) which results in lower ozone decomposition. Kinetic studies revealed that under acidic and neutral conditions, the kinetics is independent of the pH. In contrast under basic conditions, surface-bound ozonide ($O3^-$) and hydroxyl radicals are produced (equation 2.3 and

equation 2.23). Therefore it is suggested that the kinetics depends on the pH of the solution and ozone decomposition is facilitated at pH>7.[28]

2.5 Mechanisms of Reactions

The mechanisms of degradation of organic compounds in water involve either ozone (direct reaction) or free hydroxyl radicals (indirect reaction).[17]

$$O_3 + M \xrightarrow{k_{O_3}} P \tag{2.36}$$

$$\bullet OH + M \xrightarrow{k_{OH}} P \tag{2.37}$$

According to the above equations, both hydroxyl radicals and molecular ozone are prominent in ozonation of organics. However, in many cases one is more dominant than the other. The total rate of the removal of pollutant is described by the second order equation shown below:

$$-\frac{d[M]}{dt} = k_{O_3}[O_3][M] + k_{OH}[\bullet OH][M] \tag{2.38}$$

k_{O_3} is the rate constant of reaction of pollutant with ozone molecule in M^{-1} s^{-1}, and k_{OH} is the rate constant of reaction of pollutant with hydroxyl radical in M^{-1} s^{-1}.

2.6 Observed Reaction Rate

During most ozonation processes the emerging pollutant is only partially degraded to intermediates rather than a full degradation. For this reason the kinetic study of such reactions are often complicated and inaccurate. Despite this limitation, a few models have been proposed which assume a full degradation of the contaminants. Such models suggest that the removal of the contaminant using catalytic ozonation occur either in the bulk liquid phase or on the surface of the catalyst (both in homogeneous and heterogeneous reactions). The proposed kinetics is second order with respect to concentration of ozone and residual concentration of contaminant:

$$-\frac{d[M]}{dt} = k_{obs}[O_3][M] \tag{2.39}$$

By integration of the above equation with respect to time and concentration of contaminant, the rate of removal is described by equation 2.40:

$$\ln\left(\frac{[M]}{[M]_0}\right) = -k_{obs} \int [O_3]\, dt \quad (2.40)$$

According to this model the concentration of intermediates are omitted.

2.7 Contribution of Hydroxyl Radicals in Oxidation of Emerging Pollutants

Determination of the exact concentration of hydroxyl radicals is particularly challenging due to its low steady-state concentration (10^{-12} M). Elovitz and von Gunten have proposed a parameter based on the ratio of $C_{\bullet OH}$ to C_{O_3} which is defined as R_{CT}.[29]

Higher R_{CT} values correspond to higher conversion of molecular ozone to hydroxyl radicals. This parameter ranges between 10^{-6} and 10^{-9}.

$$R_{CT} = \frac{C_{\bullet OH}}{C_{O_3}} \quad (2.41)$$

By substituting $C_{\bullet OH}$ with $R_{CT}.C_{O_3}$ in equation 4 followed by integration, equation 2.42 is obtained:

$$ln\left(\frac{[M]}{[M]_0}\right) = -\left(k_{O_3} + k_{\bullet OH}.R_{CT}\right) \int [O_3] dt \quad (2.42)$$

By plotting $ln\left(\frac{[M]}{[M]_0}\right)$ against $\int [O_3] dt$, R_{CT} value can be calculated from the slope .

In order to find the fraction of pollutant degraded by hydroxyl radicals equation 2.43 is used:

$$f_{OH} = \frac{k_{OH}[\bullet OH][M]}{k_{O_3}[O_3][M] + k_{OH}[\bullet OH][M]} = \frac{k_{\bullet OH}.R_{CT}}{k_{O_3} + k_{\bullet OH}.R_{CT}} \quad (2.43)$$

By taking equations 2.40 and 2.42 into consideration, k_{obs} is described as:

$$k_{obs} = k_{O_3} + k_{\bullet OH}.R_{CT} \quad (2.44)$$

k_{O_3} and $k_{\bullet OH}$ and R_{CT} are constant parameters. Hence, the observed rate constant should be constant.

2.8 Metal oxides

A number of metal oxides have been shown to be suitable for catalytic ozonation processes. Both main group metal oxides such as Al_2O_3 and transition metal oxides such as MnO_2, TiO_2, and Fe_2O_3 have shown promising results in such processes. The efficiency of the catalysts is linked to the functional groups that cover the surface of these compounds. Some metal oxides have enhanced affinity towards less polar molecules owing to the hydrophobic nature of the functional groups present on the surface of the catalysts. Lewis acid functional groups are also among the functional groups present on the surface of some metal oxides.[2]

A variety of metal oxides bear hydroxyl groups on their surfaces which possess ion-exchange properties (main adsorption sites). The hydroxyl groups could be single (or isolated), such as silica-based metal oxides or bridged, such as hydroxyl groups found in alumina, titania, and zirconia. The ion-exchange characteristics of the surface of metal oxides depend mainly on the pH of the solution: such metal oxides exchange anions at pHs lower than the compound's pHpzc and cations at pH higher than their pHpzc.

The emerging pollutant's polarity is a crucial factor in surface adsorption; polar organic compounds such as organic ions adsorb more rapidly and efficiently on the surface of metal oxides. However, the extent of the adsorption depends on the pH of the solution. On the other hand, non-polar emerging pollutants do not adsorb on the surface of the catalyst unless the catalyst is covered with hydrophobic functional groups (such as in silica zeolites). As mentioned, Lewis acid functional groups are also present on the surface of many oxides. Despite the presence of these reactive sites, in aqueous interphase conditions these functional groups are inactive due to the dissociative reaction with water. In conditions where Lewis bases (such as phosphates, sulfate,

fluoride, and carboxylic acids) are present, metal oxides bearing such functional groups show promising surface affinities.[30]

A report by pines and Reckhow[31] in 2003 suggested that ozone degradation could not be carried out in the presence of metal oxides. Despite their claim, since then many studies have shown that in fact metal oxides do possess such catalytic properties. It is noteworthy that in such heterogeneous catalysis formation of a metal oxide-ozone surface complex is necessary for the observed reactivity.

A number of studies have described the mechanism of the aquatic ozone decomposition in heterogeneous systems. Al_2O_3, TiO_2, and MnO_2 are used as catalysts in such studies.[1]

Titania (TiO_2) was successfully used for removal of oxalic acid from water samples under acidic conditions.[28] Furthermore, metal oxides supported on silica gel, clay, Al_2O_3 and TiO_2 have been shown to be efficient catalysts for removal of organic contaminants from aqueous samples.[1] The efficiency of Fe (III) supported on alumina for removal of phenol from water samples was explored in catalytic ozonation processes by Al-Hayek *et al.*[32] Cooper and Burch[33] have examined the effects of Al_2O_3, TiO_2 supported on Al_2O_3 and Fe_2O_3 supported on Al_2O_3 in the catalytic removal of oxalic acid, chloroethanol, and chlorophenol from aqueous samples. In all cases the efficiency of such catalysts was reported as outstanding and TOC results showed a significant increase in rate of removal of the contaminants.

2.8.1 Al_2O_3

Alumina (Al_2O_3) is extensively used in catalytic ozonation for water and wastewater treatment purposes. Due to its importance in industry, the study of the structure and the chemistry associated with alumina has been a major focus throughout the literature. In order to obtain a comprehensive understanding of such catalytic ozonation processes, both physical and chemical

properties need to be taken into consideration. Other characterization of the reaction media such as pH of the solution and the nature of the contaminant also need to be considered in the study of such processes.[34]

2.8.1.1 Classification of Alumina

According to the classification by Harber in 1925, alumina is categorized into two groups: α- alumina and γ-alumina. An alternative classification of these compounds was proposed later by Stumpf *et* al. in which alumina is classified in order of $\alpha, \gamma, \delta, \kappa, \eta, i$ and χ-Al_2O_3.[34] These types of alumina differ in their crystal structures and lattice properties. Generally, α-alumina is less porous than γ-alumina and therefore its application as heterogeneous catalyst is limited.[35,36]

From a catalyst preparation standpoint, each type of alumina could be obtained by varying the temperature of heating and a particular source of alumina. Equations 2.46 to 2.49 outline examples of such conditions:[34]

$$\text{gibbsite } (Al(OH)_3) \xrightarrow{250℃} \chi\text{-}Al_2O_3 \xrightarrow{900℃} \kappa\text{-}Al_2O_3 \xrightarrow{1200℃} \alpha\text{-}Al_2O_3 \quad (2.45)$$

$$\text{bayerite } (Al(OH)_3) \xrightarrow{230℃} \eta\text{-}Al_2O_3 \xrightarrow{850℃} \Theta\text{-}Al_2O_3 \xrightarrow{1200℃} \alpha\text{-}Al_2O_3 \quad (2.46)$$

$$\text{boehmite } (AlOOH) \xrightarrow{450℃} \gamma\text{-}Al_2O_3 \xrightarrow{600℃} \delta\text{-}Al_2O_3 \xrightarrow{1050℃} \Theta\text{-}Al_2O_3 \xrightarrow{1200℃} \alpha\text{-}Al_2O_3 \quad (2.47)$$

$$\text{diaspore} \xrightarrow{450℃} \alpha\text{-}Al_2O_3 \quad (2.48)$$

Based on the classification proposed by Münster in 1957 (and further modifications by Lippens in 1961) alumina are classified in to two groups based on the preparation temperature of aluminum hydroxide: The γ–group, which refers to alumina that is prepared through the

dehydration of aluminum hydroxide at temperatures lower than 600 ℃ and δ-groups which refer to the class of alumina that are obtained similarly but at higher temperatures (900 ℃ – 1000 ℃).[34]

The surface properties of alumina are strongly influenced by the pH of the solution. At pH lower than $pH_{PZC,}$ the surface is positively charged and in contrast, at higher pHs than the $pH_{PZC,}$ negative charges are predominant on the surface.[37] (Fig 2.4)

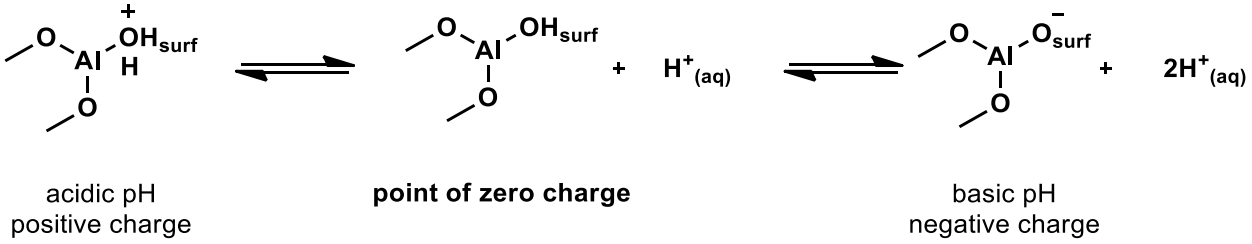

Figure 2. 4. Al_2O_3 at different pHs

This is particularly important in catalytic ozonation due to the fact that ions that are oppositely charged are attracted to the surface of the catalyst.

In catalytic ozonation processes using alumina as the catalyst, it is absolutely necessary to control the pH. pH measurements should be rigorous when working with commercial samples of alumina since these catalysts are industrially prepared by alkali precipitation from aluminum salts. These alkali contaminants could potentially result in the increase in the pH of the aqueous solution and consequently affect the efficiency of catalytic ozonation.[2]

The extent of adsorption of the organic matter on the surface of alumina has been a point of discussion in the field. Findings by Lin *et al*[38] and Álvarez *et al.*[39] suggest that adsorption on the catalyst surface is an absolute necessity for the catalytic ozonation while Ernst *et al.*[40] and Beltrán *et al.*[41] believe that the adsorbed organic molecules hinder the catalytic reactivity. The later studies suggest that ozone should be adsorbed on the surface of alumina prior to the organic matter.

In many studies, detailed mechanisms are often neglected and the outcomes of the reactions are the main focus of such reports. Nevertheless, most studies suggest that hydroxyl radicals are the main reactive species in the catalytic ozonation process. Despite the vast number of reports regarding the involvement of hydroxyl radicals in the catalytic degradation, recent findings suggest that the generation of hydroxyl radicals are not an absolute necessity for the catalytic reactivity.

The mechanism of catalytic ozonation of coumarin using alumina at its pH_{PZC} is hypothesized to involve hydroxyl radicals.[42] In order to probe the mechanism of the reaction, amplex red and NBD-Cl were used for identification of hydroxyl radicals, hydrogen peroxide and superoxide ion radicals.[43] Furthermore, TBA and phosphate experiments confirmed the role of hydroxyl radicals in the catalytic ozonation reactions.

Figure 2.5 outlines the reported alumina-mediated ozonation mechanism. Initially, aqueous ozone interacts with the hydroxyl groups on the surface of the alumina catalysts. This adsorption is known to assist the decomposition of ozone to superoxide ion radicals (identified using NBD-Cl probe) and production of oxygen (O_2). It has been shown that O_2H radicals are also produced as the result of ozone decomposition.[44] The reaction between another molecule of ozone and superoxide or $O_2H^{\bullet}$ forms ozonide ($O_3^{\bullet}$) or $O_3H^{\bullet}$ radicals.[43]

$O_3H^{\bullet}$ undergo a rapid reduction to yield hydroxyl radicals. The pH of the solution is particularly influential at this step of the mechanism. At pHs above 7, the generation of hydroxyl radicals is a result of reaction between $O_3^{\bullet -}$ and H_2O.[44] The produced hydroxyl radicals could undergo a dimerization reaction to form hydrogen peroxide (H_2O_2).[45] The concentration of hydroxyl radicals and the pH of the solution directly influence the stability and persistency of H_2O_2. Furthermore, the formation of hydrogen peroxide (H_2O_2) was confirmed with amplex red and TBA tests.

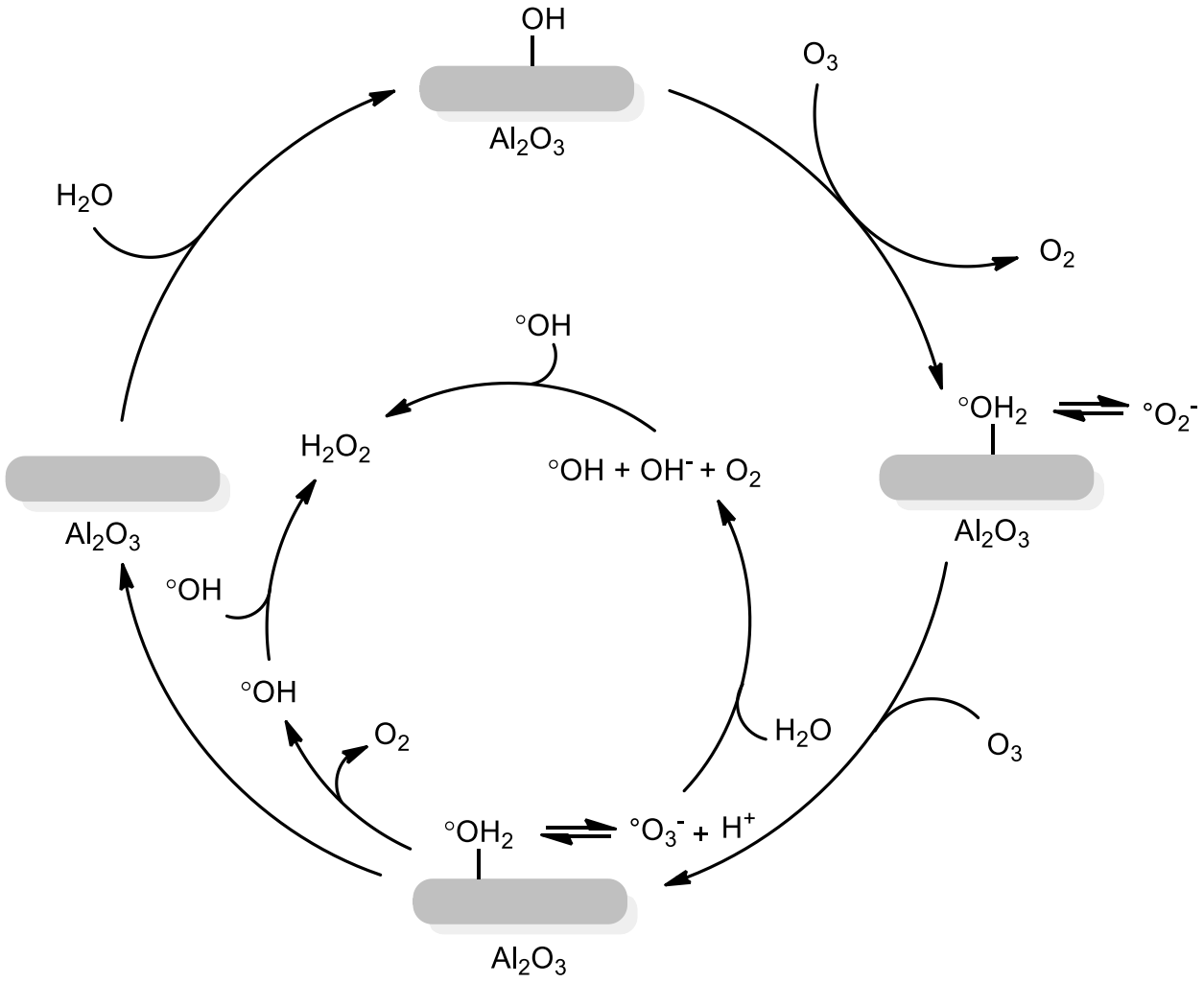

Figure 2. 5. The reported mechanism for alumina-mediated catalytic ozonation[43]

2.8.2 MnO_2

Dry MnO_2 is a well-known catalyst for the degradation of ozone to from oxygen and atomic oxygen species[2]. Many studies have reported the loss of catalytic reactivity even when traces of moisture are present. In contrast, some studies have claimed that MnO_2 is catalytically active in aqueous solutions.

Ma and Graham suggest that in order to achieve certain levels of reactivity, manganese dioxide should be prepared *in-situ*. Their findings suggest that commercial MnO_2 catalysts are ineffective for their purpose.[46] A study by Tong *et* al. suggests that the even though MnO_2 might be reactive towards the degradation of ozone, but this does not necessarily guarantee its effectiveness towards degradation of organic molecules.[47] In 1996 Andreozzi *et al.*[46] proposed that the reaction between manganese oxide and oxalic acid in a catalytic ozonation reaction possibly goes through a manganese-oxalic acid complex. Later in 2011, Orge *et al.*[48] validated such hypothesis. The later study suggests that the ozonation proceeds through the direct degradation/oxidation of adsorbed organic molecules either through molecular ozone or surface oxygenated radicals.

2.8.3 ZnO

Zinc oxide (ZnO) is a non-toxic, non-water soluble and relatively inexpensive transition metal oxide with widespread application in aqueous catalytic ozonation of various emerging pollutants.[49]

The catalytic ozonation for removal of dichloroacetic acid (DCAA) from aqueous samples were carried out by Zhai *et* al. in a series of batch experiments.[50] The mechanism of such catalytic system is proposed to involve adsorption of ozone onto the surface of the catalyst followed by generation of hydroxyl radicals. Consequently, DCAA reacts with the radicals on the surface of the catalyst and is degraded.

Jung and Choi have shown that zinc oxide is an efficient catalyst for removal of para-chlorobenzoic acid (*p*CBA) from aqueous solutions.[51] Their findings pinpoint the significance of nano-ZnO catalysts in degradation of ozone and in the removal of *p*CBA. This was judged by the

fact that R_{ct} values increase with the concentration of nano-ZnO (R_{ct} values represent the ratio of hydroxyl radicals (•OH) to ozone (O_3).

The suggested mechanism of catalytic removal of *p*CBA is outlined in equations 2.50 to 2.58. Initially ozone is adsorbed on the surface of the nano-Zno catalyst which leads to decomposition of ozone to ZnO radicals and HO_3 radicals. These species undergo a series of radical chain reactions to form hydroxyl radicals. The adsorption of *p*CBA on the surface of the catalyst followed by reaction with hydroxyl radicals present either on surface or the bulk of the solution leads to the degradation of the contaminants.[51]

$$\equiv ZnOH + O_3 \leftrightarrow \equiv ZnOH(O_3)_s \quad (2.49)$$

$$\equiv ZnOH(O_3)_s \leftrightarrow \equiv ZnO\bullet + \bullet HO_3 \quad (2.50)$$

$$\equiv ZnO\bullet + H_2O \rightarrow \equiv ZnOH + \bullet OH \quad (2.51)$$

$$\bullet HO_3 \rightarrow H^+ + \bullet O_3^- \quad (2.52)$$

$$\bullet HO_3 \rightarrow \bullet OH + O_2 \quad (2.53)$$

$$\bullet O_3^- + H_2O \rightarrow \bullet OH + O_2 + OH^- \quad (2.54)$$

$$\equiv ZnOH + O_3 \rightarrow \bullet OH \quad (2.55)$$

$$\equiv ZnOH_2^+ + R{-}COOH \leftrightarrow ZnOH_2^+ {-} HOOC{-} R \quad (2.56)$$

$$\equiv ZnOH_2^+ {-} HOOC{-} R + \bullet OH \rightarrow \text{Products} \quad (2.57)$$

Dong *et* al. carried out the aquatic catalytic ozonation of phenol using nano-ZnO (200 nm average particle size) as the catalyst. The efficiency of degradation was shown to increase by

23.7% by using the nano-sized catalyst. However, their report did not outline a mechanism for the transformation.[52]

In 2005, Huang *et* al.[53] reported the catalytic removal of 2,4,6-trichlorophenol (TCP) from aqueous samples using ZnO catalysts. This work highlights the effects of using various nano, sub-micro, and micro zinc oxides in the catalytic ozonation process. It was shown that ZnO dramatically increases the efficiency of the removal of the contaminant within 30 minutes (from 75% removal in absence of the catalyst to 99.8% in the presence of ZnO). Hydroxyl radicals were shown to be responsible for the enhancement of reactivity and the kinetics were proposed to be independent of concentration of ozone but strongly dependent on the dose of the catalyst and the size of catalysts. In addition control experiments suggest that the rates of removal of TCP were in the order of nanometer > submicrometer > micrometer. In order to investigate whether pore diffusion or surface reaction is responsible for the reactivity, the rate of TCP removal was examined by evaluating the efficiency of each particle size of ZnO. Based on calculations, it was postulated that compared to pore diffusion, surface reaction is more important in removal of TCP from water. It is believed that the lack of experimental data has thwarted the mechanistic studies on catalytic ozonation of zinc oxides. Despite this limitation, two plausible mechanisms are proposed for the catalytic ozonation of TCP in the presence of ZnO catalysts; in the first proposal the catalyst behaves exclusively as adsorbent and ozone and hydroxyl radicals act as oxidants. The contaminants rapidly adsorb on the surface of the catalysts to form chelation products with the surface. The surface complex is then oxidized with ozone or hydroxyl radicals present in the solution. The oxidation by-products are desorbed into the solution that will be homogenously degraded with the excess ozone and hydroxyl radicals. Despite the logical explanation, the authors believe that this scenario could only exist for catalysts with low adsorbabilities such as ruthenium

and copper. The second proposal consists of the simultaneous adsorption of ozone and contaminant on the surface of the catalyst. Thereafter, ozone undergoes a series of chain radical reactions to form hydroxyl radicals[46]. Ozone or hydroxyl radicals present in the bulk of the solution will then degrade/oxidize the adsorbed organic contaminants. Generation of high concentration of hydroxyl radicals through the solid-liquid interface is the main basis of such proposal.

2.8.4 Metals and Metal Oxides Supported on Metal Oxides

Metals and metal oxides supported on metal oxides (or carbon) are among the most important catalysts for decomposition of ozone to hydroxyl radicals. Even though the exact mechanism of such catalytic processes are not clear, Legube and Karpel Vel Leitner[20] propose two mechanisms for such reactions. In the first scenario, the contaminant is adsorbed on the surface of the catalyst and then oxidizes by hydroxyl radicals or molecular ozone. Finally the oxidized products desorb into the solution. In the second scenario, molecular ozone is decomposed to hydroxyl radicals on the surface of the catalysts. This is followed by adsorption of the contaminant on the surface followed by the oxidation of the later through an electron-transfer reaction. Finally the products are desorbed to the solution.

In 2005, Fonatnier *et* al.[19] reported one of the most accepted mechanism of catalytic ozonation of metals supported on inorganic compounds. The suggested mechanism involves the formation of a highly reactive metal-ozone complex on the surface of the catalyst. This complex eventually reacts with/degrades the organic molecule at the solid-liquid interface. It is interesting that the generation of hydroxyl radicals were not observed in this study.

Chapter 3

3. Experimental

3.1 Materials

Atrazine (ATZ) and γ-alumina were purchased from Alfa Aesar Co. and nano-ZnO powders were purchased from US Research Nanomaterials Inc. The average size of nano-ZnO powders were: 80-200 nm, 35-45 nm and 18 nm. All commercially available material were used without further purification.

ATZ has approximately 30 mg/L solubility in water at pH=7.5, and the pKa value of 1.64 at 20°C. A stock solution of Atrazine was prepared with the concentration of 30 mg/L in millipore water (Millipore Milli-Q water) (18 MΩ cm^{-1}). All ozonation reactions were carried out at three different pH levels (3, 5, and 7) by using buffer solutions of hydrochloric acid/potassium chloride or phosphate buffers. The ionic strength of buffers were maintained at (0.10 M) for all experiments.

Three metal oxides (ZnO, Mn_2O_3 and Fe_2O_3) loaded on γ-Alumina and γ-Alumina (metal oxide-free) were used as catalysts (for preparation procedures see Section 3.5. All ozonation reactions and adsorption tests were carried out at pH=7 by using phosphate buffer. The ionic strength of buffers were maintained at (0.1 M) for all the experiments.

3.2 Experimental Procedures

3.2.1 Adsorption of Atrazine

Atrazine adsorption tests were carried out using different particle sizes of nano-ZnO catalysts, metals loaded on γ-alumina, and metal-free γ-alumina. 1000 mL of atrazine solution (10 ppm) was treated with each nano-ZnO catalyst at room temperature (23.5±0.5°C), metals loaded on γ-alumina, and metal-free γ-alumina. The suspension was stirred with a constant speed of 700 rpm using a magnetic stirrer.

All experiments included ATZ with concentration of 10 ppm (4.63×10^{-5} M) while different amounts of nano-ZnO catalysts (1, 2, 4 and 8 grams) or 8 grams of metals loaded on γ-alumina or 8 grams of metal-free γ-alumina were added to the reactor. The reaction times were 30 minutes. Samples were withdrawn from the reactor at different intervals (2, 5, 10, 15, 20, 25 and 30 min), filtered through a 0.22 μm cellulose nitrate membrane filter, and transferred to 25 mL TOC vials. In order to determine the residual concentration of ATZ, the samples were analyzed by TOC and HPLC analyses.

Atrazine adsorption on nano-ZnO catalysts were negligible. Furthermore, adsorption of atrazine on metals loaded on γ-alumina and metal-free γ-alumina were low (Table 3.1.).

Table 3. 1. Adsorption of atrazine on γ-alumina-supported metal oxides

Atrazine adsorption on ZnO/γ-Alumina	Atrazine adsorption on Mn_2O_3/γ-Alumina	Atrazine adsorption on Fe_2O_3/γ-Alumina	Atrazine adsorption on γ-Alumina
13%	7%	4%	4%

In order to determine the kinetics of ATZ adsorption on the surfaces of catalysts, a second-order kinetics with respect to the concentration of atrazine and catalyst dose of nano-ZnO is

proposed. The kinetics is first-order with respect to the concentration of pollutant or the catalytic loading.

$$-\frac{d[M]}{dt} = k_a[M]W \quad (3.1)$$

In this equation, k_a is the adsorption rate constant in L g^{-1} s^{-1}, and W is the mass of adsorbent per litre of solution in g L^{-1} and M is atrazine concentration.[54]

3.2.2 Ozone Decomposition

Ozonation was carried out in a 1 L batch reactor. Ozone decomposition experiments were carried out in three different pH levels (3, 5, and 7). The pH was adjusted using hydrochloric acid/potassium chloride solutions or phosphate buffers. Ozone was generated using a laboratory ozone generator (OZV-8, Ozone Solutions) with corona discharge in ultra-high pure oxygen (grade = 4.3) and continuous supply of ozone. Ozone was bubbled into the liquid phase until the ozone concentration reached 8.33×10^{-5} M (4 mg L^{-1}). Ozone decomposition experiments were performed either in the presence of catalyst or catalyst-free. The experimental setup is shown in Figure 3.1.

The reactor was charged with 1 L of Millipore water at adjusted pH (3, 5, and 7) for each experiment. The suspension was stirred with a constant speed of 700 rpm with a magnetic stirrer at room temperature (23.5±0.5°C). For ozone decomposition experiments carried out in the presence of catalyst, when ozone concentration reached 8.33×10^{-5} M (4 mg L^{-1}), the oxygen cylinder valve was shut off and the ozone generator was turned off immediately. Subsequently, catalyst was added, in one portion and the reactor was immediately sealed using a glass stopper. For catalyst-free ozone decomposition experiments, procedures were identical to the above, only differing in the addition of catalyst. The Ozone concentration in aqueous phase was monitored by the electrochemical (amperometric) method over 30 minutes.

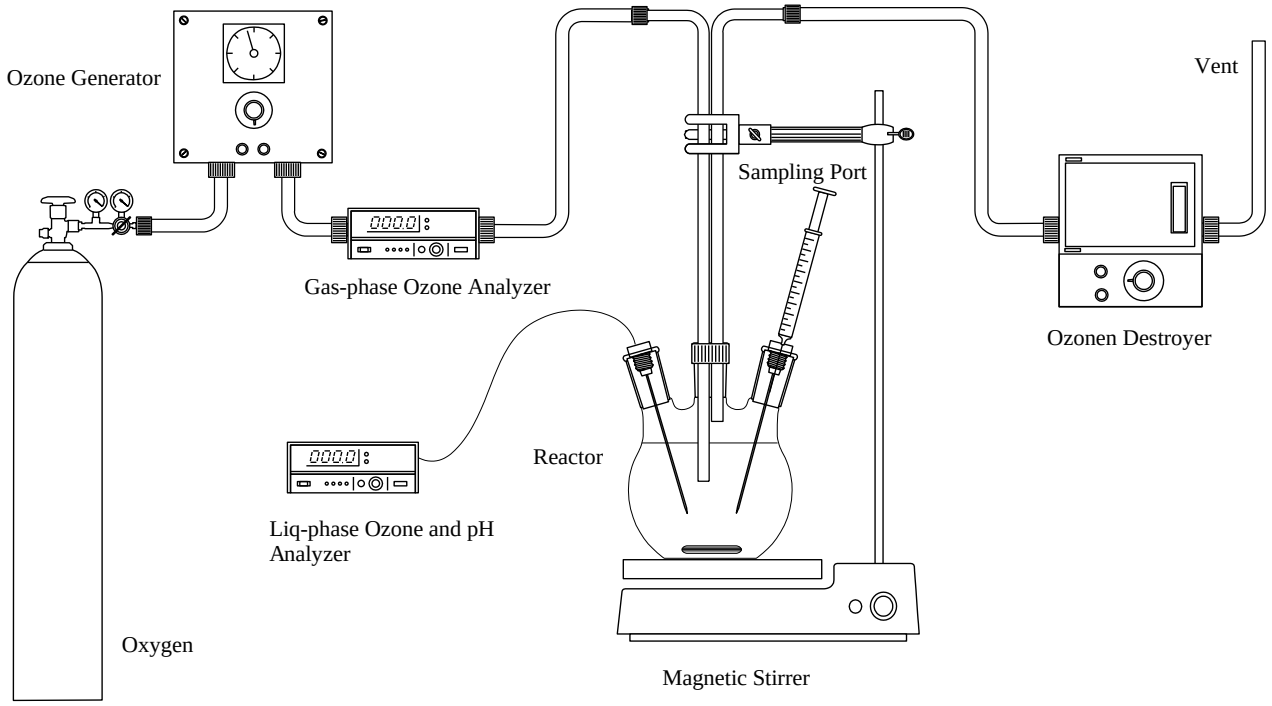

Figure 3. 1. Experimental setup for ozonation tests[55]

To investigate the effects of buffer solutions, ozone decomposition experiments were carried out in the presence buffer solutions (controlled pH) and without buffers at different pH levels. Additionally, the effects of radical scavenger was evaluated by performing the ozonation reaction in the presence of *tert*-butyl alcohol (TBA) at 1×10^{-4} M concentration. Finally the desired amount of catalyst was determined by using different doses of catalysts in the ozonation reaction.

3.2.3 Metal-Free Ozonation of Atrazine

Ozonation experiments were carried out in a 1 L batch mode reactor at room temperature (23.5±0.5°C) and 700 rpm mixing speed (Figure 3.1). The liquid and gas ozone concentration, pH,

and temperature were monitored every two seconds using a data acquisition system (cDAQ-9172, National Instruments Corp.).

The reactor was charged with 666±1 mL of buffer pH=7 (phosphate buffer). Ozone was continuously bubbled into the liquid phase until the ozone concentration reached 8.33×10^{-5} M (4 mg L^{-1}). The oxygen cylinder valve was shut off and the ozone generator was turned off immediately. Subsequently, catalyst was added in one portion to the reactor. Then 333 ±1 mL of atrazine (stock solution 30 mg/L) was added to this suspension and the rector was immediately sealed using a glass stopper. The reaction times were 30 minutes and samples were withdrawn from the reactor at different intervals (2, 5, 10, 15, 20, 25 and 30 min) and transferred to 25 mL TOC vials containing 200 µl of sodium thiosulphate (32 mM) to quench the residual ozone and stop the oxidation reaction. The residual concentration of ATZ and total organic carbon were determined by High Performance Liquid Chromatography (HPLC) and Total Organic Carbon (TOC) analyses.

3.3 Catalyst Characterization

3.3.1 Nitrogen Gas Adsorption

Nitrogen adsorption was used to characterize the nano-ZnO catalysts. Physisopriton (physical adsorption) of N_2 at 77 K was measured using an ASAP 2000 apparatus (Micromeritics Instrument Corp). Adsorption isotherms were constructed using the amount of adsorbed gas (cm^3/g) versus relative pressure (p/p_0). Similarly, nitrogen desorption (cm^3/g) was plotted versus the relative pressure (cm^3/g) (Figure 3.2, 3.3, and 3.4). Specific surface area is measured by physisorption that reflects weak van der Waals forces between the adsorbate and the adsorbent surface.[56] Results clearly suggest a type (III) isotherm according to classification proposed by Brunauer, Emmett and Teller (BET).

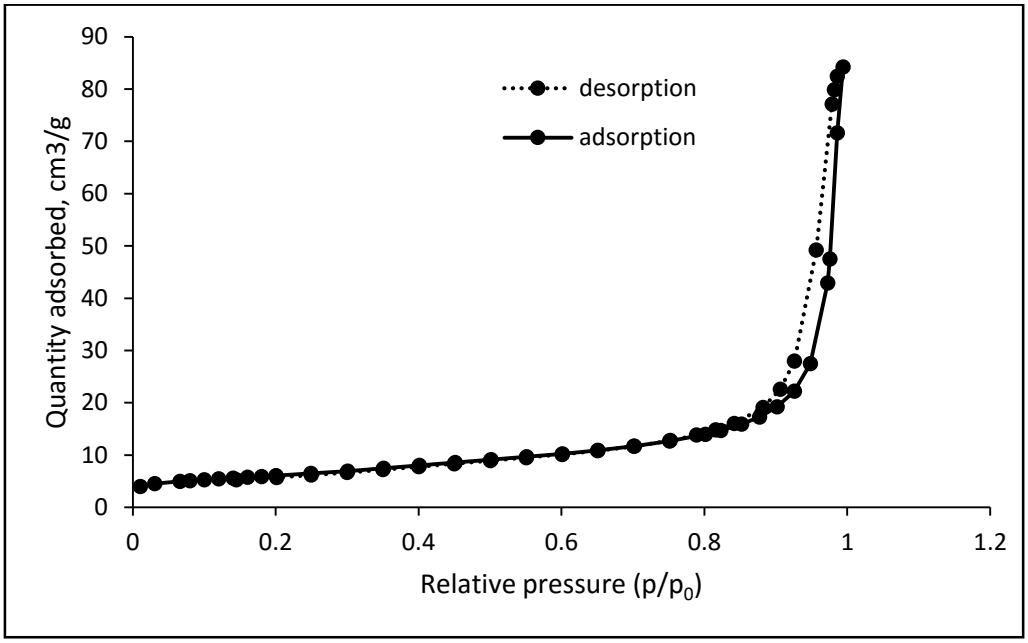

Figure 3. 2. Nitrogen adsorption-desorption isotherm for nano-ZnO (18 nm)

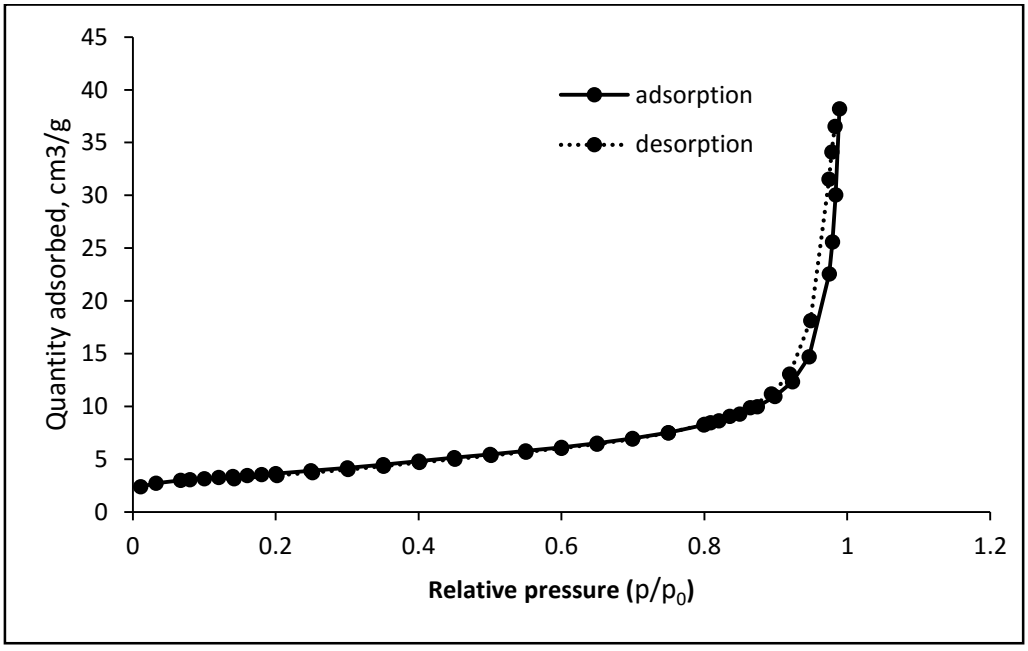

Figure 3. 3. Nitrogen adsorption-desorption isotherm for nano-ZnO (35-45 nm)

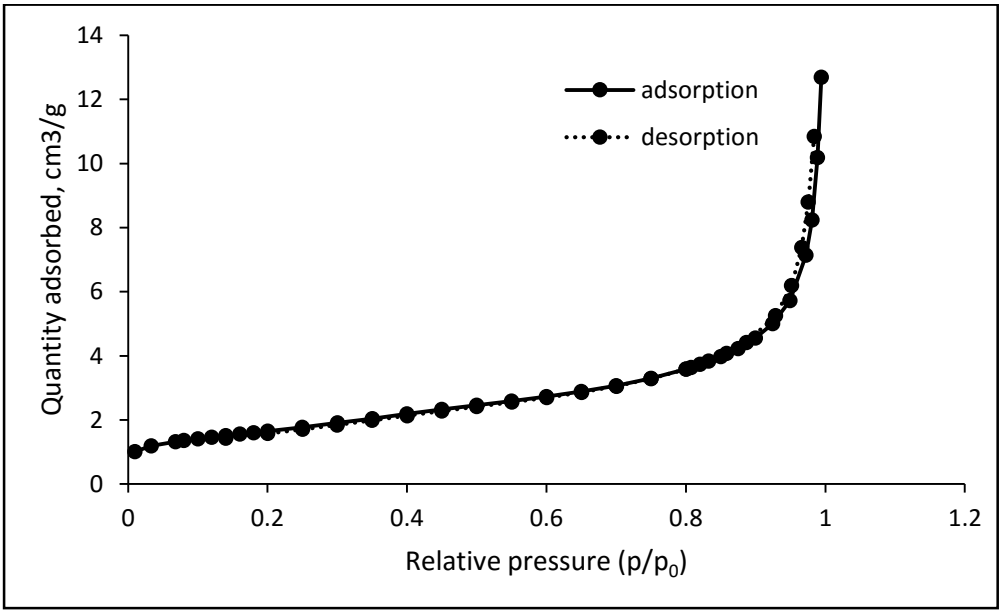

Figure 3. 4. Nitrogen adsorption-desorption isotherm for nano-ZnO (80-200 nm)

Equation (3.2) is used to quantify the equilibrium amounts of adsorbed nitrogen (n^0) on the catalyst surface at the external pressure (P) and constant temperature (T) at isothermal conditions:[57]

$$n^{0} = \int (\frac{P}{P^{0}})_{\text{T, gas, solid}} \quad (3.2)$$

Figures (3.2, 3.3., and 3.4) show that the uptake of nitrogen remains low and almost constant up to $p/p^o = 0.9$. However at $p/p^o > 0.9$, an increase in the adsorption of nitrogen takes place which is believed to be due to adsorption on the catalyst's grain boundaries.[57]

The nitrogen adsorption experiments are also used to determine average pore sizes. Based on the results, the structure of nano-ZnO catalysts are rigid with mesoporouse.[58,59]

The BET surface area for three sizes of the nano-ZnO catalysts indicate the difference in the sizes (Table 3.2)

Table 3. 2. Parameters obtained from gas adsorption with nitrogen for nano-ZnO catalysts

Catalysts	BET Surface Area (m^2/g)	Average Pore Volume ($cm^3/g)\times10^2$	Average pore Size (nm)
Nano-ZnO (18 nm)	21	6.6	12
Nano-ZnO (35-45 nm)	13	3.4	11
Nano-ZnO (80-200 nm)	6	1.1	7

3.3.2 Point of Zero Charge

Point of zero charge (PZC) measurement is a common method to quantify the adsorption on surface of catalysts. At the PZC of catalysts, the electrical charge density is equal to zero. Therefore, in aqueous solutions with pH lower than pH_{PZC} , the number of protons transferred from water to the surface of catalyst are more than hydroxide ions. This results in a build-up of positive charge and adsorption of anions on the surface. In contrast, in solutions with pH higher than pH_{PZC}, cations are adsorbed on the surface of the catalyst.

PZC measurements were carried out using nano-ZnO (80-200 nm) and γ-alumina by mass titration according to the method proposed by Noh and Schwarz.[60] For nano-ZnO (80-200 nm), three standard solutions with different pH levels (7, 9, and 11), and for γ-alumina, three standard solutions with different pH levels (5, 8, and 11) were prepared. The pH of the solution was adjusted using NaOH and/or HCl. pH meter was calibrated with standard buffers at different pH levels.

Different amounts of catalysts (1 to 10 weight percent) were added to 30 mL test tubes containing the standard solutions. The test tubes were capped and sealed immediately with Parafilm®[61] and placed on an agitator (shaker) for 24 hours at room temperature. pH meter was re-calibrated with standard solutions and the pH of each sample was recorded.

pH_{PZC} results are shown in Figure 3.5. The pH_{PZC} of nano-ZnO was within the range of 7.6-8.1.

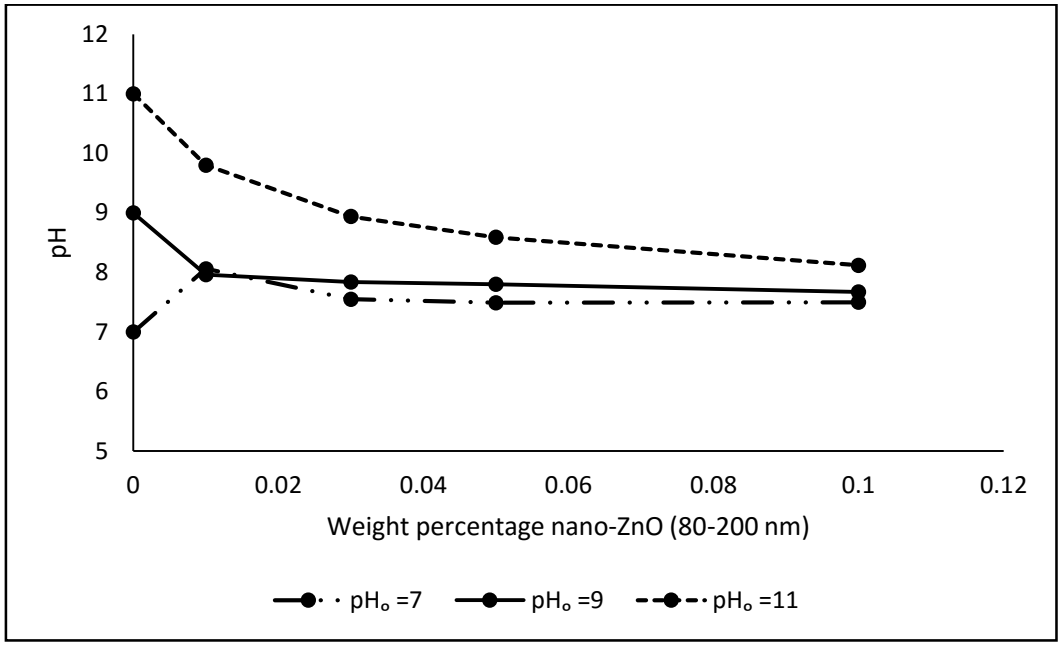

Figure 3. 5. Determination of point of zero charge for nano-ZnO

Under the conditions described above, the pH_{PZC} of γ-alumina is equal to 7.4 (Figure 3.6.).

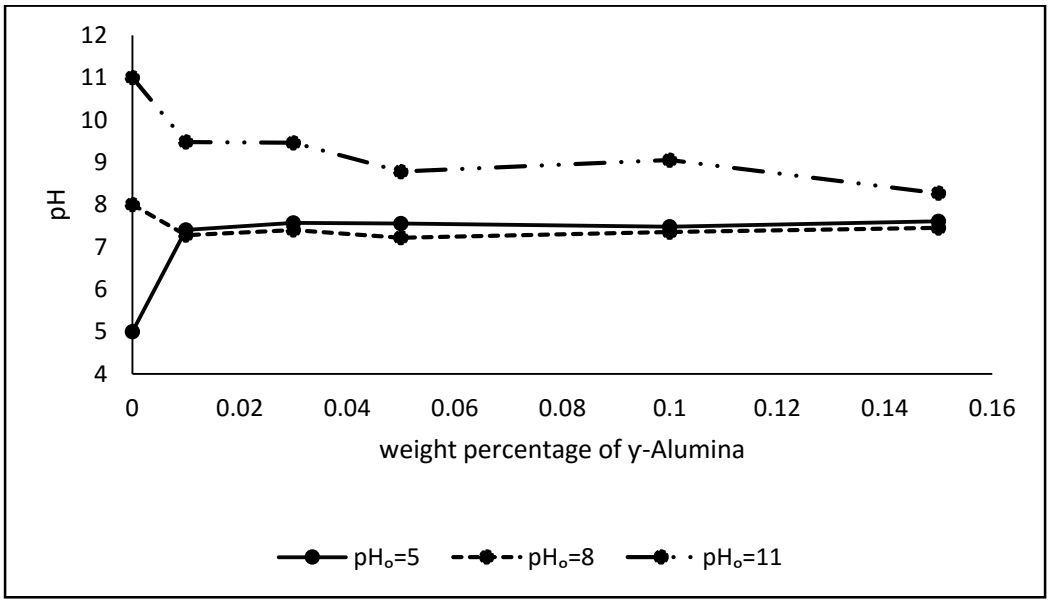

Figure 3. 6. Determination of point of zero charge for γ-alumina

3.4 Analytical Methods

Several parameters such as pH, temperature (liquid phase), liquid ozone concentration, and gas ozone content were monitored during the experiment. The residual atrazine concentration and total organic carbon were measured by HPLC and TOC in order to quantify the extent of mineralization of ATZ and identification of reaction products.

TOC is measured using a TOC-VCSH SHIMADZU automatic TOC analyzer equipped with ASI-V auto-sampler. HPLC measurements were carried out using an Agilent 1100 HPLC system (Agilent Technologies Inc.) equipped with a Luna 5u C18 (2) 100 A (250×4.60mm, 5 µm) column from Phenomenex and diode array detector at 275 nm. Acetonitrile/water (60:40, v/v) was used as the mobile phase at a constant flow rate of 1 $mL.min^{-1}$ and injection volume of 100 µl, with a retention time of approximately 15 min. Standard calibration curves were constructed by injection of standard solutions containing accurate aquatic concentrations of ATZ.

pH was measured by using a single junction pH combination electrode (R-27012-06, Cole-Parmer Inc.). Temperature and liquid ozone contents were measured by an ampere-metric ozone micro-sensor (MS-08, AMT Analysenmesstechnik, GmbH). The Indigo method was used to calibrate the ozone measurement.[54]

The liquid and gas ozone concentration, pH, and temperature were monitored every two seconds using a data acquisition system (cDAQ-9172, National Instruments Corp.).

3.5 Catalyst Preparation

Catalyst preparation was performed by dry impregnation with 10% of metal loading on *γ*-Alumina (Alfa Aesar, S_{BET} = 220 m^2/g).

Powder pellets of *γ*-alumina (Surface area = 220 m^2/g and total pore volume = 0.62 mL/g) were crushed and sieved (500 µm diameter). The amount of doped metals were 10%. Manganese (II) nitrate tetrahydrate (Sigma–Aldrich, 97%) was used as the precursor for Mn_2O_3/*γ*-alumina catalyst. Zinc (II) nitrate hexahydrate (Sigma–Aldrich, 98%) was used for preparation of ZnO/*γ*-Al_2O_3 catalyst, and $Fe(NO_3)_3.9H_2O$ (Sigma–Aldrich, 98%) was used as the precursor for Fe_2O_3/ *γ*-alumina. *γ*-alumina was evenly placed at the bottom of a 500 mL beaker. The corresponding precursor solution was added to the solids using a micropipette. Then the mixture was stirred thoroughly using a spatula and placed in the oven. The drying time depends on the nature of the substrate. The mixture was transferred to a glass watch and placed in a furnace. Afterwards, the catalyst was crushed and sieved again (500 µm diameter).[62–64] The specific conditions used for the preparation of metal oxides supported on *γ*-alumina are described in Table 3.3.

Table 3. 3. Time and temperature requirements for preparation of *γ*-alumina-supported metal oxides. Catalyst preparation was performed by dry impregnation with 10% metal loading.

Catalyst	Drying temperature (˚C)	Drying time (hr)	Calcination temperature (˚C)	Calcination time (hr)
Mn_2O_3 / γ-alumina	100	10	500	4
ZnO / γ-alumina	120	10	550	6
Fe_2O_3 / γ-alumina	120	4	700	2

Chapter 4

4. Effect of different particle sizes of Nano-ZnO on removal of atrazine from water

4.1 Ozone Self-Decomposition

Ozone self-decomposition is defined as the conversion of molecular ozone to OH radicals. In order to quantify the effects of catalyst on decomposition of ozone it is crucial to measure rates at which self-decomposition of ozone occurs in absence of catalyst. pH of the solution, and presence of buffers and radical scavenger are factors that influence to the rate of ozone self-decomposition.

4.1.1 Effect of pH

pH is one of the main influencing factors on ozone self-decomposition *vide supra*. Three aqueous standard solutions (pH= 3, 5, and 7) were prepared by using hydrochloric acid/ potassium chloride solutions or phosphate buffers. Using the experimental setup shown in Figure 3.1, ozone was continuously bubbled into the liquid phase until the ozone concentration reached 8.33×10^{-5} M (4 mg L^{-1}). The oxygen cylinder valve was shut off and the ozone generator was turned off immediately. The liquid and gas ozone concentration, pH, and temperature were monitored every two seconds using a data acquisition system (cDAQ-9172, National Instruments Corp.).

It was observed that ozone self-decomposition is significantly faster in neutral pH level compared to acidic pH levels (Figure 4.1). According to the SHB mechanism equations, under acidic conditions, hydroxyl radicals react with H^+ to form hydrogen peroxide (H_2O_2) (equation 2.6

). This contributes to the significant decrease in the rate of self-decomposition in acidic pH levels. In contrast, at pH levels higher than 6, HO_2^- and OH^- ions are produced which lead to increase in the concentration of OH radicals.

The observed rate increase in neutral condition (pH= 7), is believed to be linked to the effect of HO_2^- and OH^- ions.

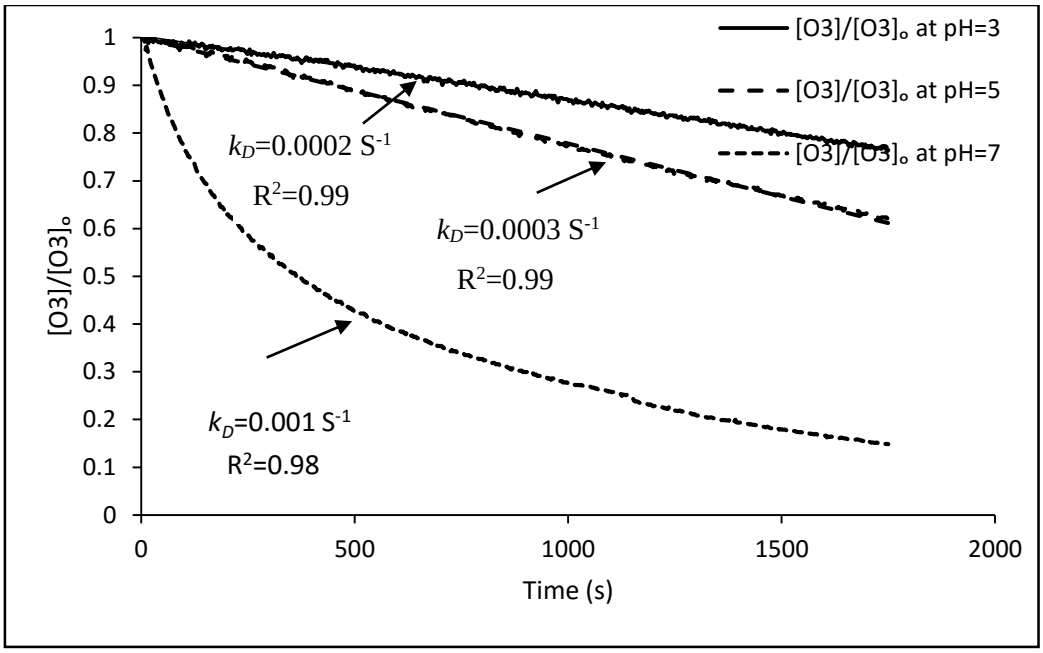

Figure 4. 1. Decomposition of ozone in different pHs and non-buffered millipore water.
$[O3]_0 = 8.33\times10^{-5}$ M (4 mg L^{-1})

4.1.2 Effect of Phosphate Buffer

The effect of phosphate buffer on the self-decomposition of ozone were evaluated according to the procedure described in section 4.1.1. with minor changes. For this purpose, two solutions were used; one with phosphate buffer (pH=7) and another without buffer at pH=7. Results show that in the presence of phosphate buffer, the rate of ozone decomposition is slightly faster (Figure 4.2).

Phosphate buffers ($H_3PO_4/H_2PO^{4-}/HPO4^{-2}$) are commonly used in ozonation reaction. These types of buffers contain ions that are generally unreactive towards ozone. However, these ions undergo slow reactions with hydroxyl radicals which increase the rate of ozone decomposition.[65]

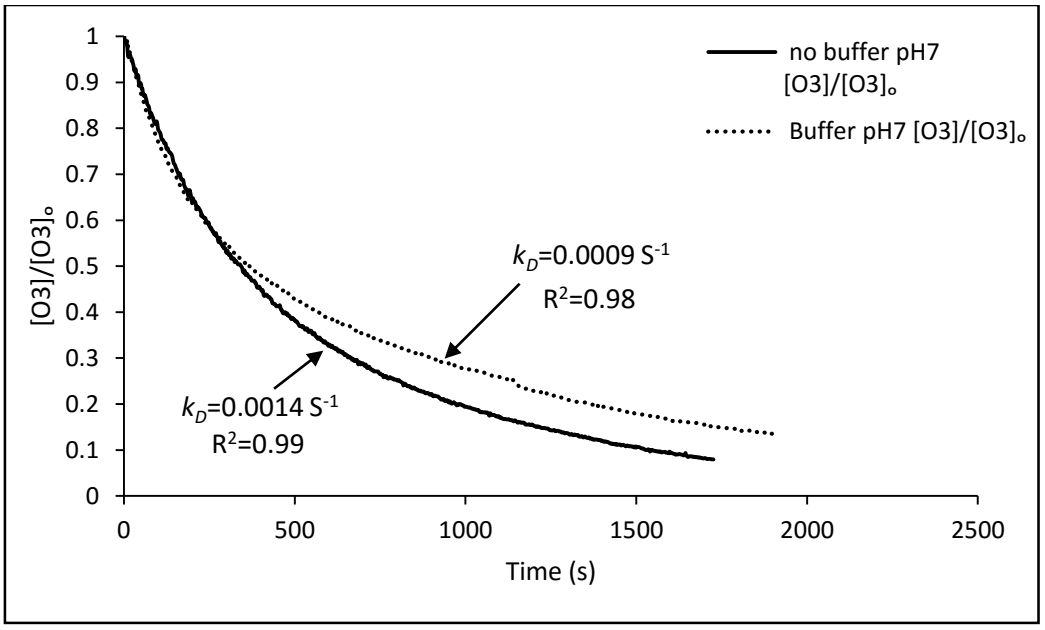

Figure 4. 2. Ozone self-decomposition in the presence of buffer solution in pH=7 and non-buffered solution $[O3]_0 = 8.33\times10^{-5}$ M, ionic strength (buffer) = 0.1 M

4.1.3 Effect of Radical Scavenger

The effect of TBA as the radical scavenger on the self-decomposition of ozone was measured experimentally according to the procedure described in section 4.1.1. with minor changes. For this purpose, two solutions containing phosphate buffers (pH=7) were prepared. To one of these solutions TBA (1×10^{-4} M) the radical scavenger was added and the other did not

contain this additive. TBA was chosen as the suitable scavenger based on its commercial availability, and un-reactivity towards adsorption on ZnO surface.

Results suggest that the rate of ozone decomposition is reduced from 85% ozone decomposition without scavenger to 50% ozone decomposition in the presence of TBA (Figure 4.3.). It is likely that the observed rate difference is related to the removal of hydroxyl radicals by TBA (*vide supra*).[28,66]

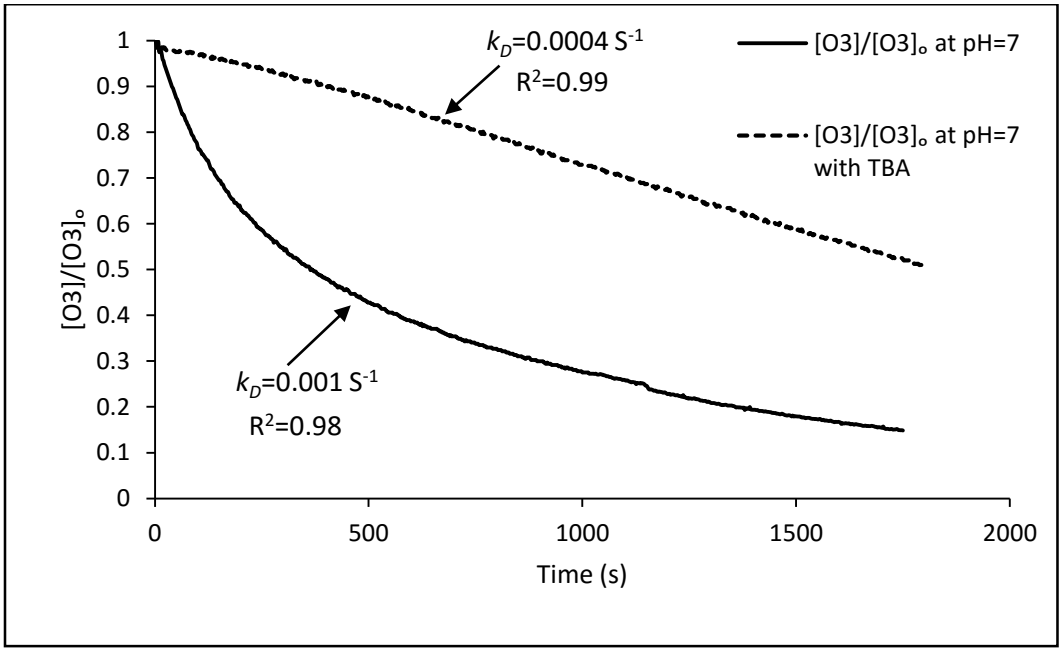

Figure 4. 3. Ozone decomposition in the presence of radical scavenger. $[O3]_0 = 8.33\times10^{-5}$ M, $[TBA]_0 = 1\times10^{-4}$ M, phosphate buffer pH = 7, ionic strength 0.1 M

4.1.4 Effect of Catalyst Dose on Ozone Decomposition Rate

The amount of ZnO catalyst directly influences the ozone decomposition. In order to investigate and quantify such effects, a series of experiments were carried out using process described in section 4.1.1. with minor changes. Standard phosphate buffer solutions (pH=7)

containing various amounts of the nano-ZnO (35-45 nm) were prepared (0, 1, 2, 4, and 8 grams). Results show that by increasing the amount of catalyst (up to 8 $g.L^{-1}$) the ozone decomposition rate is increased (Figure 4.4).

By plotting the rate constants (k_D (s^{-1})) against the catalyst dose Figure 4.5 is obtained. Based on these data, 8 grams was chosen as the desired catalytic dose.

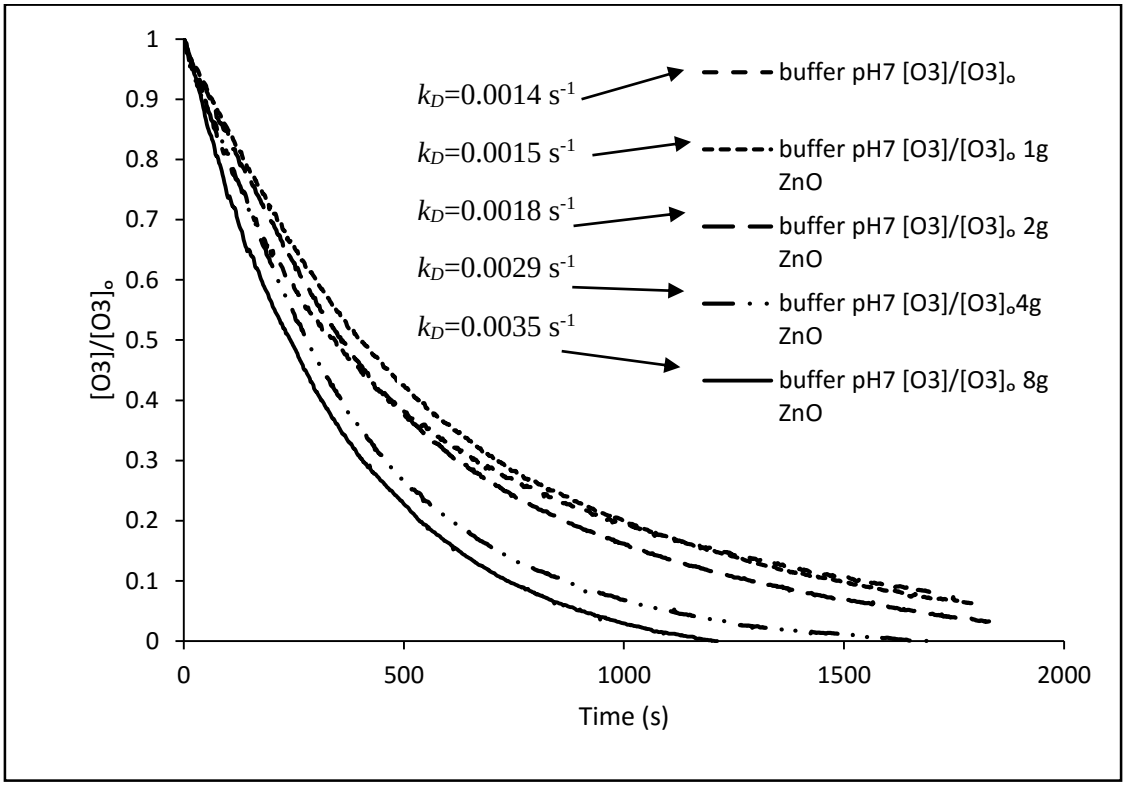

Figure 4. 4. Effect of catalyst dose (nano-ZnO (35-45 nm)) on ozone decomposition rate. $[O_3]_0 = 8.33\times10^{-5}$ M, ionic strength (buffer) = 0.05 M, pH = 7

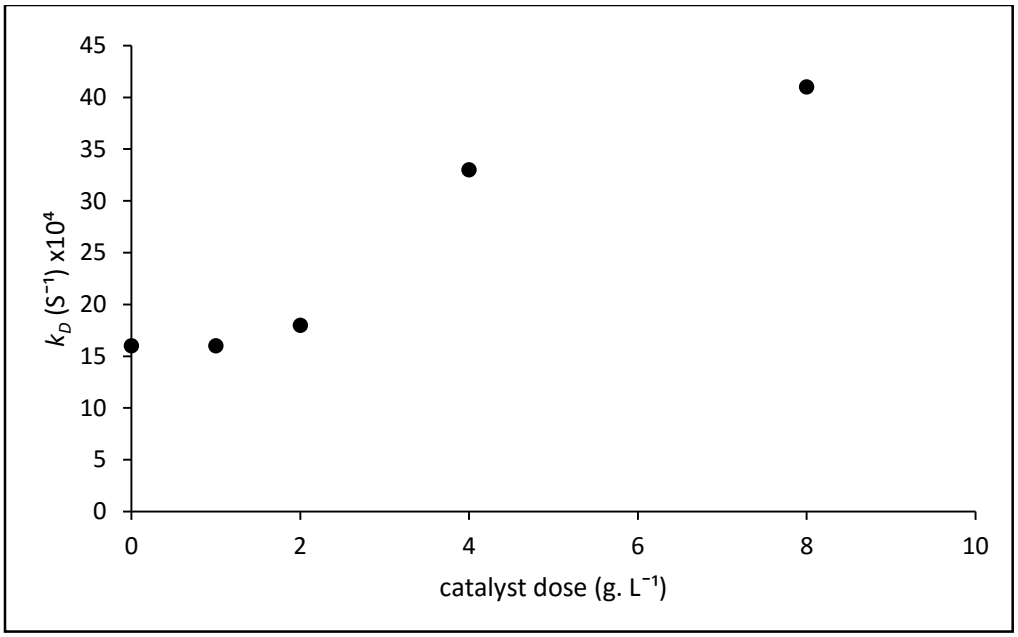

Figure 4. 5. Ozone decomposition rate in the presence of different dose of catalysts. $[O_3]_0$ =8.33×10^{-5} M, ionic strength (buffer) = 0.05 M, pH = 7

4.2 Ozone Decomposition in the Presence of nano-ZnO Catalyst

In order to investigate the effect of pH and radical scavenger on the rate of ozone decomposition a series of measurements were carried out using the catalyst dose of 8 g.L^{-1} and the initial ozone concentration of 8.33×10^{-5} M (4 mg L^{-1}).

4.2.1 Effect of pH

The effect of pH on the decomposition rate of ozone was investigated using a series of experiments with the following conditions: The reactor was charged with 1000±1 mL of buffer pH=7 or 5 (phosphate buffer). Ozone was continuously bubbled into the liquid phase until the concentration reached 8.33×10^{-5} M (4 mg L^{-1}). The oxygen cylinder valve was shut off and the ozone generator was turned off immediately. Subsequently, nano-ZnO (35-45 nm) catalyst (8 g.L^{-1}) was added in one portion to the reactor. The rector was immediately sealed using a glass stopper

and stirred for 30 mins. The liquid and gas ozone concentration, pH, and temperature were monitored every two seconds using a data acquisition system (cDAQ-9172, National Instruments Corp.).

Results suggest that ozone decomposition rate at pH=7 is higher than pH=5 (79%). This is believed to be linked to the higher concentration of hydroxyl radicals at pH=7 (Figure 4.6).

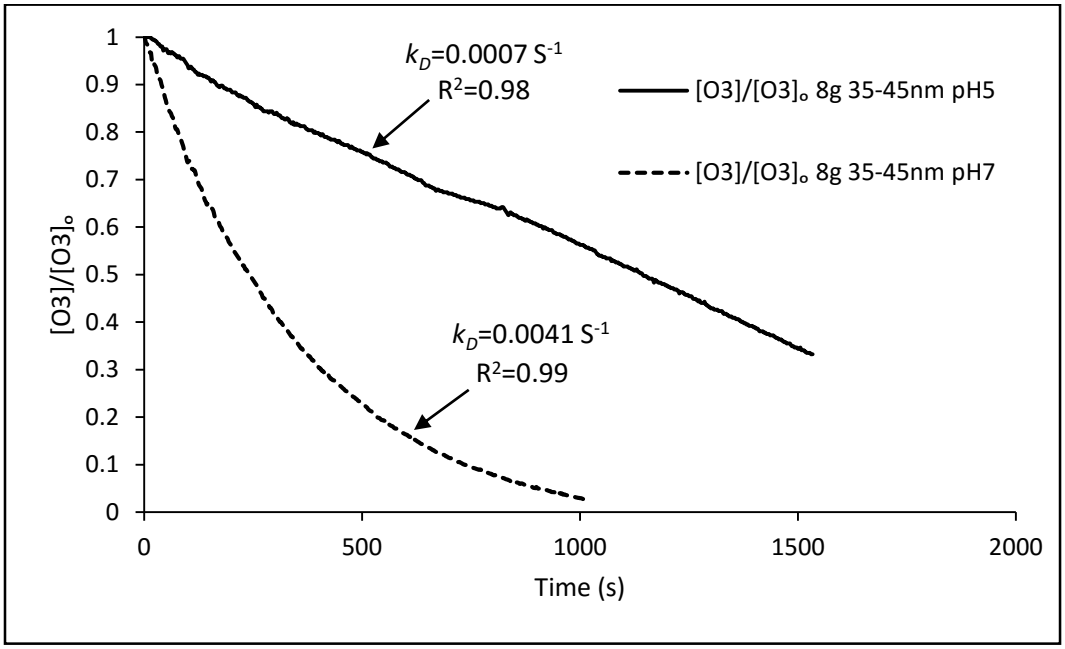

Figure 4. 6. Effect of pH on ozone decomposition catalyzed by nano-ZnO (35-45 nm). $[O3]_0$= 8.33×10^{-5} M, catalyst dose= 8.0 g.L^{-1}, ionic strength (buffer) = 0.1 M

4.2.2 Effect of Scavenger

The influence of radical scavenger on the rate of ozone decomposition was quantified by an experiment carried out using the same setup as described in section (3.2.2.) at pH=7 (phosphate buffer), and in the presence of 1×10^{-4} M TBA.

Similar to the results obtained from ozone self-decomposition experiments, a noticeable decrease is observed in the rate of ozone decomposition in the presence of TBA (80% decrease) (Figure 4.7.).

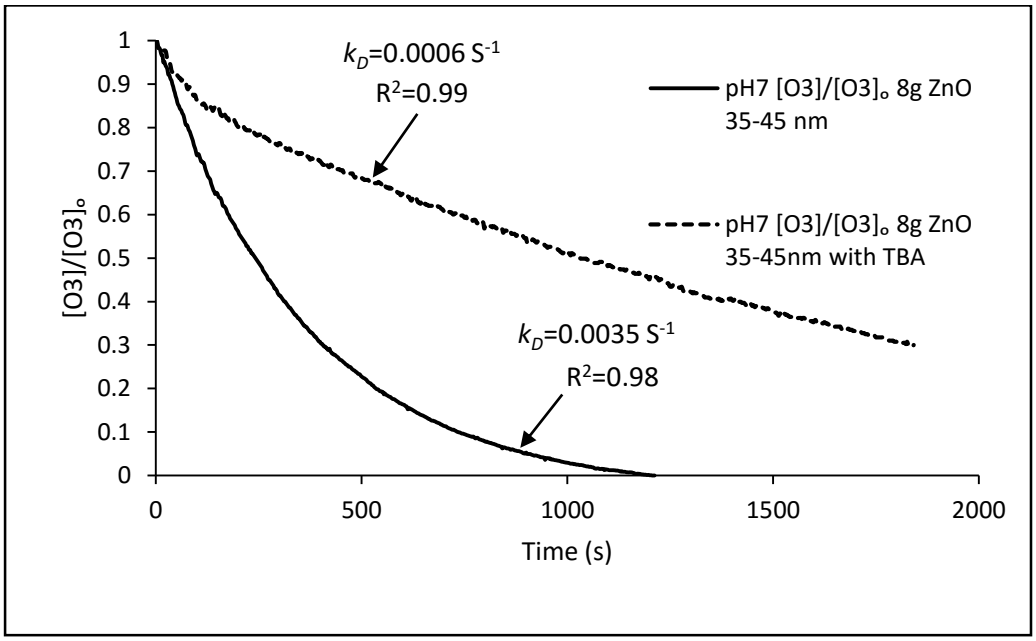

Figure 4. 7. Ozone decomposition in the presence of 8g nano-ZnO catalyst (35-45 nm) and 1×10^{-4} M TBA, $[O3]_0 = 8.33\times10^{-5}$ M, ionic strength (buffer) = 0.1 M

4.3 Effect of Different Sizes of nano-ZnO on Ozone Decomposition

A typical condition was utilized to evaluate the effect of various sizes of nano-ZnO catalysts on the rate of decomposition of ozone. The experimental setup was similar to that in section 3.2.2., using three different sizes of nano-ZnO (18 nm, 35-45 nm, and 80-200 nm).

Based on the results presented in Figure 4.8., the rate of ozone decomposition are similar for different sizes of nano-ZnO catalyst. R^2 values show good fit and the three k_D values are close in quantity.

It is generally accepted that in the presence of nano-ZnO catalysts, the rate of ozone decomposition is enhanced and therefore the rate of production of hydroxyl radical is accelerated. This is believed to be related to the facile adsorption of molecular ozone on the surface of nano-ZnO catalyst followed by an electron-transfer from catalyst's surface to the molecule of ozone. This electron transfer leads to the oxidation of O_3 to form O_3^- ions and OH radicals.[53]

4.3.1 Comparison between findings and previously published results

Huang *et al.* suggested that micro, sub-micro and nano ZnO decompose ozone at different rates. This is believed to be related to increase in surface area; nano-sized ZnO are more catalytically active in decomposition of molecule of ozone in comparison to micro and sub-micro sizes, possibly due to a larger surface area.[53] Unfortunately multiple efforts towards reproduction of results published by Huang *et al.* (i.e. removal of TCP using various macro-, micro-, and nano-sized ZnO catalysts) were unsuccessful. This could be due to fast reactions between TCP and ozone in absence of the metal catalyst.

Based on the results presented here, the rate difference between different sizes of nano-ZnO in ozone decomposition experiments are negligible (Figure 4.8). The absence of such rate enhancement is believed to be linked to the poor adsorption properties of the catalyst surface (*vide infra*).

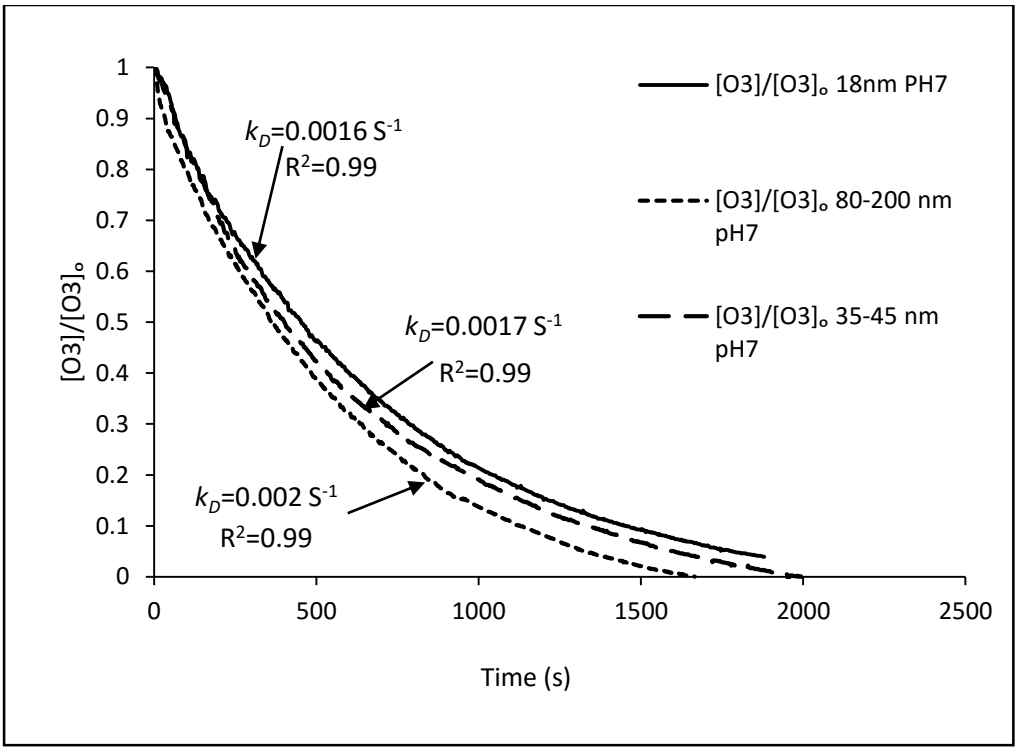

Figure 4. 8. Comparison between different sizes of nano-ZnO on ozone decomposition, catalyst dose=8 g.L^{-1}, $[O_3]_0$ = 8.33×10^{-5} M, ionic strength (buffer) = 0.1 M.

4.4 Metal-Free Ozonation of Atrazine

In order to gain insight into the reaction mechanism, *tert*-butyl alcohol (TBA) was added as the radical scavenger (1×10^{-4} M). TBA has low affinities towards adsorption on most catalyst surfaces and has been used frequently to eliminate hydroxyl radicals.[65] TBA experiments are used to probe the role of hydroxyl radicals in the reaction mechanism. In other words, the difference between the rates of reactions that are carried out in the presence of TBA and reactions that do not contain this additive could elucidate whether the reaction proceeds through hydroxyl radicals or molecular ozone.

HPLC results show that atrazine removal in the presence of TBA is 32% and without TBA is 56%

(Figure 4.9.). Similarly the rate of ozone decomposition in the presence of TBA is lower than that under the same conditions but without TBA (Figure 4.10). It is interesting to note that a noticeable drop in concentration of ozone was observed during the first few seconds of the start of the reaction which is indicative of a rapid degradation of ozone (Figure 4.10).

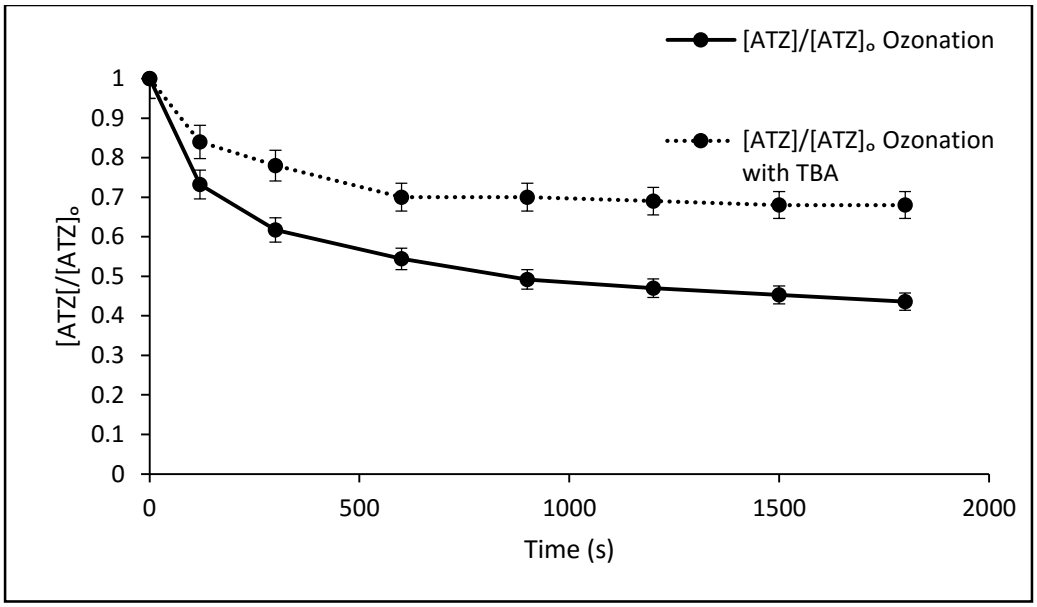

Figure 4. 9. Effect of radical scavenger on the removal of atrazine at ozonation at pH=7,$[O3]_0$ =8.33×10^{-5} M, $[ATZ]_0$ = 4.62×10^{-5} M, when applies $[TBA]_0$ =1×10^{-4} M, ionic strength (buffer) = 0.1 M.

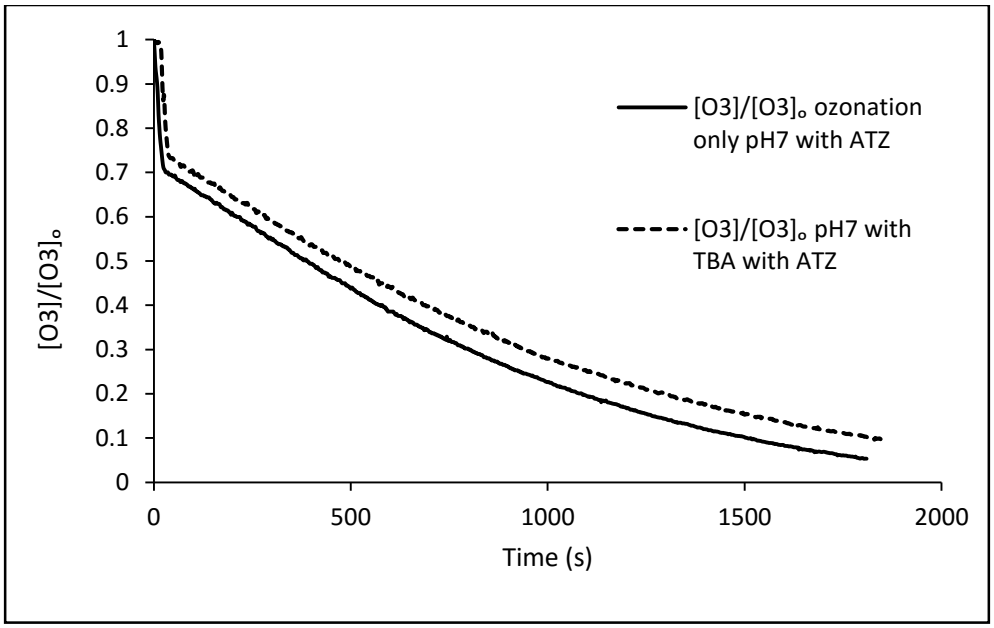

Figure 4. 10. Effect of radical scavenger on the rate of non-catalytic ozonation of atrazine at pH=7. $[O3]_0$ $=8.33\times10^{-5}$ M, $[ATZ]_0 = 4.62\times10^{-5}$ M, when applies $[TBA]_0 =1\times10^{-4}$ M, ionic strength (buffer) = 0.1 M.

TOC results show that total organic carbon of all samples withdrawn from reactor remained unchanged over 30 minutes. This suggests that during ozonation of atrazine, the concentration of the emerging pollutant decreases. However, the degradation is not complete and other stable intermediates are formed. deisopropylatrazine (DIA), deethylatrazine (DEA), 2-chloro-4-ethylimino-6-isopropylaminos-triazine (ATZ-imine), 4-acetamido-2-chloro-6-isopropylamino-s-triazine (CDET), 6-amino-2-chloro-4-ethylimino-s-triazine (DIA-imine), deethyldeisopropylatrazine (DEDIA), 4-acetamido-6-amino-2-chloro-s-triazine (CDAT) and 4-acetamido-2-chloro-6-isopropylaminos-triazine (CDIT) are common stable intermediates formed during ozonation of atrazine.[67,68]

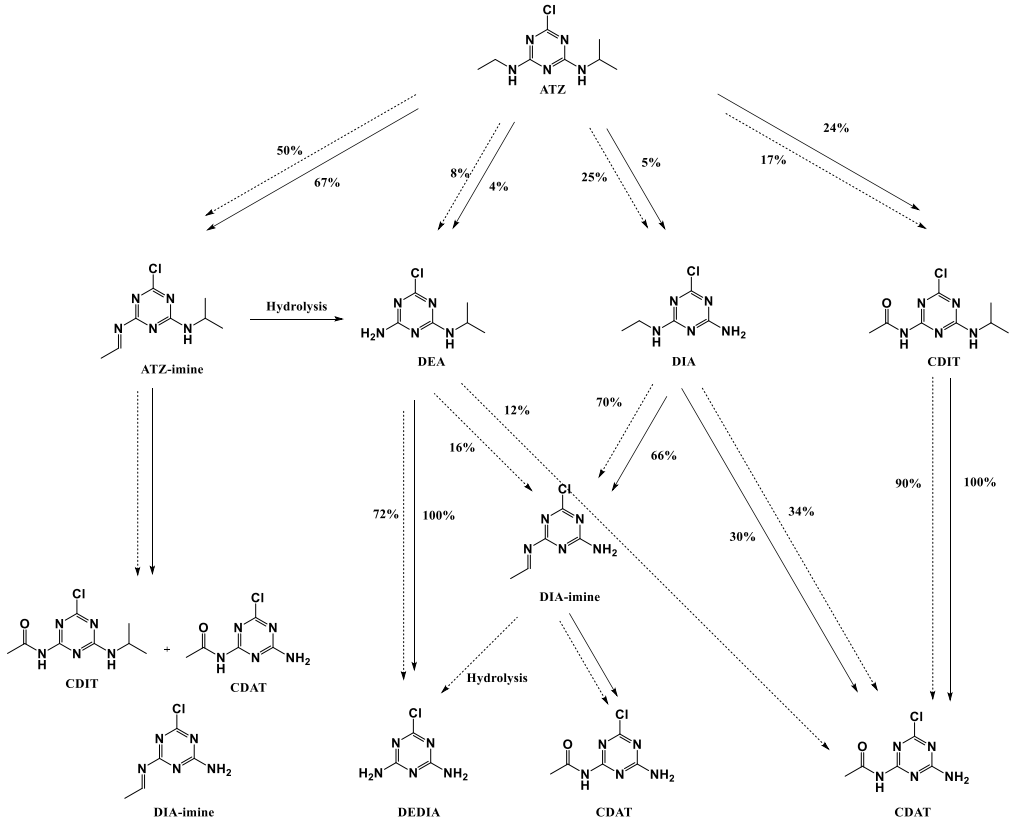

Figure 4. 11. Atrazine degradation pathways by ozone and OH radicals. Solid lines represent molecular ozone-assisted degradations and dashed lines represent OH radical-assisted pathways (image reproduced directly from the literature precedence).[67]

The data corresponding to decomposition rates of ozone suggest that the decomposition mechanism goes through hydroxyl radicals rather than molecular ozone.

Furthermore, R_{ct} values for both experiments were calculated (see Appendix B). The R_{ct} for atrazine removal *via* metal-free ozonation is 4.69×10^{-9} and that for ozonation of atrazine in the presence of TBA is calculated as 1.11×10^{-9}. These data suggest that atrazine removal in ozonation mainly proceeds through hydroxyl radicals rather than molecular ozone.

4.5 Effect of Different Particle Sizes of nano-ZnO on Catalytic Ozonation

Huang *et al*. have studied the rate of degradation of Trichloro phenol (TCP) in the presence of different sizes of ZnO catalysts. They found that degradation of TCP using nano-sized ZnO catalysts are faster than sub-micro sizes and sub-micro sizes are faster than micro-sized catalysts.[53]

A similar trend was envisioned for the rate of removal of atrazine between different nano-sized ZnO. In order to examine this hypothesis, three sizes of nano-ZnO were used for removal of Atrazine under the conditions described in section 3.2.2.

Results show that the rate of ozone decomposition and ATZ removal in the presence of nano-ZnO is higher than metal-free ozonation, possibly due to the presence of hydroxyl radicals (Figure 4.11. and Figure 4.12.). However, the size of the nano-ZnO catalysts have minimal effects on the rate of ozone decomposition and ATZ removal. On the other hand, the adsorption of Atrazine on the surface of nano-ZnO is negligible suggesting that the reaction occurs in the bulk of the solution rather than the surface of the catalyst (section 3.2.1.).

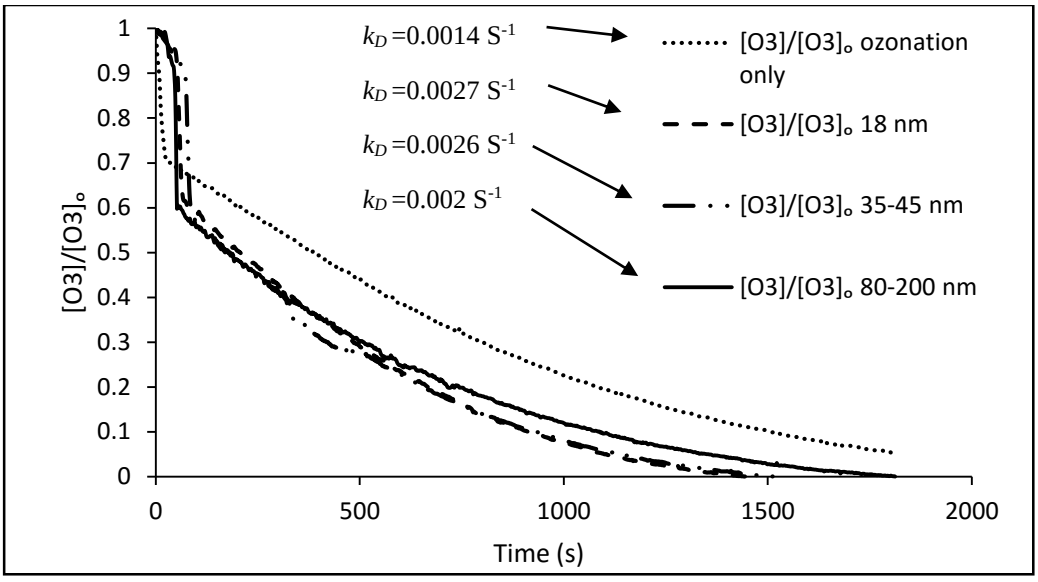

Figure 4. 12. Comparison between effect of different particle sizes of Nano-ZnO on ozone decomposition in the presence of atrazine in water at pH=7 (phosphate buffer), $[O3]_0$ =8.33×10^{-5} M, $[ATZ]_0$ = 4.62×10^{-5} M

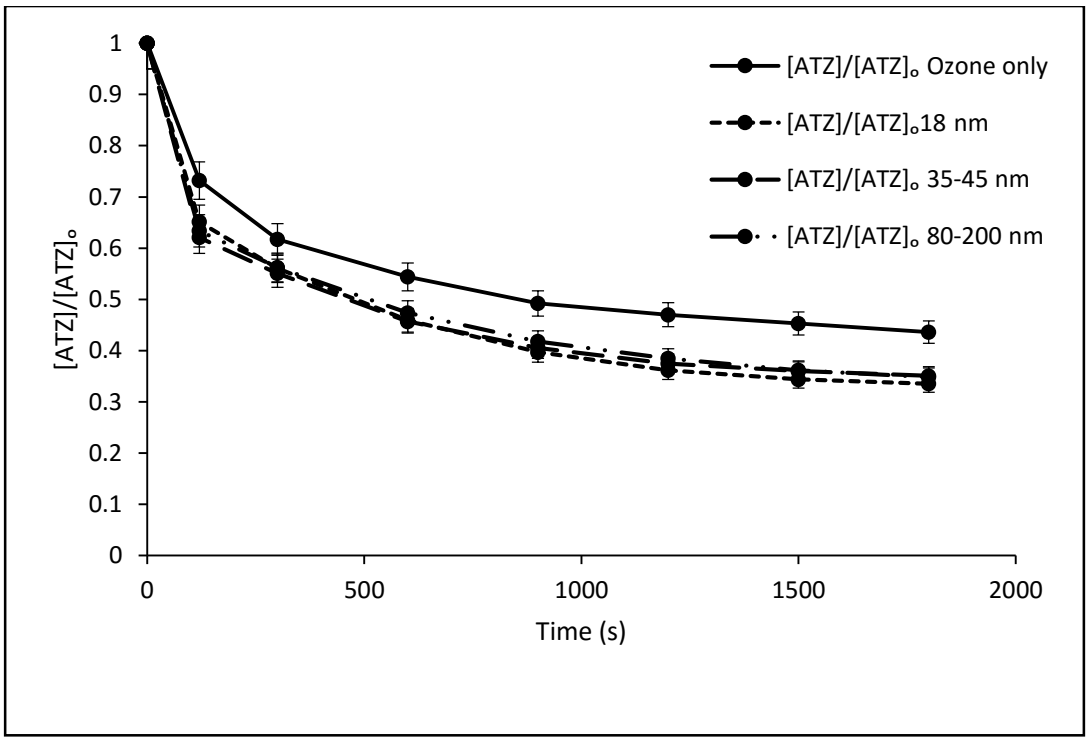

Figure 4. 13. Comparison between effect of non-catalytic and catalytic ozonation on atrazine removal from water at pH=7 (phosphate buffer), $[O3]_0$ =8.33×10^{-5} M, $[ATZ]_0$ = 4.62×10^{-5} M

The mechanism of ATZ removal has been shown to proceed through hydroxyl radicals. This work has shown that decomposition of ozone using nano-ZnO proceeds through radicals. In order to explore the presence of this type of mechanism in the removal of ATZ, two experiments were carried out (section 3.2.2.), one in the presence of TBA (1×10^{-4} M) and the other without the scavenger.

Results show that the residual concentration of ATZ in the presence of TBA is 45% and without TBA this value is 65% of its initial concentration (Figure 4.13.).

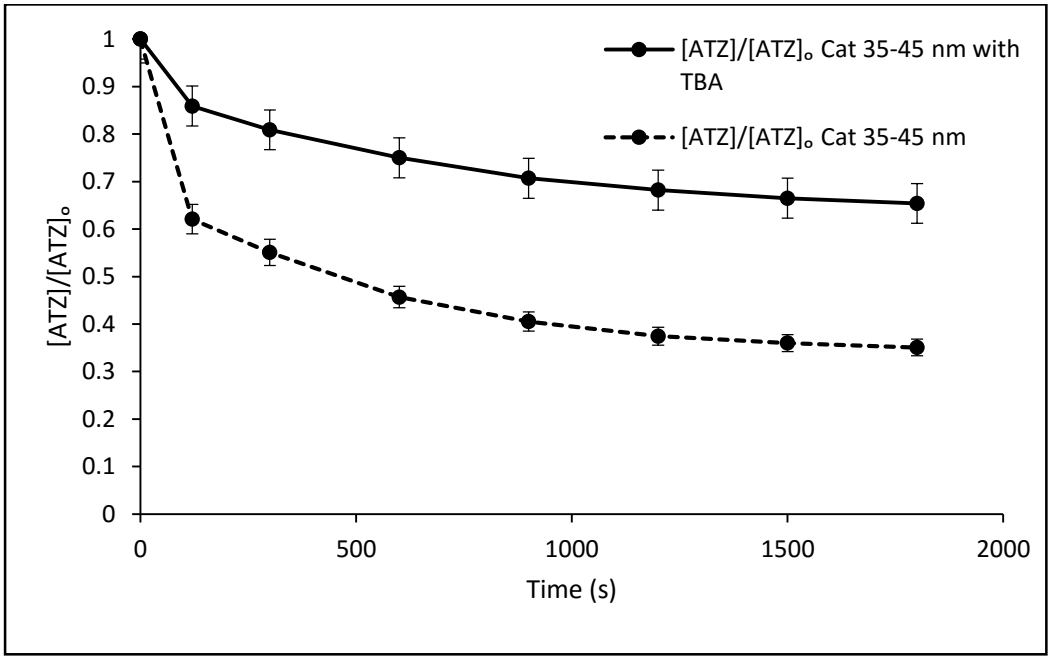

Figure 4. 14. Radical scavenger effect on catalytic ozonation (nano-ZnO 35-45nm) of atrazine at pH=7. $[O3]_0$ =8.33×10^{-5} M, $[ATZ]_0$ = 4.62×10^{-5} M, when applies $[TBA]_0$ = 1×10^{-4} M ionic strength (buffer) = 0.1 M.

The rate of ozone decomposition in water in the presence of TBA was 26% lower than the experiment without TBA (Figure 4.14.).

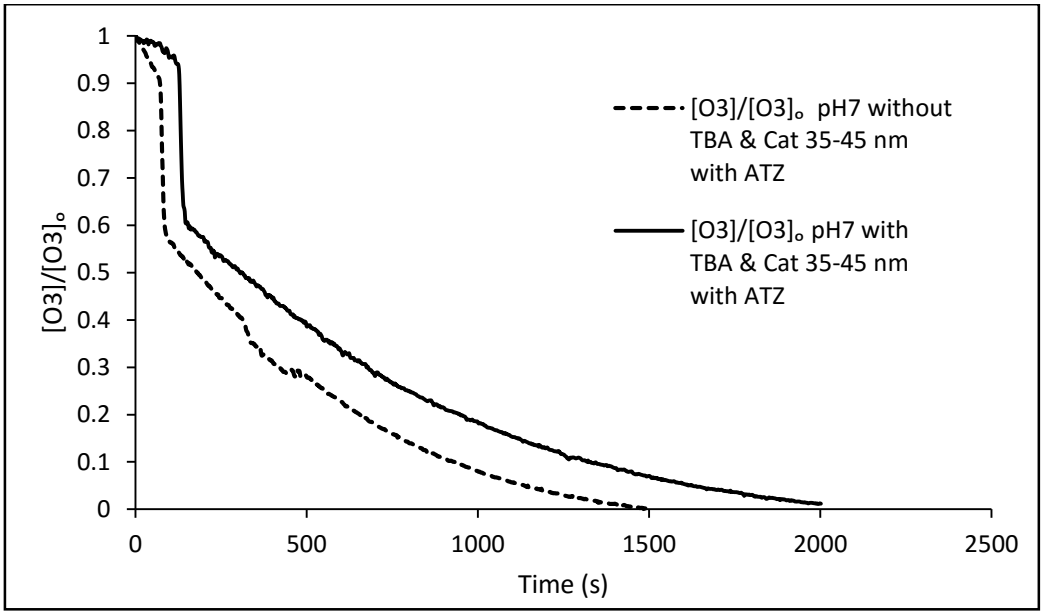

Figure 4. 15. Effect of radical scavenger ($[TBA]_0 = 1\times10^{-4}$ M) on the ozone decomposition in the presence of 8g nano-ZnO (35-45 nm) and $[ATZ]_0=4.64\times10^{-5}$ M., $[O3]_0 = 8.33\times10^{-5}$ M, ionic strength (buffer) = 0.1 M

As mentioned earlier, TBA reacts with labile hydroxyl radicals in the solution, effectively removing them from the solution. It is evident that without the hydroxyl radicals the rate of reaction decreases significantly. However TBA does not completely terminate the catalytic ozonation meaning that hydroxyl radicals are only partially involved in the mechanism. The residual reactivity could be linked to the direct reaction of molecular ozone. These results agree with the previous findings regarding the decomposition of ozone (*i.e.* removal of Atrazine in the presence of nano-ZnO catalysts involve hydroxyl radicals).

Furthermore, R_{ct} values for atrazine removal using nano-ZnO (35-45 nm)/O_3) and other nano-ZnO (35-45 nm)/O_3/TBA was calculated (Appendix B). R_{ct} for atrazine removal using nano-ZnO (35-45 nm)/O_3 is 9.48 $x10^{-9}$ and in the presence of nano-ZnO (35-45 nm)/O_3/TBA is 1.58$x10^{-}$

[9]. These data suggest that atrazine removal in the presence of nano-ZnO (35-45 nm)/O_3 mainly proceeds through hydroxyl radicals rather than molecular ozone.

4.6 Discussion

Previous reports have suggested that some organic compounds can chelate to the surface of the heterogeneous catalysts. This complex is oxidized in the presence of ozone and hydroxyl radicals and the oxidation products and by-products are desorbed into the solution. The oxidation is continued in the bulk of the solution to degrade the remaining organic compounds.[53] Furthermore, based on the adsorption experiment, atrazine does not effectively adsorb on the surface of nano-ZnO.

Legube and Karpel Vel Leitner have proposed two possible mechanisms for degradation of micropolutants in the presence of metals or metal oxides supported on metal oxides or carbon[20]; first, adsorption of micropolutant on the surface of catalyst followed by the oxidation of the organic matter by molecular ozone or hydroxyl radicals. Second, oxidation of ozone to hydroxyl radicals *via* electron transfer from the surface of the metals followed by the degradation of the emerging pollutant. In 2005, Fonatnier *et* al.[19] reported that the mechanism involves the formation of a highly reactive metal-ozone complex which eventually leads to the degradation of the organic molecule. In their study, it was observed that degradation of organic molecules does not involve hydroxyl radicals and the ozone molecules are directly involved in the mechanism. It is believed that molecular ozone is adsorbed on the surface of nano-ZnO followed by the oxidation of the ozone molecule. This leads to the production of OH radicals.

All in all, it is reasonable to assume that reaction is carried out in the bulk and the rate is independent of the surface area of the catalyst. This is probably the reason for the observed similar reaction rates for different particle sizes of nano-Zno catalysts.

Chapter 5

5. The effect of alumina based catalysts on catalytic ozonation of atrazine in water

5.1 Effect of Catalyst Dose on Ozone Decomposition Rate

Mn_2O_3/γ-alumina

To investigate the catalytic role of Mn_2O_3/γ-alumina, standard phosphate buffer solutions (pH=7) were prepared. The reactor was charged with different amounts of Mn_2O_3/γ-alumina (0, 0.5,1, 2, and 3 grams) and subjected to ozonation conditions described in section 3.2.

Figure 5.1. illustrates the rate of ozone decomposition in the presence of different amounts of Mn_2O_3/γ-alumina catalysts. This linear correlation suggests that the rate of decomposition and the amount of Mn_2O_3/γ-alumina follows a pseudo first-order kinetics. (Figure 5.1.).

By plotting the rate constants (k_D (s^{-1})) against the catalyst dose, a graph is obtained (Figure 5.2.). This plot shows that by increasing the dose of catalyst the rate of ozone decomposition is increased.

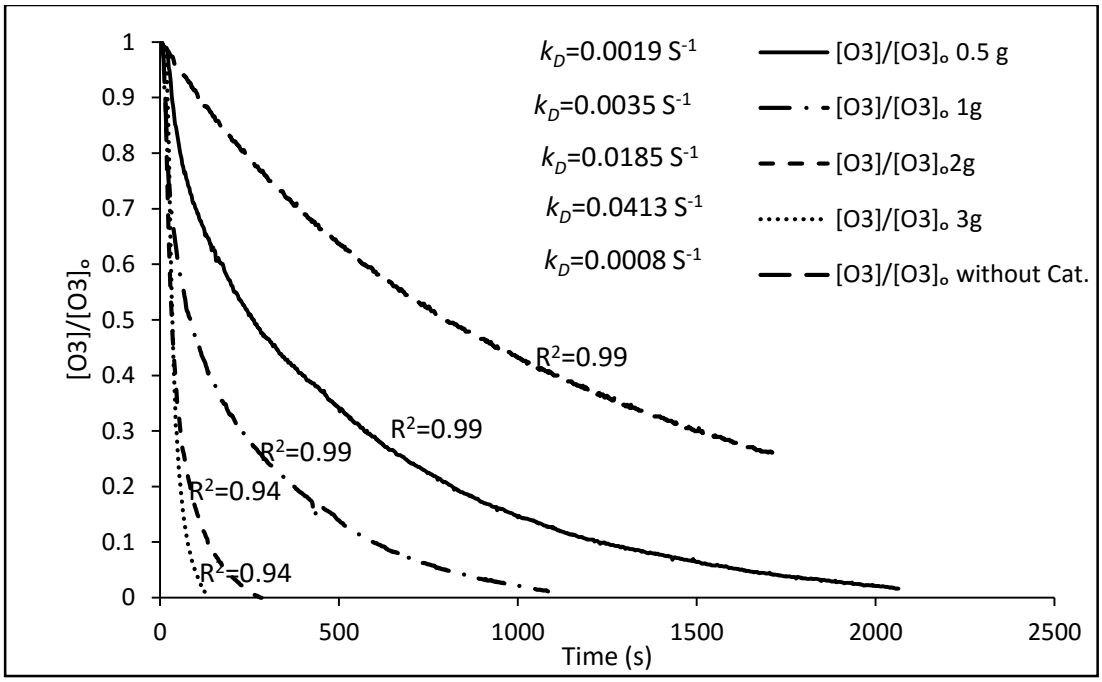

Figure 5. 1. Effect of catalyst dose Mn_2O_3/γ-alumina on ozone decomposition rate. $[O_3]_0$ =8.33×10^{-5} M, ionic strength (buffer) = 0.05 M, pH = 7

It was observed that the rate of ozone decomposition increases by using more catalyst.

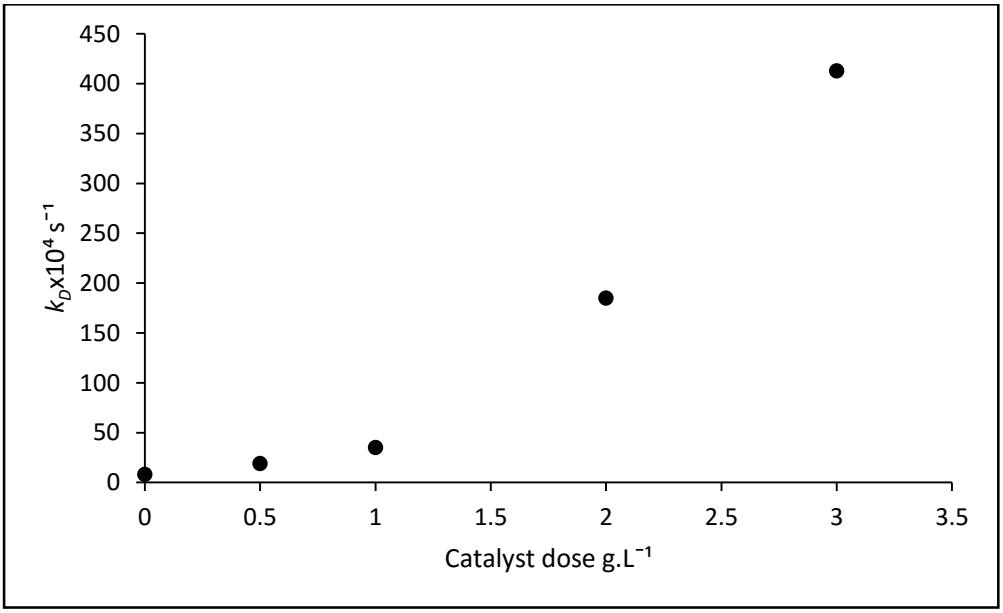

Figure 5. 2. Ozone decomposition rate in the presence of different dose of Mn_2O_3/γ-alumina. $[O_3]_0$ =8.33×10^{-5} M, ionic strength (buffer) = 0.05 M, pH = 7

Standard phosphate buffer solutions (pH=7) were prepared and were charged with different amounts of Fe_2O_3/γ-alumina, or ZnO/γ-alumina, or metal-free *γ*-alumina (0, 1, 2, 4 and 8 grams) according to the procedure described in section 4.1.

γ-Alumina

Results suggest that ozone decomposition in the presence of different amounts γ-alumina follows a pseudo first-order kinetics (Figure 5.3.).

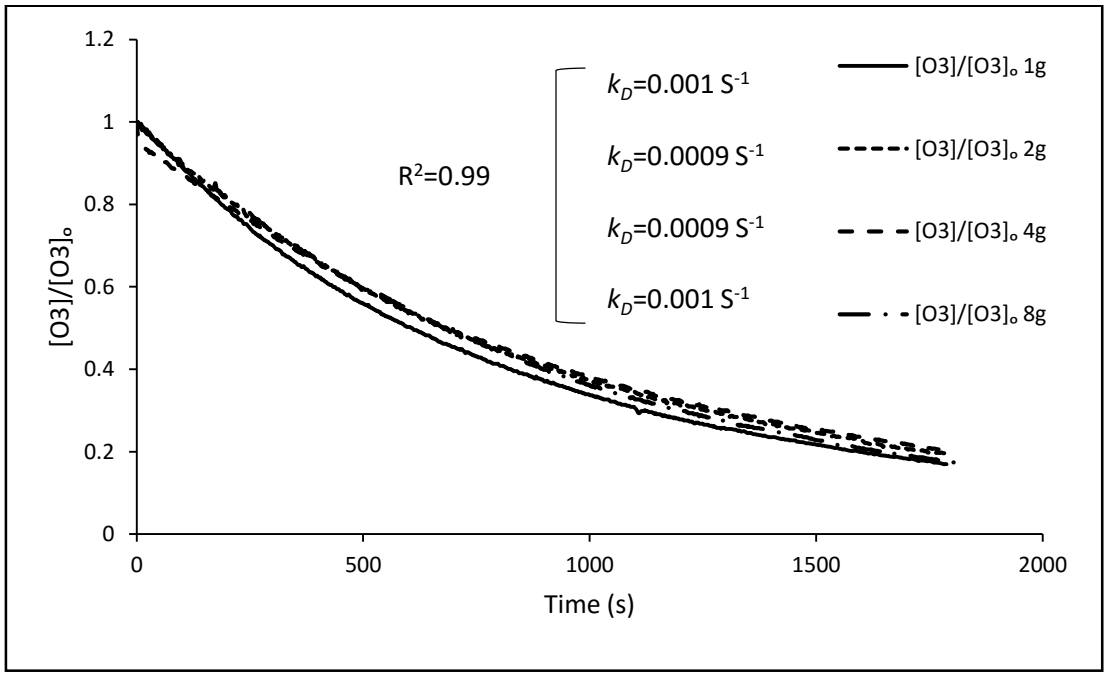

Figure 5. 3. Effect of catalyst dose γ-alumina on ozone decomposition rate. $[O_3]_0 = 8.33\times10^{-5}$ M, ionic strength (buffer) = 0.05 M, pH = 7

Additionally, it was observed that for catalyst doses higher than 2 grams, the amount of catalyst has negligible influence on the rate of ozone decomposition (Figure 5.4.).

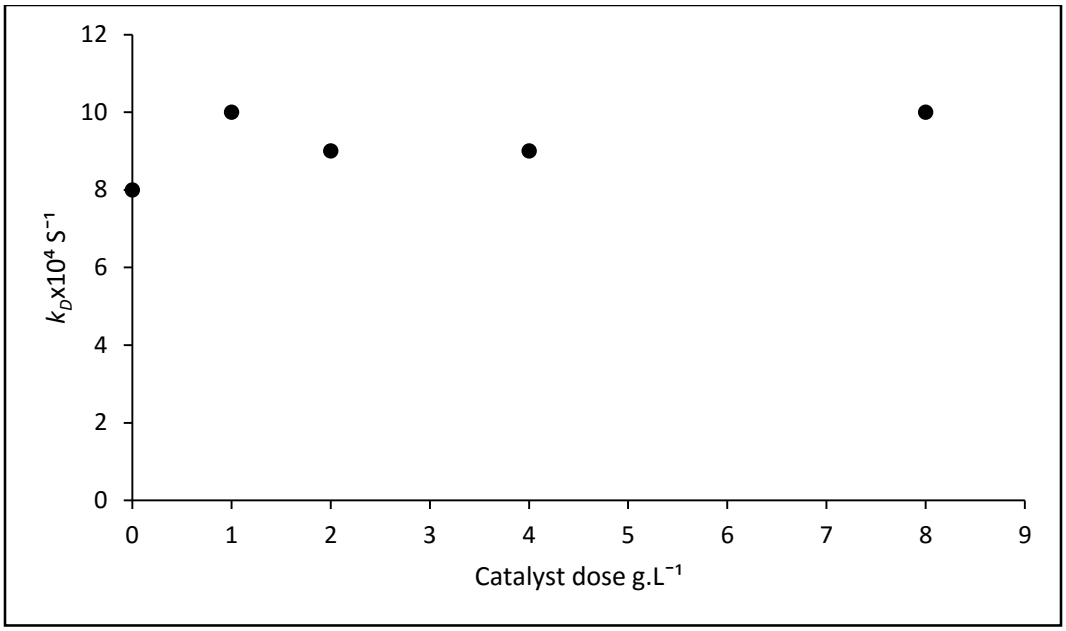

Figure 5. 4. Ozone decomposition rate in the presence of different dose of catalysts. $[O_3]_0$ =8.33×10^{-5} M, ionic strength (buffer) = 0.05 M, pH = 7

Fe_2O_3/γ-alumina

It was observed that ozone decomposition in the presence of different amounts of Fe_2O_3/γ-alumina catalyst follows pseudo first-order kinetics (Figure 5.5.).

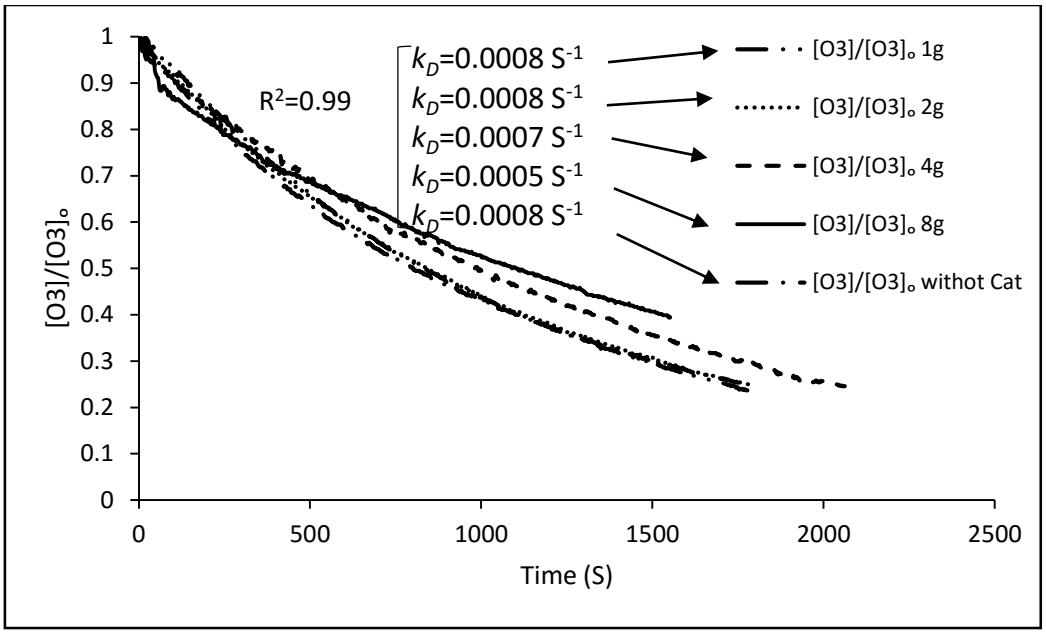

Figure 5. 5. Effect of catalyst dose Fe_2O_3/γ-alumina on ozone decomposition rate. $[O3]_0 = 8.33\times10^{-5}$ M, ionic strength (buffer) = 0.05 M, pH = 7

Results suggest that at higher doses, an increase in the amount of catalyst dose results in decrease in rate of ozone decomposition (Figure 5.6.).

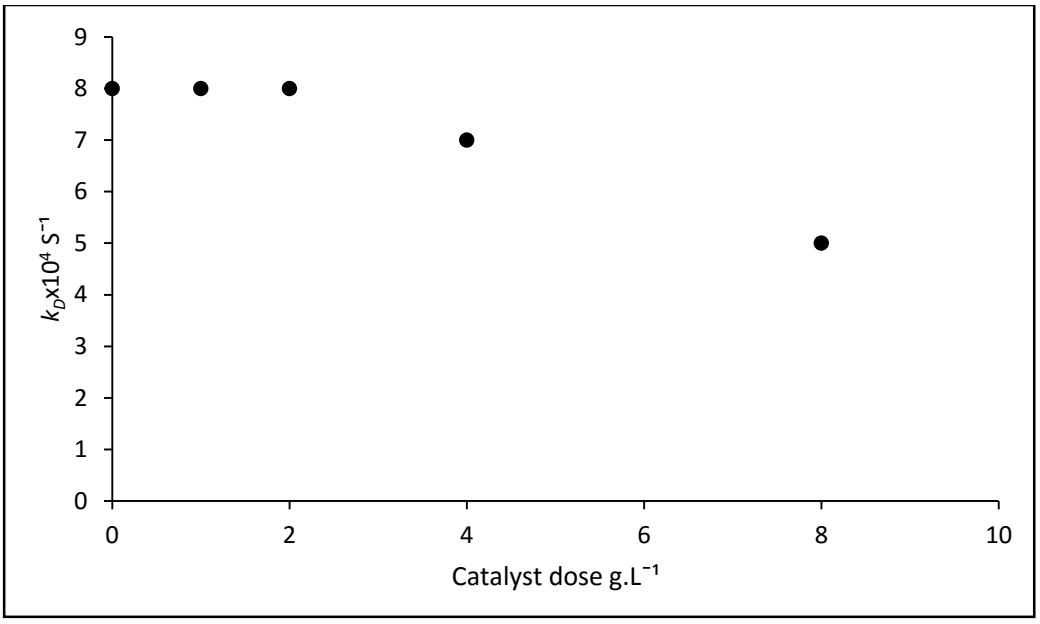

Figure 5. 6. Ozone decomposition rate in the presence of different dose of catalysts. $[O_3]_0$ =8.33×10^{-5} M, ionic strength (buffer) = 0.05 M, pH = 7

ZnO/γ-alumina

Results show that ozone decomposition in the presence of different amounts of ZnO/γ-alumina catalyst follows pseudo first-order kinetics (Figure 5.7.). A slight increase in the rate of ozone decomposition is observed by using 1 gram of catalyst. However, when increasing the catalyst dose to 8 grams a decline is observed in the rate of ozone decomposition (Figure 5.8.).

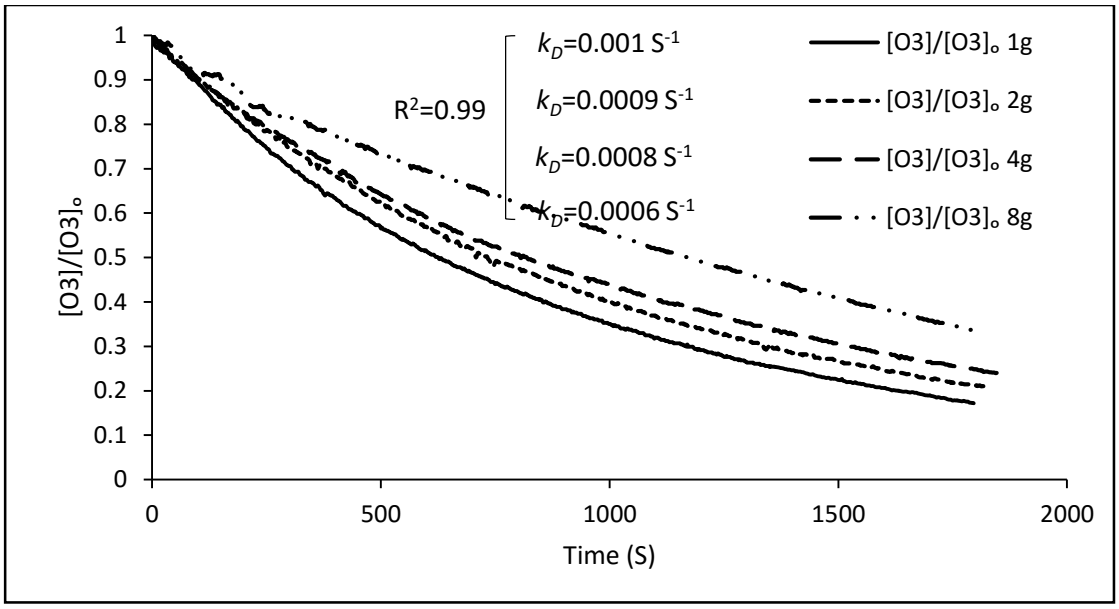

Figure 5. 7. Effect of catalyst dose ZnO/γ-alumina on ozone decomposition rate, $[O3]_0=8.33\times10^{-5}$ M, ionic strength (buffer) = 0.05 M, pH = 7

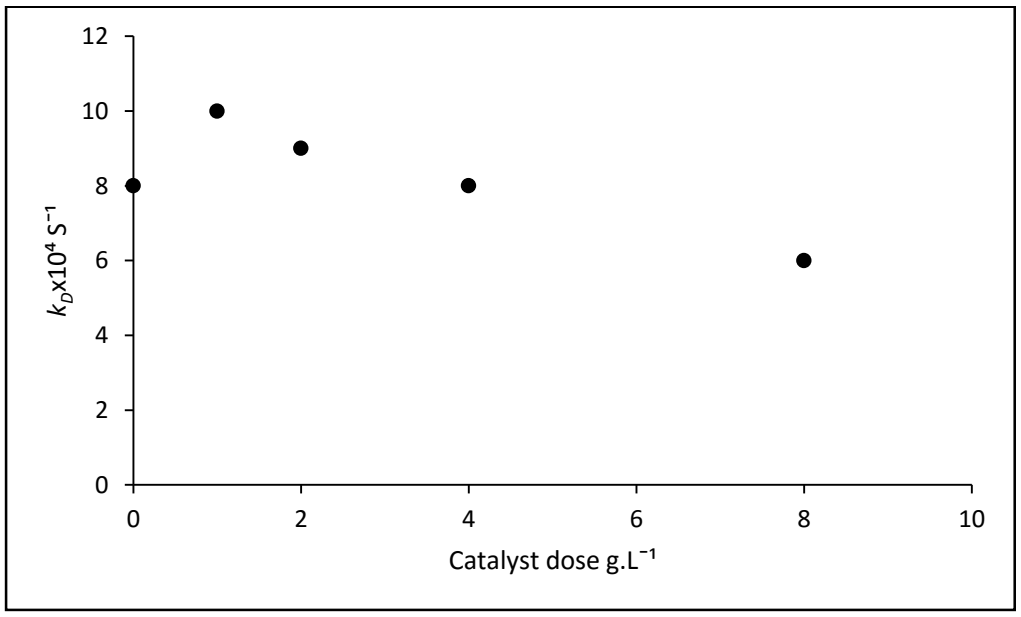

Figure 5. 8. Ozone decomposition rate in the presence of different dose of ZnO/γ-alumina. $[O_3]_0$ =8.33×10^{-5} M, ionic strength (buffer) = 0.05 M, pH = 7

Based in the result described above, a slight rate enhancement is achieved by using more than 2 grams of catalyst. However, this does not justify the extra cost of using excess amounts of these catalysts. Therefore, 2 grams was chosen as the desired dose.

In addition, similar rates of ozone decomposition is observed for ZnO/γ-alumina, Fe_2O_3/γ-alumina, and γ-alumina catalysts (Figure 5.9). R^2 values show good fit and the three k_D values are close in quantity. Interestingly, the rates of ozone decomposition using Mn_2O_3/γ-alumina catalyst are faster than other γ-alumina-supported metal oxides and metal-free γ-alumina. This might be related to the relatively faster rate of production of hydroxyl radicals using Mn_2O_3/γ-alumina compared to the other catalysts.

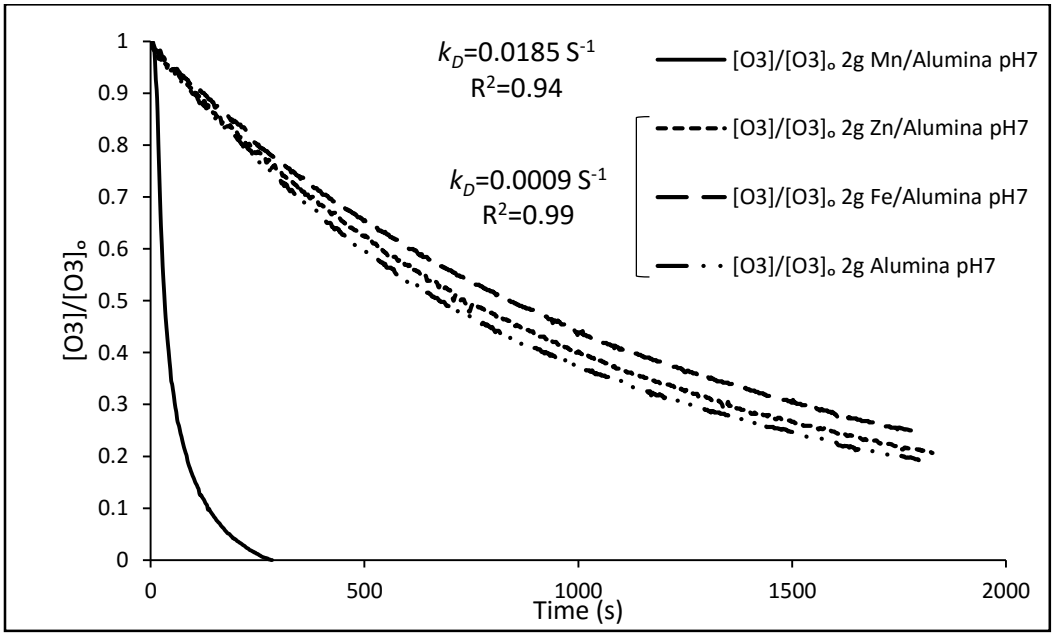

Figure 5. 9. Comparison between ozone decomposition rates by using different metals supported on γ-Alumina**,** catalyst dose=8 g.L^{-1}, $[O_3]_0$ = 8.33×10^{-5} M, ionic strength (buffer) = 0.1 M.

5.2 The Effect of pH Levels on Ozone Decomposition in the Presence of Mn_2O_3 /γ-Al_2O_3

The influence of pH on the rate of decomposition of ozone was investigated using conditions described in section 3.2.1.

The rates of ozone decomposition were compared at pH= 5 and 7 in the presence of Mn_2O_3 /γ-Al_2O_3 as the model catalyst. pH=7 was chosen as optimal, based on a faster ozone decomposition at this pH.

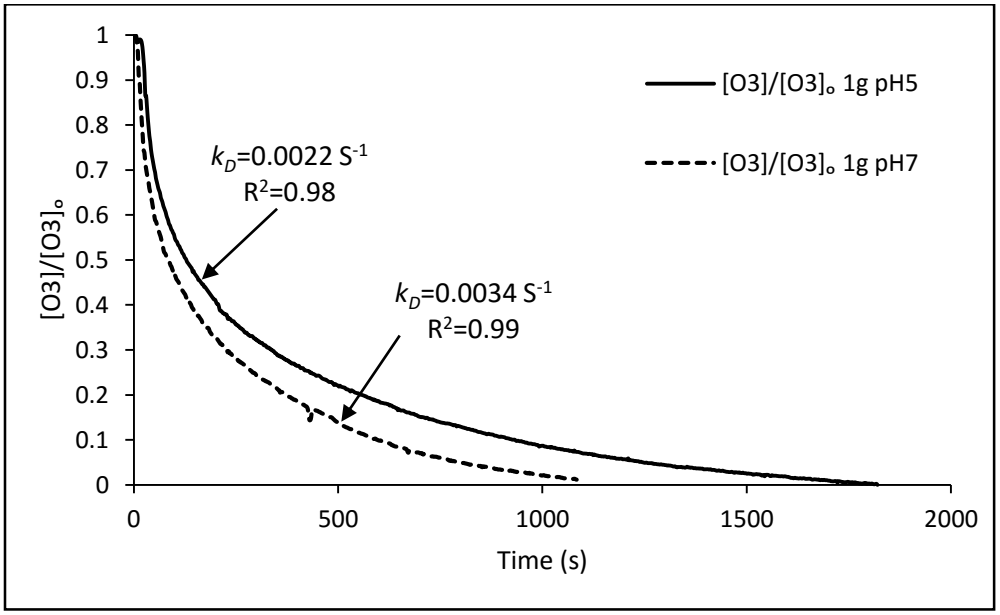

Figure 5. 10. Effect of pH on ozone decomposition catalyzed by Mn_2O_3 / γ-Al_2O_3, $[O3]_0$= 8.33×10^{-5} M, catalyst dose= 1.0 g.L^{-1}, ionic strength (buffer) = 0.1 M

5.3 Effect of Different Metals Loaded on γ-Alumina on Catalytic Ozonation

The experimental procedures, apparatus and measurements were identical to that of section 3.2. The removal of atrazine was measured using the same HPLC system, conditions and mobile phases as described in section 3.2.

Results show that ZnO/γ-alumina, Fe_2O_3/γ-alumina and γ-alumina catalysts possess similar rates of ozone decompositions (Figure 5.11.). Gratifyingly, Mn_2O_3/γ–alumina proved to be superior over other catalysts in the ozone decomposition experiments. However, when catalytic ozonation conditions were employed in the presence of atrazine, it was observed that that ZnO/γ-alumina, Fe_2O_3/γ-alumina, and γ-alumina catalysts have similar rates of atrazine removal (65%) while Mn_2O_3/γ-alumina was less effective towards the degradation (10%) (Figure 5.12.).

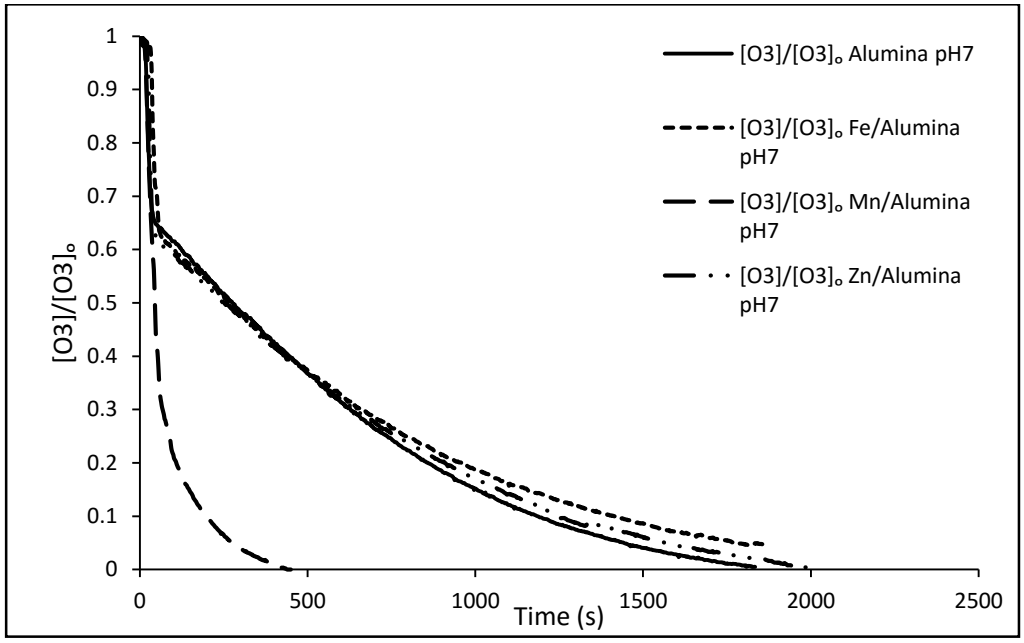

Figure 5. 11. Comparison between effect of different metals loaded on γ-Alumina on ozone decomposition in the presence of atrazine in water at pH=7 (phosphate buffer), $[O3]_0 = 8.33\times10^{-5}$ M, $[ATZ]_0 = 4.62\times10^{-5}$ M

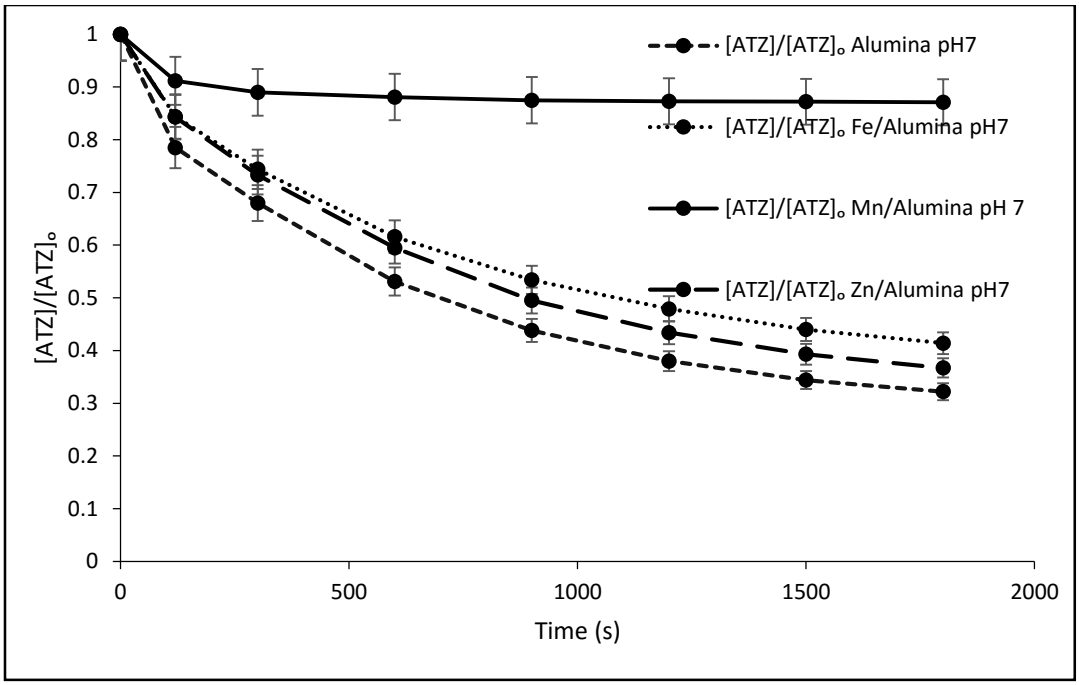

Figure 5. 12. Comparison between effect of different metals loaded on γ-Alumina on catalytic ozonation on atrazine removal from water at pH=7 (phosphate buffer), $[O3]_0 = 8.33\times10^{-5}$ M, $[ATZ]_0 = 4.62\times10^{-5}$ M

5.4 Effect of Radical Scavenger

In order to examine whether the catalytic ozonation involves hydroxyl radicals and/or molecular ozone as the reactive species, four experiments were carried out (see section 3.2.1.), two in the presence of TBA (1×10^{-4} M) and the others without the scavenger.

It was observed that the rate of atrazine removal with Mn_2O_3/γ-alumina in the presence of TBA is almost zero and without TBA is approximately 10%. In other words, in catalytic ozonation reactions carried out in the presence of TBA results in a 10% decrease in removal of ATZ (Figure 5.13.). Furthermore, the rate of atrazine removal using ZnO/γ-alumina in the presence of TBA is 39% and without TBA with ZnO/γ-alumina is 64% its initial concentration, showing a 25% decline (Figure 5.14.).

In MnO_2/γ-alumina-catalyzed ozonation reactions, TBA completely terminates the ozone decomposition suggesting that in the presence of Mn_2O_3/γ-alumina, ozone decomposition occurs at a very fast rate (all ozone molecules are decomposed within the first 2 minutes). However results obtained from the atrazine removal experiments for Mn_2O_3/γ-alumina show an enhancement in the rate of removal only within the first 2 minutes time frame (Figure 5.13.). These observations substantiate the strong influence of molecular ozone on degradation of ATZ and the partial involvement of hydroxyl radicals in the mechanism.

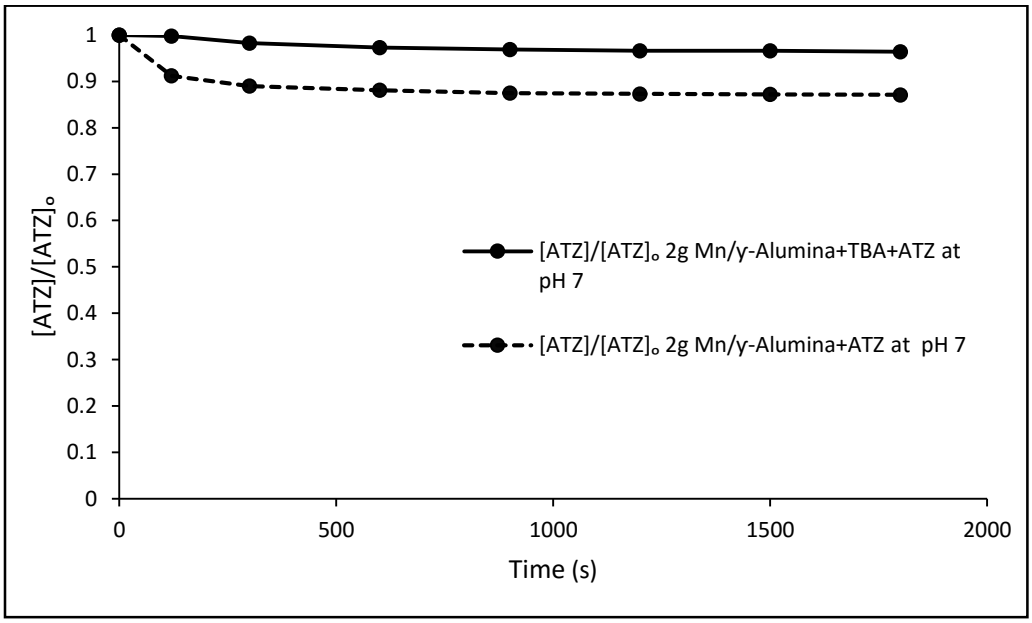

Figure 5. 13. Radical scavenger effect on catalytic ozonation (Mn_2O_3/γ-alumina) of atrazine at pH=7.$[O3]_0$ =8.33×10^{-5} M, $[ATZ]_0$ = 4.62×10^{-5} M, when applies $[TBA]_0$ = 1×10^{-4} M ionic strength (buffer) = 0.1 M.

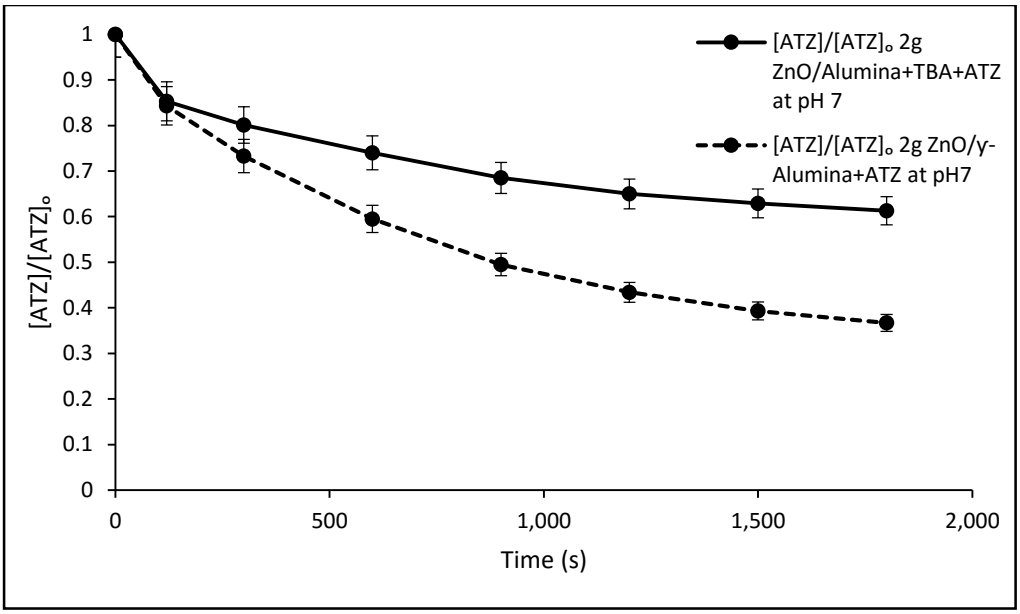

Figure 5. 14. Radical scavenger effect on catalytic ozonation (ZnO/γ-alumina) of atrazine at pH=7. $[O3]_0$ $=8.33\times10^{-5}$ M, $[ATZ]_0 = 4.62\times10^{-5}$ M, when applies $[TBA]_0 = 1\times10^{-4}$ M ionic strength (buffer) = 0.1 M.

R_{ct} for experiments of atrazine removal *via* ZnO/γ-alumina/O_3 and other ZnO/γ-alumina/O_3/TBA were calculated (Appendix B). R_{ct} values for atrazine removal by ZnO/γ-alumina/O_3 is 8.5 $x10^{-9}$ and in the presence of ZnO/γ-alumina/O_3/TBA is 2.1 $x10^{-9}$. Furthermore, R_{ct} values for atrazine removal using Mn_2O_3/O_3 and other Mn_2O_3 / γ-alumina /O_3/TBA were calculated (Appendix B). R_{ct} for atrazine removal using Mn_2O_3/ γ-alumina /O_3 is 4.4 $x10^{-9}$ and in the presence of Mn_2O_3/ γ-alumina /O_3/TBA is -1.3 $x10^{-9}$.

R_{ct} values show the contribution of hydroxyl radicals in the mechanism of removal of ATZ. However, the difference in R_{ct} values for Mn_2O_3/ γ-alumina/O_3/TBA experiments are smaller than ZnO/ γ-alumina/O_3/TBA experiments. This suggests that in Mn_2O_3/ γ-alumina/O_3 systems, despite the effective formation of hydroxyl radicals (from ozone decomposition experiment), the small difference in R_{ct} values suggest that molecular ozone is more effective in the mechanism of removal.

5.5 Discussion

Similar to our observations, Lin *et* al.[27] and Kasprzyk and Nawrocki[69,70] have independently reported that rate of ozone decomposition in the presence of alumina is almost zero.

Nawrocki reported a similar reactivity for ozone decomposition on alumina. However, significant catalytic reactivity was observed in the removal of emerging pollutants which is believed to be linked to the adsorption on the surface of alumina. The proposed mechanism of catalytic ozonation on alumina consists of formation of a hydrophobic layer of emerging pollutant on the surface of alumina and reaction of molecular ozone with the emerging pollutant. Ozone is considered as a non-polar molecule with 0.46 D dipole moment which has low affinity towards solvation in polar solvents such as water. The hydrophobic layer of emerging pollutant provides a suitable non-polar interface for solid-liquid interactions. As a result, ozone could effectively migrate towards the non-polar hydrophobic layer and react with the emerging pollutant. The authors conclude that the rate enhancement in removal of emerging pollutants in the catalytic ozonation is observed without incorporation of hydroxyl radicals.[38] Álvarez *et* al.[39] , Ernst *et* al.[40] and Beltrán *et* al.[41] independently confirmed this mechanism and emphasized on the importance of adsorption of organic molecules on the catalyst surface in catalytic ozonation processes.

Ernst *et* al.[40] suggested that organic molecules do not adsorb on the surface of the catalyst during the catalytic ozonation process. According to the proposed mechanism, atomic oxygen is produced from decomposition of ozone which reacts with hydroxyl groups on the surface of alumina to form O_2H radicals. This is followed by the reaction with another molecule of ozone to generate O_3^- radicals. These species could decompose to O_2 or OH radicals which react with organic molecules in the surface of catalyst or in the bulk liquid phase.

Zhang *et* al.[71] and Pines and Reckhow[24] suggested that degradation of oxalate in catalytic ozonation does not incorporate hydroxyl radicals. However, according to Amir Ikhlaqa *et al.*[43] degradation of Coumarin on alumina in catalytic ozonation proceeds through hydroxyl radicals and the relevant chain reactions.

Based on the (often controversial) mechanisms suggested by different groups, the mechanism of catalytic ozonation on alumina and alumina-supported metal oxides are not fully understood. Based on the results presented here, it is observed that the rates of removal of atrazine in the presence of metals supported on γ-Al_2O_3 and metal-free γ-Al_2O_3 are faster than systems without the catalysts. However, the rate of removal of atrazine in the presence of Mn_2O_3/γ-Al_2O_3 was slower than γ-Al_2O_3, Fe_2O_3/γ-Al_2O_3 and ZnO/γ-Al_2O_3, despite the clear rate difference between ozone decomposition in the presence of Mn_2O_3/γ-Al_2O_3 compared to the other catalysts. Furthermore, experiments in the presence of TBA suggest that degradation of atrazine is likely to involve molecular ozone as the reactive species.

In many catalytic ozonation systems the ozone molecule and the emerging pollutant compete for active site on the surface of the catalyst. However, based on the adsorption studies, atrazine has a low affinity towards such adsorption. It is logical to assume that ozone reacts with the hydroxyl groups of the catalyst to form a highly reactive metal-ozone complex. This layer could react with a molecule of atrazine through electron transfer mechanism. In such system, the degradation of atrazine does not proceed through hydroxyl radicals (as mentioned in section 3.3.7.) and instead ozone molecules are directly involved in the mechanism.

5.6 Typical experimental errors

1. Errors associated with pH control

As mentioned, the pH level of the solution greatly influences ozone decomposition and hence the catalytic ozonation of the organic molecule. In the presence of catalysts the pH of the solution changes from its original level mostly due to the presence of inorganic impurities of the catalyst. Therefore, it is crucial to control the pH of the solution during and after the catalytic ozonation reactions.

2. Errors associated with adsorption on the surface of catalyst

In some cases, catalyst-free ozonation reactions could lead to a partial degradation of the organic contaminant. Additionally, some of the organic molecules might adsorb on the surface of the catalyst and lead to a false negative error in determining the residual concentration of the emerging pollutant. Hence, when evaluating the effects of catalytic ozonation, the combined adsorption and metal-free ozonation reactions should be taken into consideration.

3. Reproducibility of Experimental Measurements

In order to validate the experimental data, ozone self-decomposition and a few atrazine removal experiments were performed by using a randomly selected catalyst 3 to 5 times. The results showed that the data was consistent (±5%) within 30 minutes.

Furthermore, to evaluate the HPLC calibration methods and TOC results, various standard solutions were prepared. The results exhibited excellent consistency (±5%). As an example, the effects of radical scavenger on catalytic ozonation (ZnO/γ-alumina) of atrazine was run three times which show < ±5% error. Error bars are illustrated in Figure 5.15.

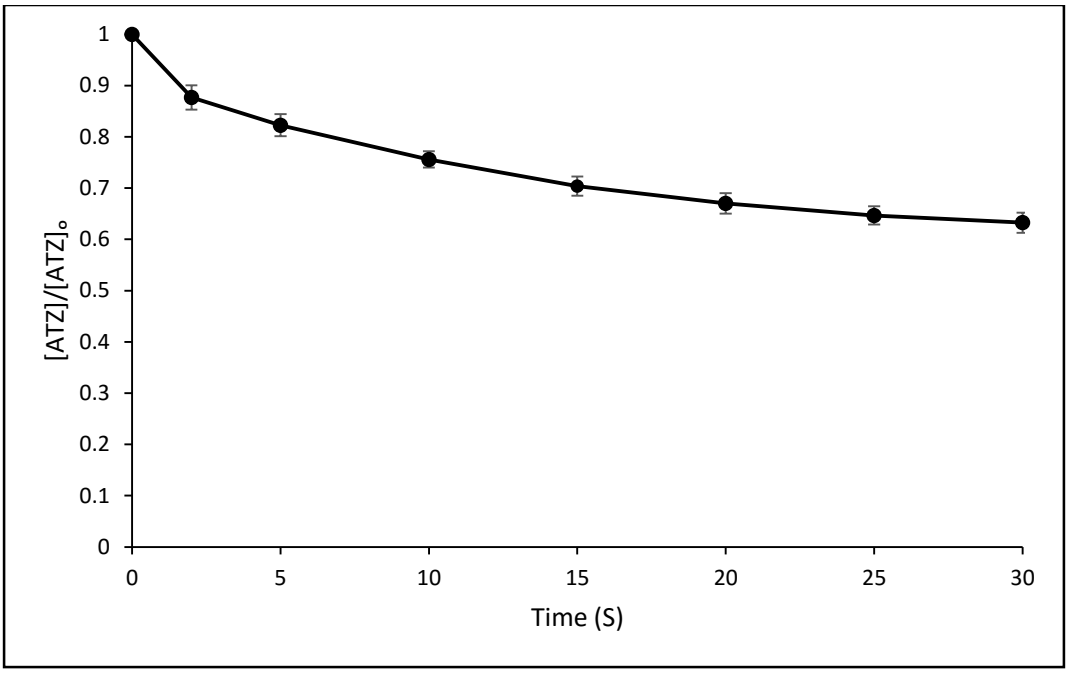

Figure 5. 15. Radical scavenger effect on catalytic ozonation (ZnO/γ-alumina) of atrazine at pH=7. $[O3]_0$ =8.33×10^{-5} M, $[ATZ]_0$ = 4.62×10^{-5} M, $[TBA]_0$ = 1×10^{-4} M ionic strength (buffer) = 0.1 M.

Chapter 6

6. Summary and conclusion

The highlights and findings corresponding to the effects of different sizes of nano-ZnO in the catalytic ozonation of ATZ removal are summarized below:

- nano-ZnO catalysts increase the rate of ozone decomposition and atrazine removal *via* production of hydroxyl radicals as oxidative intermediates.
- Different particle sizes of nano-ZnO catalysts have minimal effect on the rate of ozone decomposition and atrazine removal.
- Adsorption of ATZ on nano-ZnO surface is a negligible.
- A metal-organics chelate is proposed as the reactive species in the mechanism of removal of ATZ.
- The logical explanation for the similar rates of ATZ removal by various sizes of nano-ZnO could be linked to the possible occurrence of the catalytic ozonation reactions in the bulk of the solution rather than the surface of the catalysts.

The highlights and findings for the effects of alumina based catalysts on catalytic ozonation of atrazine in water are summarized below:

- Metals supported on γ-Al_2O_3 and metal-free γ-Al_2O_3 are associated with faster rates of ATZ reactions compared to metal-free ozonation.
- Mn_2O_3/γ-Al_2O_3 catalysts exhibited superior reactivity to the other γ-Al_2O_3-based catalysts in ozone decomposition. However, the rate of removal of ATZ was slower than γ-Al_2O_3, Fe_2O_3/γ-Al_2O_3 and ZnO/γ-Al_2O_3.

- A reactive metal-ozone complex is proposed as the reactive species, which oxidizes ATZ through an electron transfer mechanism.
- Reactions in the presence of TBA show that molecular ozone is probably involved in the degradation of ATZ

6.1 Recommendation for Future Work

Results reported in this thesis have demonstrated that the rate of catalytic ozonation of atrazine using various sizes of nano-ZnO catalysts are similar and associated with partial degradation of the contaminant. This is believed to be due to the low adsorption of the contaminant on the catalysts possibly due to the low polarity of the contaminant. As a future direction for this project, it seems logical to screen a spectrum of non-polar and polar contaminants using the adsorption tests outlined in section 3.2.1 and the catalysts described in this thesis. Having established the correct combination of catalyst-contaminant it is proposed to carry out a series of catalytic ozonation experiments to examine the effects of particle size on nano-ZnO/O_3 catalytic ozonation. Furthermore, based on the promising results obtained in ozone decomposition experiments using metals supported on γ-alumina and metal-free γ-alumina (section 4.5 and 5.3), these catalysts could be used for catalytic ozonation of the aforementioned pollutant(s).

Another proposed direction for this project consists of carrying out thorough toxicological studies in order to investigate the toxicity of the catalytic ozonation by-products of atrazine degradation. From an environmental safety standpoint, this is particularly alluring as it has been shown that the catalytic ozonation of atrazine results in incomplete degradation of the contaminant. These smaller by-products could be potentially harmful for the environment. The degradation products are identified using mass spectrometry techniques and a plausible fragmentation pattern will be

suggested for ATZ different ionization conditions. Finally, attempts will be made to understand the source of toxicity of the intermediates in the degradation process and their potential effects on the environment.

References

(1) Kasprzyk-Hordern, B.; Ziółek, M.; Nawrocki, J. Catalytic Ozonation and Methods of Enhancing Molecular Ozone Reactions in Water Treatment. *Appl. Catal. B Environ.* **2003**, *46* (4), 639–669.

(2) Nawrocki, J. Catalytic Ozonation in Water: Controversies and Questions. Discussion Paper. *Appl. Catal. B Environ.* **2013**, *142-143*, 465–471.

(3) Pham, T.-T.; Rondeau, B.; Sabik, H.; Proulx, S.; Cossa, D. Lake Ontario: The Predominant Source of Triazine Herbicides in the St. Lawrence River. *Can. J. Fish. Aquat. Sci.* **2000**, *57* (S1), 78–85.

(4) Wan, M. T.; Kuo, J.; McPherson, B.; Pasternak, J. Agricultural Pesticide Residues in Farm Ditches of the Lower Fraser Valley, British Columbia, Canada. *J. Environ. Sci. Health. B.* **2006**, *41* (5), 647–669.

(5) Stover, J.; Hamill, A. S. Pesticide Contamination of Surface Waters Draining Agricultural Fields : Pesticide Contamination Classification and Abatement Measures. [http://agrienvarchive.ca/download/glwq_1.pdf]

(6) Wu, M.; Quirindongo, M.; Sass, J.; Wetzler, A. Still Poisoning the Well. *Nat. Resour. Def. Counc. Washington, DC* **2010**.

(7) Waller, S. A.; Paul, K.; Peterson, S. E.; Hitti, J. E. Agricultural-Related Chemical Exposures, Season of Conception, and Risk of Gastroschisis in Washington State. *Am. J. Obstet. Gynecol.* **2010**, *202* (3), 241.

(8) Swan, S. H.; Kruse, R. L.; Liu, F.; Barr, D. B.; Drobnis, E. Z.; Redmon, J. B.; Wang, C.; Brazil, C.; Overstreet, J. W.; Future Families Research Group, Semen Quality in Relation

to Biomarkers of Pesticide Exposure. *Environ. Health Perspect.* **2003**, *111* (12), 1478.

(9) Kettles, M. K.; Browning, S. R.; Prince, T. S.; Horstman, S. W. Triazine Herbicide Exposure and Breast Cancer Incidence: An Ecologic Study of Kentucky Counties. *Environ. Health Perspect.* **1997**, *105* (11), 1222.

(10) Winchester, P. D.; Huskins, J.; Ying, J. Agrichemicals in Surface Water and Birth Defects in the United States. *Acta Paediatr.* **2009**, *98* (4), 664–669.

(11) Villanueva, C. M.; Durand, G.; Coutté, M.-B.; Chevrier, C.; Cordier, S. Atrazine in Municipal Drinking Water and Risk of Low Birth Weight, Preterm Delivery, and Small-for-Gestational-Age Status. *Occup. Environ. Med.* **2005**, *62* (6), 400–405.

(12) Levine, M. J. *Pesticides a Toxic Time Bomb in Our Midst*; Greenwood Publishing Group, **2007**.

(13) Pathak, R. K. Various Techniques for Atrazine Removal. *Int. Conf. Life Sci. Technol.* **2011**, *3*, 19–22.

(14) Abigail, M. E. A.; Lakshmi, V. Microbial Degradation of Atrazine, Commonly Used Herbicide. *Int. J. Adv. Biol. Res.* **2012**, *2*, 16–23.

(15) Sotelo, J. L.; Beltran, F. J.; Benitez, F. J.; Beltran-Heredia, J. Ozone Decomposition in Water: Kinetic Study. *Ind. Eng. Chem. Res.* **1987**, *26*, 39−43.

(16) Buehler, R. E.; Staehelin, J.; Hoigne, J. Ozone Decomposition in Water Studied by Pulse Radiolysis. 1. Perhydroxyl (HO_2)/hyperoxide (O_2^-) and HO_3/O_3^- as Intermediates. *J. Phys. Chem.* **1984**, *88* (12), 2560–2564.

(17) Beltrán, F. *Ozone Reaction Kinetics for Water and Wastewater Systems*; CRC Press, **2003**.

(18) Oyama, S. T. Chemical and Catalytic Properties of Ozone. *Catal. Rev.* **2000**, *42* (3), 279–

322.

(19) Fontanier, V.; Farines, V.; Albet, J.; Baig, S.; Molinier, J. Oxidation of Organic Pollutants of Water to Mineralization by Catalytic Ozonation. *Ozone Sci. Eng.* **2005**, *27* (2), 115–128.

(20) Legube, B. Catalytic Ozonation: A Promising Advanced Oxidation Technology for Water Treatment. *Catal. Today* **1999**, *53* (1), 61–72.

(21) Gracia, R.; Aragües, J. L.; Ovelleiro, J. L. Study of the Catalytic Ozonation of Humic Substances in Water and Their Ozonation Byproducts. *Ozone Sci. Eng.* **1996**, *18* (3), 195–208.

(22) Piera, E.; Calpe, J. C.; Brillas, E.; Domènech, X.; Peral, J. 2,4-Dichlorophenoxyacetic Acid Degradation by Catalyzed Ozonation: TiO_2/UV/O_3 and Fe(II)/UV/O_3 Systems. *Appl. Catal. B Environ.* **2000**, *27* (3), 169–177.

(23) Hart, E. J.; Sehested, K.; Holoman, J. Molar Absorptivities of Ultraviolet and Visible Bands of Ozone in Aqueous Solutions. *Anal. Chem.* **1983**, *55* (1), 46–49.

(24) Pines, D. S.; Reckhow, D. A. Effect of Dissolved cobalt(II) on the Ozonation of Oxalic Acid. *Environ. Sci. Technol.* **2002**, *36* (19), 4046–4051.

(25) Mills, A.; Le Hunte, S. An Overview of Semiconductor Photocatalysis. *J. Photochem. Photobiol. A Chem.* **1997**, *108* (1), 1–35.

(26) Bulanin, K. M.; Lavalley, J. C.; Lamotte, J.; Mariey, L.; Tsyganenko, N. M.; Tsyganenko, A. A. Infrared Study of Ozone Adsorption on CeO 2. *J. Phys. Chem. B* **1998**, *102* (35), 6809–6816.

(27) Lin, J.; Kawai, A.; Nakajima, T. Effective Catalysts for Decomposition of Aqueous Ozone. *Appl. Catal. B Environ.* **2002**, *39* (2), 157–165.

(28) Beltran, F. J.; Rivas, J.; Alvarez, P.; Montero-de-Espinosa, R. Kinetics of Heterogeneous Catalytic Ozone Decomposition in Water on an Activated Carbon. *Ozone-Science Eng.* **2002**, *24* (4), 227–237.

(29) Elovitz, M. S.; von Gunten, U. Concept. *Ozone Sci. Eng.* **1999**, *21* (3), 239–260.

(30) Nawrocki, J.; Dunlap, C.; Li, J.; Zhao, J.; McNeff, C. V.; McCormick, a.; Carr, P. W. Part II. Chromatography Using Ultra-Stable Metal Oxide-Based Stationary Phases for HPLC. *J. Chromatogr. A* **2004**, *1028* (1), 31–62.

(31) Pines, D. S.; Reckhow, D. A. Solid Phase Catalytic Ozonation Process for the Destruction of a Model Pollutant. *Ozone Sci. Eng.* **2003**, *25* (1), 25–39.

(32) Al-Hayek, N.; Legube, B.; Doré, M. Ozonation Catalytique (Fe III/$A1_2O_3$) Du Phénol et de Ses Produits D'ozonation. *Environ. Technol. Lett.* **1989**, *10* (4), 415–426.

(33) Cooper, C.; Burch, R. An Investigation of Catalytic Ozonation for the Oxidation of Halocarbons in Drinking Water Preparation. *Water Res.* **1999**, *33* (18), 3695–3700.

(34) Kasprzyk-Hordern, B. Chemistry of Alumina, Reactions in Aqueous Solution and Its Application in Water Treatment. *Adv. Colloid Interface Sci.* **2004**, *110* (1-2), 19–48.

(35) Shirai, T.; Watanabe, H.; Fuji, M.; Takahashi, M. Structural Properties and Surface Characteristics on Aluminum Oxide Powders. *Technology* **2009**, *9*, 23–31.

(36) Yalamaç, E.; Trapani, A.; Akkurt, S. Sintering and Microstructural Investigation of Gamma–alpha Alumina Powders. *Eng. Sci. Technol. an Int. J.* **2014**, *17* (1), 2–7.

(37) Yopps, J. .; Fuerstenau, D. The Zero Point of Charge of Alpha-Alumina. *J. Colloid Sci.* **1964**, *19* (1), 61–71.

(38) Kasprzyk-Hordern, B.; Raczyk-Stanisławiak, U.; Świetlik, J.; Nawrocki, J. Catalytic

Ozonation of Natural Organic Matter on Alumina. *Appl. Catal. B Environ.* **2006**, *62* (3-4), 345–358.

(39) Álvarez, P. M.; Beltrán, F. J.; Pocostales, J. P.; Masa, F. J. Preparation and Structural Characterization of Co/Al2O3 Catalysts for the Ozonation of Pyruvic Acid. *Appl. Catal. B Environ.* **2007**, *72* (3-4), 322–330.

(40) Ernst, M.; Lurot, F.; Schrotter, J. C. Catalytic Ozonation of Refractory Organic Model Compounds in Aqueous Solution by Aluminum Oxide. *Appl. Catal. B Environ.* **2004**, *47* (1), 15–25.

(41) Beltrán, F. J.; Rivas, F. J.; Montero-De-Espinosa, R. A TiO_2/Al_2O_3 Catalyst to Improve the Ozonation of Oxalic Acid in Water. *Appl. Catal. B Environ.* **2004**, *47* (2), 101–109.

(42) Ikhlaq, A.; Brown, D. R.; Kasprzyk-Hordern, B. Mechanisms of Catalytic Ozonation on Alumina and Zeolites in Water: Formation of Hydroxyl Radicals. *Appl. Catal. B Environ.* **2012**, *123-124*, 94–106.

(43) Ikhlaq, A.; Brown, D. R.; Kasprzyk-Hordern, B. Mechanisms of Catalytic Ozonation: An Investigation into Superoxide Ion Radical and Hydrogen Peroxide Formation during Catalytic Ozonation on Alumina and Zeolites in Water. *Appl. Catal. B Environ.* **2013**, *129*, 437–449.

(44) Zhang, T.; Li, C.; Ma, J.; Tian, H.; Qiang, Z. Surface Hydroxyl Groups of Synthetic α-FeOOH in Promoting OH Generation from Aqueous Ozone: Property and Activity Relationship. *Appl. Catal. B Environ.* **2008**, *82* (1-2), 131–137.

(45) Suh, M.; Bagus, P. S.; Pak, S.; Rosynek, M. P.; Lunsford, J. H. Reactions of Hydroxyl Radicals on Titania , Silica , Alumina , and Gold Surfaces Reactions of Hydroxyl Radicals

on Titania , Silica , Alumina , and Gold Surfaces. *J. Phys. Chem. B* **2000**, *104* (12), 2736–2742.

(46) Andreozzi, R.; Insola, a.; Caprio, V.; Marotta, R.; Tufano, V. The Use of Manganese Dioxide as a Heterogeneous Catalyst for Oxalic Acid Ozonation in Aqueous Solution. *Appl. Catal. A Gen.* **1996**, *138* (1), 75–81.

(47) Tong, S. P.; Liu, W. P.; Leng, W. H.; Zhang, Q. Q. Characteristics of MnO2 Catalytic Ozonation of Sulfosalicylic Acid and Propionic Acid in Water. *Chemosphere* **2003**, *50* (10), 1359–1364.

(48) Orge, C. a.; Órfão, J. J. M.; Pereira, M. F. R. Catalytic Ozonation of Organic Pollutants in the Presence of Cerium Oxide-Carbon Composites. *Appl. Catal. B Environ.* **2011**, *102* (3-4), 539–546.

(49) Wang, J.; Jiang, Z.; Zhang, L.; Kang, P.; Xie, Y.; Lv, Y.; Xu, R.; Zhang, X. Sonocatalytic Degradation of Some Dyestuffs and Comparison of Catalytic Activities of Nano-Sized TiO_2, Nano-Sized ZnO and Composite TiO_2/ZnO Powders under Ultrasonic Irradiation. *Ultrason. Sonochem.* **2009**, *16* (2), 225–231.

(50) Zhai, X.; Chen, Z.; Zhao, S.; Wang, H.; Yang, L. Enhanced Ozonation of Dichloroacetic Acid in Aqueous Solution Using Nanometer ZnO Powders. *J. Environ. Sci.* **2010**, *22* (10), 1527–1533.

(51) Jung, H.; Choi, H. Catalytic Decomposition of Ozone and Para-Chlorobenzoic Acid (pCBA) in the Presence of Nanosized ZnO. *Appl. Catal. B Environ.* **2006**, *66* (3-4), 288–294.

(52) Dong, Y. M.; Wang, G. L.; Jiang, P. P.; Zhang, A. M.; Yue, L.; Zhang, X. M. Simple

Preparation and Catalytic Properties of ZnO for Ozonation Degradation of Phenol in Water. *Chinese Chem. Lett.* **2011**, *22* (2), 209–212.

(53) Huang, W. J.; Fang, G. C.; Wang, C. C. A Nanometer-ZnO Catalyst to Enhance the Ozonation of 2,4,6-Trichlorophenol in Water. *Colloids Surfaces A Physicochem. Eng. Asp.* **2005**, *260* (1-3), 45–51.

(54) Gottschalk, C.; Libra, J. A.; Saupe, A. *Ozonation of Water and Waste Water: A Practical Guide to Understanding Ozone and Its Applications: Second Edition*; **2010**.

(55) Guzman-Perez, C. a.; Soltan, J.; Robertson, J. Kinetics of Catalytic Ozonation of Atrazine in the Presence of Activated Carbon. *Sep. Purif. Technol.* **2011**, *79* (1), 8–14.

(56) Ghosh Dastidar, T.; Netravali, A. Cross-Linked Waxy Maize Starch-Based "Green" Composites. *ACS Sustain. Chem. Eng.* **2013**, *1* (12), 1537–1544.

(57) Dehabadi, L.; Wilson, L. D. Polysaccharide-Based Materials and Their Adsorption Properties in Aqueous Solution. *Carbohydr. Polym.* **2014**, *113*, 471–479.

(58) Thommes, M. Physical Adsorption Characterization of Nanoporous Materials. *Chemie-Ingenieur-Technik* **2010**, *82* (7), 1059–1073.

(59) Julkapli, N. M.; Ahmad, Z.; Akil, H. M. X-Ray Diffraction Studies of Cross Linked Chitosan with Different Cross Linking Agents for Waste Water Treatment Application. *AIP Conf. Proc.* **2009**, *1202*, 106–111.

(60) Noh, J. S.; Schwarz, J. A. Effect of HNO_3 Treatment on the Surface Acidity of Activated Carbons. *Carbon N. Y.* **1990**, *28* (5), 675–682.

(61) Ferro-García, M. a.; Rivera-Utrilla, J.; Bautista-Toledo, I.; Moreno-Castilla, C. Adsorption of Humic Substances on Activated Carbon from Aqueous Solutions and Their Effect on the

Removal of Cr(III) Ions. *Langmuir* **1998**, *14* (7), 1880–1886.

(62) Rezaei, E.; Soltan, J.; Chen, N. Catalytic Oxidation of Toluene by Ozone over Alumina Supported Manganese Oxides: Effect of Catalyst Loading. *Appl. Catal. B Environ.* **2013**, *136-137*, 239–247.

(63) Sun, Y.; Wu, Y.; Shan, H.; Wang, G.; Li, C. Studies on the Promoting Effect of Sulfate Species in Catalytic Dehydrogenation of Propane over Fe_2O_3/Al_2O_3 Catalysts. *Catal. Sci. Technol.* **2015**, *5* (2), 1290–1298.

(64) Chen, J. C.; Tang, C. T. Preparation and Application of Granular ZnO/Al_2O_3 Catalyst for the Removal of Hazardous Trichloroethylene. *J. Hazard. Mater.* **2007**, *142* (1-2), 88–96.

(65) Hoigné, J.; Bader, H.; Haag, W. .; Staehelin, J. Rate Constants of Reactions of Ozone with Organic and Inorganic Compounds in water—III. Inorganic Compounds and Radicals. *Water Res.* **1985**, *19* (8), 993–1004.

(66) Qi, F.; Xu, B.; Chen, Z.; Ma, J.; Sun, D.; Zhang, L. Influence of Aluminum Oxides Surface Properties on Catalyzed Ozonation of 2,4,6-Trichloroanisole. *Sep. Purif. Technol.* **2009**, *66* (2), 405–410.

(67) Acero, J. L.; Stemmler, K.; Von Gunten, U. Degradation Kinetics of Atrazine and Its Degradation Products with Ozone and OH Radicals: A Predictive Tool for Drinking Water Treatment. *Environ. Sci. Technol.* **2000**, *34* (4), 591–597.

(68) Beltrán, F. J.; García-Araya, J. F.; Álvarez, P. M.; Rivas, J. Aqueous Degradation of Atrazine and Some of Its Main by-Products with Ozone-Hydrogen Peroxide. *J. Chem. Technol. Biotechnol.* **1998**, *71* (4), 345–355.

(69) Kasprzyk, B.; Nawrocki, J. Preliminary Results on Ozonation Enhancement by a

Perfluorinated Bonded Alumina Phase. *Ozone Sci. Eng.* **2002**, *24* (1), 63–68.

(70) Kasprzyk-Hordern, B.; Nawrocki, J. The Feasibility of Using a Perfluorinated Bonded Alumina Phase in the Ozonation Process. *Ozone Sci. Eng.* **2003**, *25* (3), 185–197.

(71) Zhang, T.; Li, W.; Croué, J. P. Catalytic Ozonation of Oxalate with a Cerium Supported Palladium Oxide: An Efficient Degradation Not Relying on Hydroxyl Radical Oxidation. *Environ. Sci. Technol.* **2011**, *45* (21), 9339–9346.

APPENDIX A.

Two instances of data fitting of models used to describe the kinetics of ozonation processes (pseudo first order)

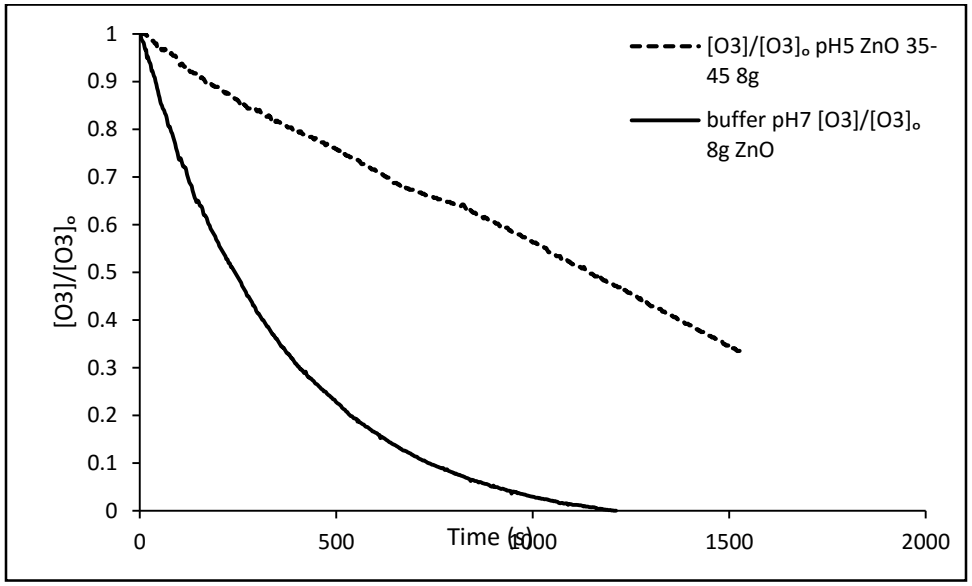

Figure A. 1. Ozone decomposition in the presence of different pH levels. $[O3]_0 = 8.33\times10^{-5}$ M, phosphate buffer used at pH = 5 and pH = 7, ionic strength 0.1 M

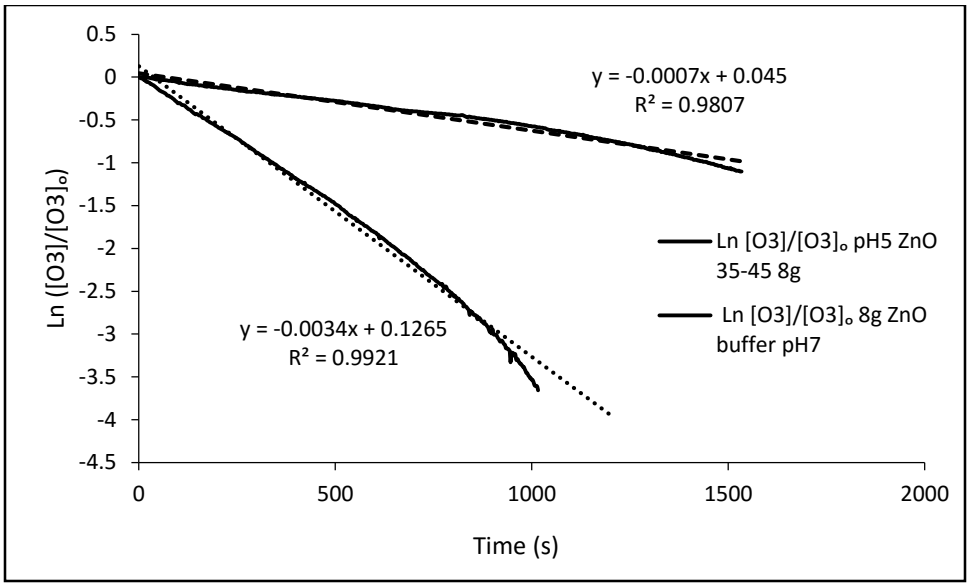

Figure A. 2. Ozone decomposition in the presence of different pH levels. $[O3]_0 = 8.33\times10^{-5}$ M, phosphate buffer used at pH = 5 and pH = 7, ionic strength 0.1 M

APPENDIX B.

Examples of Experimental Data to calculate the R_{ct}

$$R_{ct} = \frac{-slope - k_{O_3}}{k_{OH}}$$

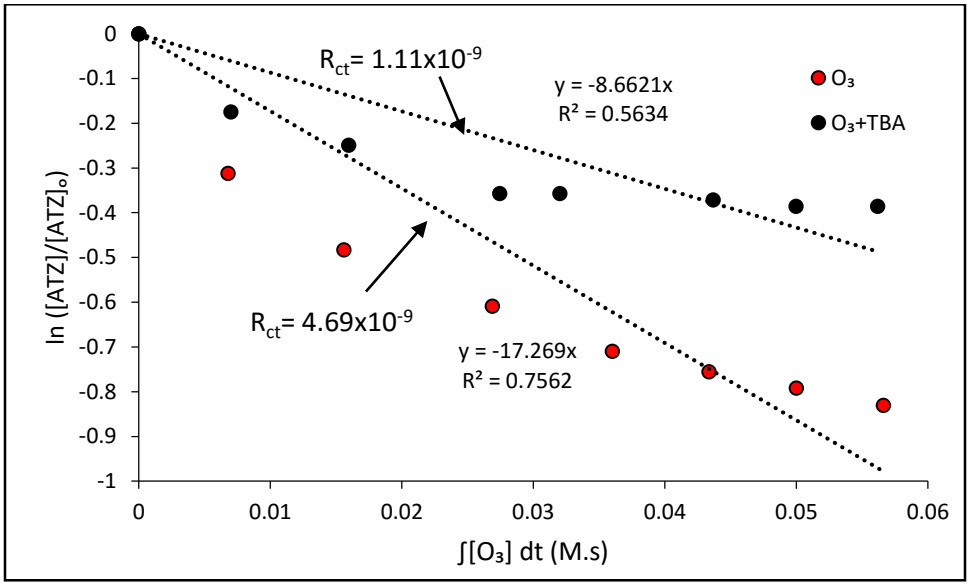

Figure B. 1. R_{ct} parameter for atrazine at non-catalytic ozonation at pH=7. $[O3]_0$ =8.33×10^{-5} M, $[ATZ]_0$ = 4.62×10^{-5} M, when applies $[TBA]_0$ =1×10^{-4} M, ionic strength (buffer) = 0.1 M.

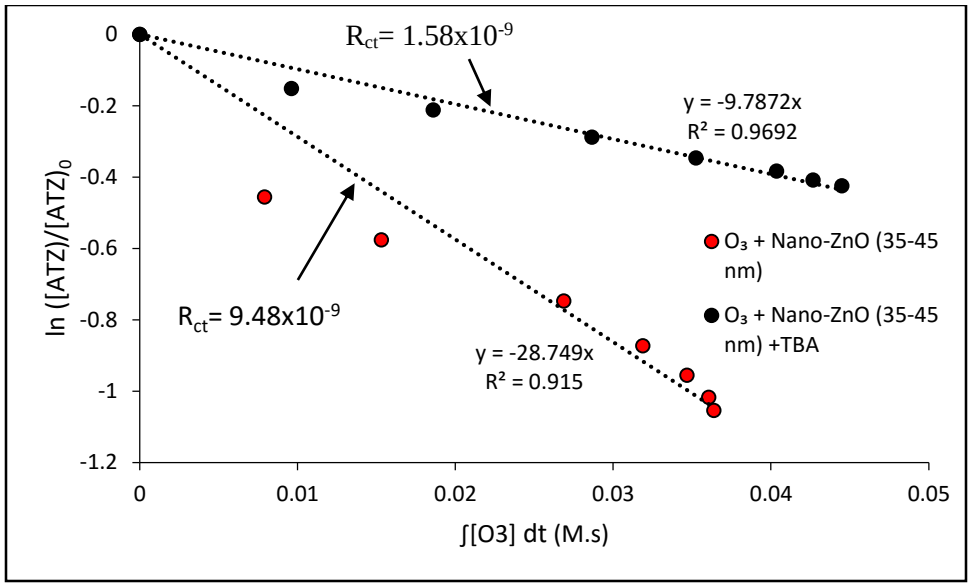

Figure B. 2. R_{ct} parameter for atrazine at catalytic ozonation (Nano-ZnO 35-45 nm) at pH=7. $[O3]_0$ =8.33×10^{-5} M, $[ATZ]_0$ = 4.62×10^{-5} M, when applies $[TBA]_0$ =1×10^{-4} M, ionic strength (buffer) = 0.1 M.

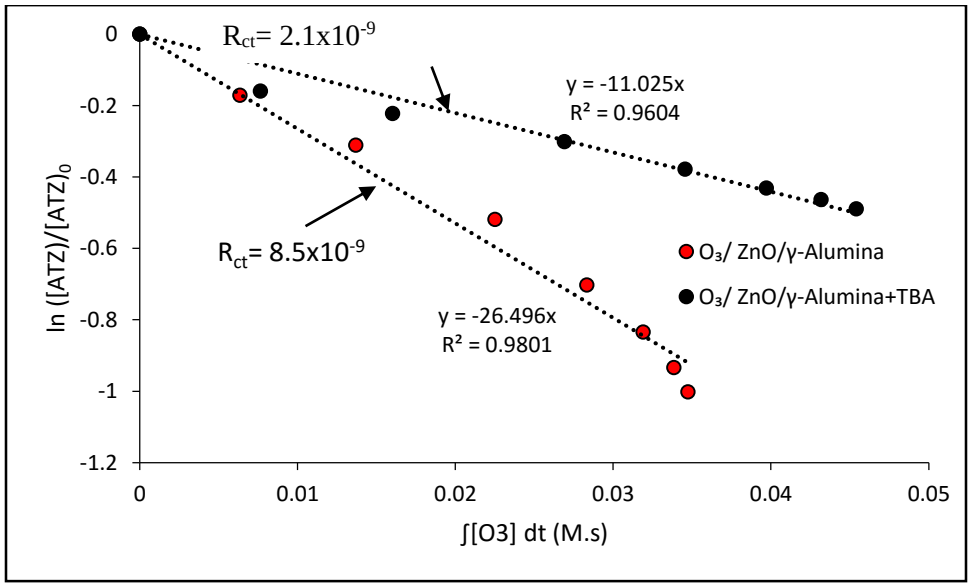

Figure B. 3. R_{ct} parameter for atrazine at catalytic ozonation (ZnO/γ-Alumina) at pH=7. $[O3]_0$ =8.33×10^{-5} M, $[ATZ]_0$ = 4.62×10^{-5} M, when applies $[TBA]_0$ =1×10^{-4} M, ionic strength (buffer) = 0.1 M.

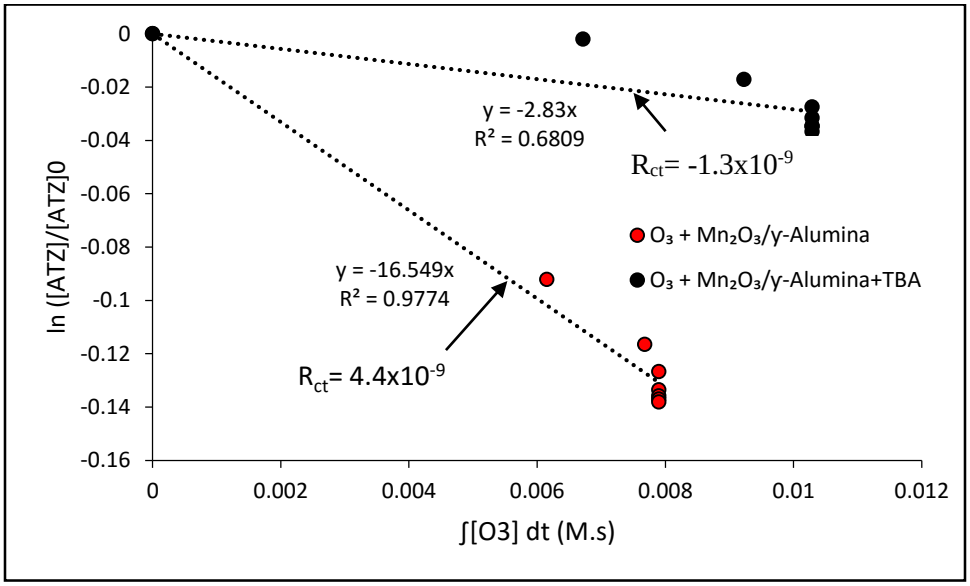

Figure B. 4. R_{ct} parameter for atrazine at catalytic ozonation (Mn_2O_3/γ-Alumina) at pH=7. $[O3]_0$ $=8.33\times10^{-5}$ M, $[ATZ]_0 = 4.62\times10^{-5}$ M, when applies $[TBA]_0 =1\times10^{-4}$ M, ionic strength (buffer) = 0.1 M.